Winter 2009

Chemical sensors based on swellable polymer microparticles and molecular imprinted polymers

John Ong'any Osambo
University of New Hampshire, Durham

CHEMICAL SENSORS BASED ON SWELLABLE POLYMER MICROPARTICLES AND MOLECULAR IMPRINTED POLYMERS

By

JOHN ONG'ANY OSAMBO

B.S., Egerton University, Njoro, Kenya, 1992

DISSERTATION

Submitted to the University of New Hampshire
in Partial Fulfillment of
the Requirements for the Degree of

Doctor of Philosophy

in

Chemistry

December, 2009

This dissertation has been examined and approved.

Dissertation Director, Dr. W. Rudolf Seitz
Professor of Chemistry

Dr. Gary R. Weisman
Professor of Chemistry

Dr. Sterling A. Tomellini
Professor of Chemistry

Dr. Roy P. Planalp
Associate Professor of Chemistry

Dr. Donald C. Sundberg
Professor (Emeritus) of Material Science

9/17/2009

Date

DEDICATION

This dissertation is dedicated to my mother Margaret Owuonda Ong'any, my wife Caren Ong'any Osambo, my children, Nancy, Fiona, and Eric, and my brothers, Peter Ong'any and Leonard Ong'any for their love, support, and encouragement.

and

In memory of my late father, Washington Ong'any Osambo, the late Dr. Geoffrey William Griffin, the director of Starehe Boys' Centre and School Nairobi, and my late sister Gladys Adhiambo. Your memories will forever live in me.

"To whom much has been given, much shall be required"
"The path of duty is the way to glory"

ACKNOWLEDGEMENTS

First I would like to express my sincere gratitude to my research advisor, Professor W. Rudolf Seitz for his constant support, guidance, encouragements, and mentoring during my graduate studies at University of New Hampshire. I also thank my committee members: Prof. Gary R. Weisman, Prof. Sterling Tomellini, Prof. Donald Sundberg, and Prof. Roy Planalp for challenging me to become a better chemist.

I would like to thank other faculty members in Chemistry department especially those who taught me the courses for providing me with a good chemistry background to enable me complete this task.

I am also very thankful to my fellow group members (both past and present) for their friendly and cooperative atmosphere which made my work in the laboratory enjoyable.

Many thanks to Cindi Rohwer, Peggy Torch, Susan Higgins, Kathy Gallagher, Bob Constantine, and Amy Lindsay for their help and friendship.

Finally, I would like to thank University of New Hampshire and especially the Department of Chemistry for both admitting me to the PhD. program and also offering me the necessary financial support in the form of teaching assistantship, and also the National Institute of Health for the research funds.

TABLE OF CONTENTS

LIST OF TABLES

LIST OF FIGURES

ABSTRACT

CHEMICAL SENSORS BASED ON SWELLABLE POLYMER MICROPARTICLES AND MOLECULAR IMPRINTED POLYMERS

By

John O. Osambo

University New Hampshire, December 2009

Swellable thermoresponsive and lightly cross-linked polymer microparticles were prepared for the development of chemical sensors for various target analytes. The swelling and shrinking of the polymer particles as a function of concentration of target analytes has been investigated using turbidity and fluorescence measurements at suitable pH values.

Chemical sensors that respond to transition metal ions such as Cu^{2+}, Ni^{2+}, Zn^{2+}, and Pb^{2+} were prepared by copolymerizing N-Isopropylacrylamide (NIPAAm) with ligands such as; 2,2'-acylamidodiacetic acid (AIDA), dibutyl-2,2'-(3 vinylphenylazanediyl) diacetate (DVPAA), N-((4'-methyl-2,2'-bipyridin-4yl)methyl)-N-propylacrylamide (NMPPAAm), and N,N-bis(pyridine-2-ylmethyl)prop-2-en-1-amine (NBPMPA). The microparticles were either labeled with 9-vinylanthracene (9-VA) / 2-Naphthylmethacrylate (2-NMA), or fluorescein o-acrylate / methacryloxethyl thiocarbonyl rhodamine B fluorophore pairs.

The particles were cross-linked using between 5-8% N, N-methylenebisacrylamide (MBA) and stabilized in acetonitrile using poly (styrene-co-acrylonitrile). The microparticles were suspended in pH 6 MOP buffer with ionic strength adjusted to 0.1M. The shrinking and swelling properties of the polymer microparticles with change in analyte concentration were evaluated by fluorescence measurements. Fluorescence intensity ratios of the acceptor to the donor fluorophores in the microparticles were calculated at different analyte concentrations.

Another method was developed for preparing sensors that respond to both β-D-glucopyranose and theophylline molecules by imprinting them in to a lightly cross-linked polymer network prepared by dispersion polymerization in water and acetonitrile, respectively. The molecular imprinting of β-D-glucopyranose and theophylline was achieved by using acrylamide and methacrylic acid (MAA), respectively, as functional monomers.

The theophylline imprinted polymer particles were labeled with fluorescein o-acrylate and methacryloxethyl thiocarbonyl rhodamine B fluorophores. MBA and poly (styrene-co-acrylonitrile) were used as cross-linker and stabilizer respectively in the polymer synthesis. Fluorescence measurements were used to monitor the swelling and shrinking of the polymer particles. The particles responded to theophylline concentration as low as 10^{-7}M in pH 7 buffer. In the preparation of β-D-glucopyranose imprinted polymer particles, poly (vinyl pyrrolidone) (PVP) was used as the stabilizer. The particles were immobilized in

10% poly (vinyl alcohol) (PVA) membranes and suspended in MOP buffer pH 7 for turbidity measurement. It was shown that these particles respond to β-D-glucopyranose concentration as low as 10^{-5}M.

CHAPTER 1

INTRODUCTION

1. 1 Background of Chemical Sensors

There has been a tremendous increase in demand for sensors, especially chemical sensors, in the last fifty years. This has resulted in extensive research on the development of sensors, particularly chemical sensors. The number of published papers in this field has increased by about 50% per year during the last decade [1]. The journals in the field of chemical sensors include: *Chemical Sensor, Chemical Sensor Technology, Sensors, Chemical Senses, Biosensors and Biotechnology, and Sensors and Actuators [2].* Several reviews and books have also been published on chemical sensors [3]. According to Janata, over 2000 papers have been published on this subject over the last four years [4]. A similar growth rate has also been experienced in other categories of sensors.

A chemical sensor can be defined as a device which provides information about the chemical composition of its environment [5]. It consists of a physical layer with a transducer coupled with a chemically selective component that transforms chemical information into an analytically useful signal [6]. The two basic components of a chemical sensor are shown in figure 1.1. One is the recognition phase where specific interaction with the target analyte allows it to be recognized, and the transducer which converts the recognition event into a useful electrical signal that can be amplified. The magnitude of the electrical signal produced depends on the extent of this interaction and is related to concentration of the target

analyte. However, this is possible if the interaction is selective to only the target analyte in the presence of other sample components.

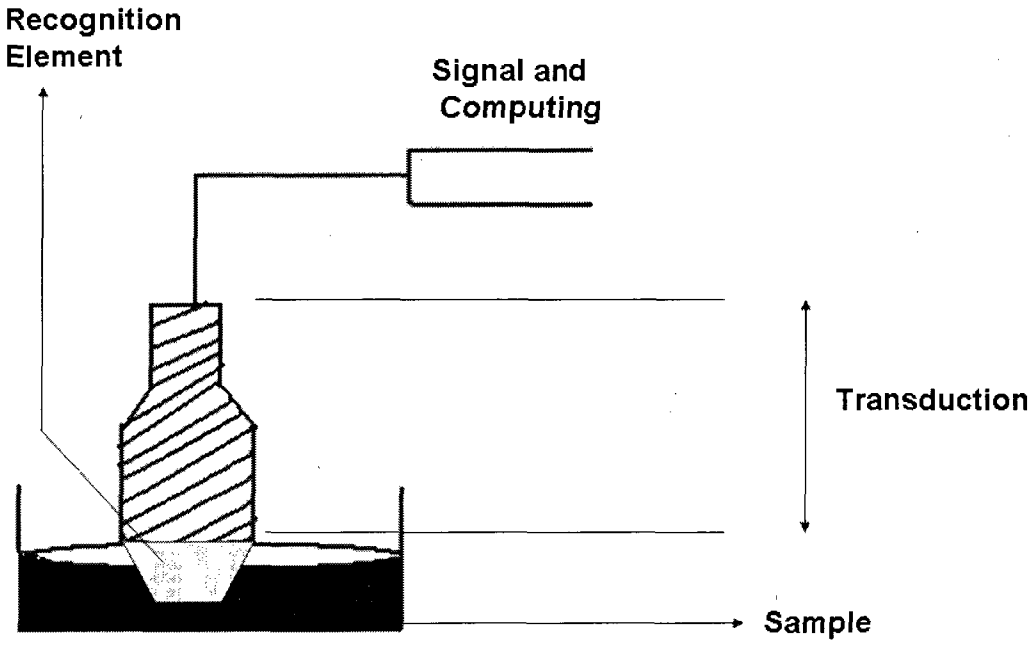

Figure 1.1: General model of chemical sensors

The sensor thus provides an experimental response related to the quantity of chemical specie [5]. In case the concentration or quantity of the target analyte varies in the sample, the measurements of the sensor should also change in a way that reflects the change in concentration or quantity of the target analyte. It can be used to either detect or quantitatively monitor a specific target analyte in a matrix containing many chemical species. The sensor must be able to interact with the target chemical specie with some degree of selectivity [6].

The sensing element which provides selectivity for the target analyte can be based upon the following properties: chemical reactivity, shape, and size. The chemical recognition of the target analyte is based on the interactions between the target analyte and the sensing element of the sensor. These interactions are usually

in the form of selective binding between the target analyte and the sensing element and are detected by a transducer. Size and shape are the common properties used by most sensing mechanisms for selective recognition of either molecules or ions. A good example of interaction that utilizes the selective binding of molecules is the antibody-antigen interaction which has been exploited for development of optical sensors [7]. Enzymes have been used in the construction of glucose and lactase sensors [8, 9].

The high growth rate experienced in the field of sensors is attributed to several features:

(i) Desire to depart from conventional instrumentation.

Conventional instrumentation methods involve transportation of the sample to the laboratory and then treating the sample before analyzing it. This involves several steps that are laborious, time consuming, expensive and also a potential source of error in the analysis.

(ii) Applications.

Chemical sensors have a wide range of applications including *in situ* analysis in industrial manufacturing plants and bioreactors. This is an advantage in that it saves time, cost and labor. This also reduces the possibility of degradation and contamination of samples during transportation. It is widely used in industries for monitoring chemical reactions, process control, and in both environmental and security monitoring.

(iii) Ability to be used in inhospitable environments.

Sensors can be used to continuously take measurements in environments that are considered either inhospitable or hazardous over a period of time. They can be used to remotely monitor chemical or biological processes by being placed at the site of monitoring.

There are several transduction methods involved in chemical sensing including: optical, thermal, electrical and chemical. Biosensors use biological host molecules such as antibodies, enzymes, and receptors for chemical recognition.

The first sensor was built by William von Siemens in 1860 [6]. He used copper wire to measure temperature. Since then, many chemical sensors have been developed.

A properly developed chemical sensor should possess key features such as: high selectivity, high sensitivity, low detection limit, fast response time, high stability, long lifetime and reliability. A sensor that has high selectivity has its output dependent only on the presence of the target analyte and responds highly selectively to that target analyte in the presence of other components in the sample matrix. Most sensors respond to the analyte of interest but also exhibit minor responses to other species present in the matrix. These species may cause minor or major interference in the analysis process and lead to poor recognition of target analytes. Achieving high selectivity with sensors has been one of the most challenging tasks in the development of chemical sensors and has been a major objective in the field of sensors for many years [3].

1. 2 Classification of Sensors

Sensors can be classified in terms of (i) type of recognition process as in semiconductor, immunochemical, and enzymatic sensors, (ii) type of sensing layer as in surface active and bulk phase sensors, (iii) size of sensor device as in nano, micro and macro sensors, (iv) sensor application as in clinical and environmental sensors, (v) mode of transduction as in the electrochemical sensors. The four major subclasses of chemical sensors based on the mode of transduction are; electrochemical, optical, mass, and thermal. They are based on measurements of the physical quantities of electrical, optical, mass, and heat respectively.

1.2.1 Electrochemical Sensors

Electrochemical sensors are the oldest and most common type of chemical sensors. In these types of sensors, the mode of transduction is electrical which involving changes in current, resistance, charge polarity, and, or voltage. They are classified as amperometric, conductimetric, and potentiomentric sensors depending on whether current, resistance, and potential difference respectively is the analytical measurement obtained [1, 110]. pH electrodes, ion-selective electrodes (ISEs) and ion-selective field effect transistors (ISFETs) are common examples of potentiometric electrochemical sensors. Amperometric electrochemical sensors are used to determine the concentration of a wide range of redox active chemical species, especially in biological samples. It consists of a biochemical recognition element such as an enzyme or a substrate. The interaction between the

enzyme and the substrate produces current that is proportional to the extent of the redox process.

1.2.2 Thermal Sensors

Thermal sensors operate by measuring either the heat energy evolved or absorbed during a chemical reaction. The sensor consists of a thermal probe with a thin layer of a thermally sensitive reagent on its surface. A physical or chemical process taking place at the surface of the probe produces a temperature change due to either absorption or evolution of heat energy. For thermal sensors involving chemical reactions for transduction, the enthalpy change of the reaction depends on its stoichiometry; the temperature change is proportional to the quantity of the reagents at the surface of the probe. Few papers have been published about thermal sensors in the past decade, making it the smallest subclass of sensors [1].

1.2.3 Optical Sensors

These sensors use interaction of the analyte with electromagnetic radiation to produce signals. In this type of sensor, a sample is irradiated with light of a particular wavelength and then the intensity of either absorbed or emitted light is being used to determine the extent of interaction. These sensors operate in a similar way to spectroscopic techniques whereby light is transmitted from the source to the sample and from the sample back to the detector without interacting with the environment. Optical sensors can detect and monitor both charged and uncharged analytes, an advantage over electrochemical sensors. The field of fiber optic chemical sensors (FOCS) has grown rapidly in the past decade because of

advances in optoelectrical components developed for the telecommunications industry [11-12]. These sensors have the advantage of operating at different wavelengths and longer distances with decreased attenuation and are widely used in navigation, medical and telecommunication fields.

FOCS have three major components: light source, detector, and optical fiber. Light is transmitted by either optical fibers or planar waveguides within the sensor. Complexing agents that interact with the target analyte at the surface or end of the fiber are introduced at the surface of the fiber. These complexing agents provide the mechanism of selective recognition of the target analyte from the sample matrix. There are two types of designs of fiber optic sensors:

(i) Direct spectroscopic sensors where the fiber is used only as a light guide separating the sensing end from the monitoring instrument. In this case spectral analysis can be obtained directly through the fiber.

(ii) Reagent-mediated sensors where the optical fiber is combined with a chemical reagent that interacts with the target analyte. In this case the change in optical properties such as refractive index, transmittance, absorbance, fluorescence, or chemiluminescence is used to measure the concentration of the analyte. The chemical reagent can either be immobilized at the tip of an optical fiber as in a *distal-type* FOCS or it can be immobilized along the core of an optical fiber as in a *fied-type* FOCS.

Bergman reported the first type of optical sensor for oxygen in 1968 [113]. The sensor contained a thin film containing a fluorescent dye and was used to monitor the partial pressure of atmospheric oxygen by luminescence quenching. In

1978, Seitz constructed the first H_2O_2 sensor based on chemiluminescence [14]. In his experiment, horseradish peroxidase was immobilized in a polyacrylamide gel on the end of optical fiber. Chemiluminescence was produced when H_2O_2 diffused into the peroxidase phase in the presence of excess luminol. In 1980, Peterson provided the first description of the construction of a pH fiber optic sensor based on absorbance of reflected light [15]. Polyacrylamide microspheres containing a dye indicator, phenol red, and microspheres of polystyrene packed into cellulose dialysis tubing at the end of optical fiber was used. The polystyrene microspheres were used for light scattering. This sensor could be used to monitor the pH of biological fluids.

Another fiber optic chemical sensor based on fluorescence was developed by Seitz in 1983 [16]. This sensor was used to monitor Al^{3+} ions, and contained Morin immobilized on cellulose powder attached to a fiber optic bundle. The reaction between Al^{3+} and Morin produces a fluorescent complex that can be monitored by measurement of fluorescence intensity. Recently, NRL researchers have developed a fiber optic biosensor that uses antibodies, lectins, and antibiotics at the surface of an optical fiber [17]. The system is designed to detect environmental pollutants, hazardous chemicals, and also biological substances with high selectivity. They have developed a portable sensor and tested on site for detection of explosives in ground water. Other successful fiber optic sensors have been developed to monitor pH, O_2, and CO_2 in beer fermentation and human blood [18].

There are several types of optical sensors that have been developed for various applications. Surface Plasmon Resonance (SPR) is a type of optical sensor that measures changes in refractive index at the surface of the sensor. The method

is highly sensitive and is widely used in the fields of chemistry and biochemistry to characterize biological surfaces and to monitor bioaffinity interactions in biological samples without the need of molecular labels or tags. The advantages of fiber optic chemical sensors include the ability to monitor in difficult or hazardous locations such as *in situ* gas diagnostics, volcano fumaroles, industrial combustion of glass furnaces, and in waste incineration industries.

1.2.4 Mass Sensors

Mass sensors measure the mass of a substance placed on the sensor surface. An example of an extremely sensitive mass sensor is the Quartz Crystal Microbalance (QCM). It is capable of measuring mass changes in the nanogram range. QCM are piezoelectric devices fabricated from a thin plate of quartz with electrodes affixed to each side of the plate. In 1880, the Curie brothers first observed the piezoelectric effect by noting that compressed quartz crystals produce an electric potential. They also observed that applying an electric potential to the crystal deforms it [10]. In piezoelectric sensors, a potential is applied to the crystal which generates acoustic waves that travel either through the bulk of the crystal or along its surface. A chemical layer which interacts with the target analyte is then applied to the top of the crystal. Polymers, antibodies, enzymes, and inorganic complexes have been used as chemical layers. The increase in the mass causes a change in the frequency of the propagating wave. The change in frequency of the propagating wave is measured and used to determine the increased mass of the target analyte at the surface of the crystal. Selectivity in mass sensors is achieved

by adding a chemically sensitive layer that is selective to the target analyte [19]. Mass sensors have numerous advantages such as cheapness, low power required, and high sensitivity. Disadvantages of piezoelectric sensors are that they are affected by both moisture and changes in temperature [20].

1.3. Chemical Sensors Based on Polymer Swelling

Swellable polymer microspheres have attracted much attention due to their wide application in sensors, medical, analytical separations, and mechanical engineering [21]. These polymers swell and shrink depending on changes of environmental conditions such as temperature, pH, and ionic strength, a factor that has lead to increased research focusing on the stimuli-responsive hydrogels. Many researchers have reported on the potential of stimuli-responsive hydrogels for use in several biomedical applications such as drug delivery, biomimetic, actuators, bioseparation, and development of surfaces with switchable hydrophilic-hydrophobic properties. Among these stimuli, pH and temperature have been extensively studied because they are important environmental factors in the human body.

Lightly cross-linked polymers swell and shrink with changes in their environment. This phenomenon was first described by Tanaka in 1978 [21]. It has been used to construct a single fiber optic pH sensor [22]. Since then there has been considerable research on the use of swellable polymers for sensors, and for controlled drug delivery [21]. Rooney studied the use of swellable polymers for reflectance-based sensing [23]. His work involved both the use of bulk membranes that were pH-sensitive, and also the use of pH-sensitive polymer microparticles that

were embedded in a non-swellable pH-insensitive hydrogel [20]. He determined that the change in reflection observed in the bulk pH-sensitive membranes was due to water entering the polymer as it swelled in acidic medium.

W. R. Seitz and co-workers also developed a pH sensing device by derivatizing a polystyrene membrane and binding it to a substrate. [24]. As the membrane swells and shrinks, the intensity of the reflected and scattered light changes due to a change in the refractive index of the membrane. The membrane swells and shrinks reversibly without cracking except when subjected to extremely harsh conditions. Two problems encountered with these types of membranes are their ability to delaminate on the surface of the substrate during the swelling and shrinking and also the possibility of cracking when the membranes dry out. One way of reducing the mechanical problem caused by cracking of membranes is by keeping the membranes wet by storing them in a suitable solvent such as water.

The Seitz research group also developed a fiber optic sensor instrument to monitor the change in reflectance at the distal end of two long optical fibers [25, 26]. They used swellable polymer microspheres immobilized in hydrogel membranes and monitored the change in reflectance as the polymer reversibly swelled and shrunk. In this design, a portion of the light that reaches the membrane at the tip of the indicator fiber is reflected back by the fiber-membrane interface while some light is reflected back by the particles embedded in the hydrogel membrane. The light that is reflected back by the fiber-membrane interface is considered unwanted background signal while the light pulse reflected back by the particles embedded in the membrane is the analytical signal required. Figure.1.2 shows a fiber optic sensor

based on polymer swelling. Despite the fact that this instrument has a low signal to noise ratio, it can be used to make multiple measurements in real time from one location.

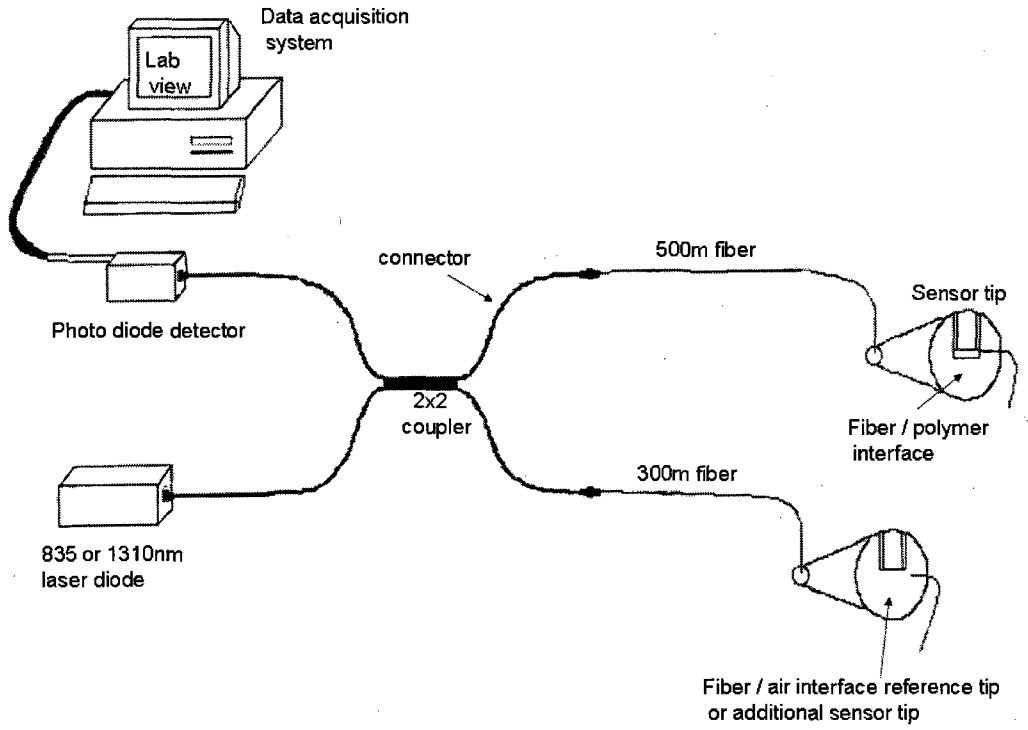

Figure 1.2: *Schematic diagram of fiber optic chemical sensor based on polymer swelling.*

Polymer swelling has also been widely used in molecular recognition processes and drug delivery systems [21]. Wenzhe Fan prepared lightly cross-linked theophylline-templated copolymer microparticles of N-Isopropylacrylamide (NIPAAm) and methacrylic acid (MAA) [27]. The particles were found to selectively bind to theophylline at pH 7, but not to caffeine which has a similar structure to theophylline. At this pH, addition of theophylline at temperatures above the phase

transition temperature of the polymer caused the particles to shrink. In 2005, Nicholas Peppas prepared a hydrophilic polymer imprinted with glucose using poly (hydroxyethylmethacrylate) (poly (HEMA)) in water [28]. In his work, he used poly (ethylene glycol) dimethacrylate with a nominal poly (ethylene glycol) (PEG) length of 600 designated as PEG600DMA as a cross-linker. The glucose-imprinted polymers showed increased recognitive capacity compared to non-imprinted polymer. Peppas also prepared monodisperse nanoparticles by copolymerizing ethylene glycol with N-Isopropyl acrylamide for biomedical applications [29]. The particles were found to respond quickly to temperature changes in the environment mainly due to their small size.

1.4. Sensors Based on Ratiometric Fluorescent Indicators for Metal Ion Determination

Ions such as Zn^{2+}, Ca^{2+}, and Cu^{2+} are important for sustaining life. All of these ions are incorporated into a variety of organics which perform specific metabolic functions in either plants or animals. They also participate in functions as diverse as electron transport, enzymatic catalysis, and neuronal communication [30]. Due to their hazardous effects on both ecosystem and human health, depending on the dose and toxicity, determining their concentrations in the aquatic environment is of tremendous importance. Copper is an integral metal ion in several biological pathways with major functions inside organisms including both electron transfer and oxygen metabolism and transit [31]. Copper is also essential in enzymes that act as free radical scavengers, in hormone biosynthesis, and in biosynthesis of collagen

and elastin, structural components of skin, tendons, and the extracellular matrix [30]. It is able to control the growth of organisms, and because of this, it has been used in some cidal agents such as antibacterial and antiplaque agents in mouthwashes and toothpastes.

Even though copper is an essential trace nutrient to both plants and animals, in sufficient amounts, it can be poisonous and fatal to the organisms and hence there is a need to determine both its concentration and its chemical nature. It is thought to play an important role in pathogenesis of several neurodegenerative diseases, such as Wilson's, Alzheimer's, and in prion protein diseases like Creutzfeld-Jakob's disease [32]. Menke's and Wilson's diseases are due to the body's inability to metabolize copper effectively. Both diseases are the result of deficient copper transport and demonstrate the importance of copper regulation and homeostasis. Although under normal conditions, free copper is believed to be maintained in the range of fentomolar quantities, the total concentration of copper is at the micromolar level. [30, 33-35].

Environmental monitoring of copper as a pollutant is essential because changes in its concentration in the environment could result in adverse biological effects considering that nanomolar Cu^{2+} is toxic to the blue mussel (*Mytilus edulis*) [36, 37]. High copper intake has been implicated in infant liver damage, and concentrations above 31μM can be deleterious according to the World Health Organization (WHO) [38]. Drinking water can be a potential source of copper exposure. It is also important to understand that the chemical nature of copper is important in determining its biological availability both in the environment and food.

Common analytical methods that have been used in determining concentrations of copper ions in either the environment or food include atomic absorption spectrometry (AAS), electrochemical methods, inductively coupled plasma emission spectrometry (ICP-ES), inductively coupled plasma mass spectroscopy (ICP-MS), and also fluorescence spectroscopy using fluorescence indicators. Both AAS and ICP-MS measure total copper concentrations, and have one major disadvantage in that they destroy the sample [39-42]. Fluorescence spectroscopy using fluorescent indicators is considered most suitable because of its high sensitivity and lower detection limit. The method is able to detect copper (II) ions in the nanomolar range.

Fluorescent indicators have been used for years especially for detection and quantitative analysis of metal ions and also in determination of complex stability constants. Most of these indicators are metallofluorescent indicators containing aromatic molecules which bind to metal ions in solution with some degree of affinity and stoichiometry introducing a change in fluorescence intensity. These types of fluorescent indicators have both selectivity and sensitivity problems and are therefore less useful for quantification of the metal ions. Also their application in biological environments is limited by the narrow range of suitable fluorophores available since most fluorophores are hydrophobic and cannot be used in aqueous media.

An advantage of the indicators is that reliable complex stability constants can be obtained, because the concentrations of free ligand and the complex can be accurately measured by spectroscopy without disturbing the equilibrium [43]. In this

thesis, a ratiometric fluorescent indicator using swellable polymer microparticles was developed. One of the advantages of the indicator is that the fluorophores are polymerized in hydrophobic media and can be used in hydrophilic media. Early results with fluorescent indicators for Cu^{2+} ions in tissues and cells presented difficulty in relating fluorescent intensity to the analyte concentration. Calibrating such a system was intractable as variations in fluorophore concentration, cell thickness, excitation intensity, and inner filter effects could all be misconstrued as changes in analyte concentration.

Another type of indicator involves fluorescent molecules covalently bonded to non-fluorescent ligands that bind to the metal ions with some degree of selectivity. In these indicators, detectable response is modulated by photoinduced electron transfer (PET) effects from the fluorophore to the resulting metal ion complex producing changes in fluorescence emission intensity upon binding of the metal ion to the ligand. This makes the method useful for direct determination of soluble heavy metal ions including, Hg^{2+}, Cu^{2+}, Ni^{2+}, and Cd^{2+}.

In 1996, the research group of Prof. Richard Thompson at the University of Maryland School of Medicine developed a fiber optic biosensor for Cu^{2+} and Co^{2+} ions based on fluorescence energy transfer with an enzyme transducer. They used an enzyme carbonic anhydrase labeled at a suitable site with a fluorophore, and a colored but non-fluorescent inhibitor. They observed that the metal ion binding to the active site permits binding of the colored inhibitor to the enzyme resulting in Förster resonance energy transfer (FRET) from the fluorescent label to the inhibitor and a reduction of both fluorescence intensity and lifetime [44].

In 2003, Alexander Hopt and co-workers developed a copper sensor based on fluorescence quenching caused by binding of Cu^{2+} with a fluorescent ligand [45]. They used tetrakis-(4-sulfophenyl) porphine (TSPP) with an emission wavelength of 645nm as the fluorescent ligand. They demonstrated that TSPP binds selectively with copper and not with other divalent metal ions. In 2008, Rahini Yasmeen and co-workers from Indiana University Purdue University used red fluorescent protein, DsRed, to selectively analyze Cu^{2+} ions by relating fluorescence quenching of DsRed with the concentration of Cu^{2+} ions. Their results indicate that Cu^{2+} ion binding by DsRed showed fluorescence quenching reversibility with addition of a metal ion chelator such as EDTA [46]. They also performed studies to identify possible amino acid residues involved in the binding of the Cu^{2+} ions to the DsRed proteins. The fluorescence response of these indicators to ion binding results can also arise from fluorescence quenching by heavy metal ions.

An improved version of fluorescent metal ion indicator is the ratiometric fluorescent indicator. In this type of indicators, the ratio of fluorescence intensities at two different emission wavelengths is related to the analyte concentration. Ratiometric fluorescent indicators are increasingly being used in many areas of biology. They are used for quantitative determination of intracellular free calcium both *in vitro* and *in vivo*, membrane potentials, pH, and other important physical variables [47]. In these sensors, either one fluorophore with two emission wavelengths of reasonable resolution, or two fluorophores with different excitation and emission wavelengths are used and their fluorescence intensities are measured. In these two sensors, FRET is the mechanism under which they function. For

ratiometric fluorescence indicators involving two fluorophores, one fluorophore (donor) is excited. Energy transfer to the other fluorophore (acceptor) is observed as quenching and enhancement of the fluorescence intensities of the donor and acceptor respectively.

The FRET efficiency (*E*) increases with a decrease of distance (r) between the two fluorophores, and also with an increase in overlap region between the emission and excitation spectra of the donor and the acceptor respectively as discussed in a later chapter of this thesis. In the ratiometric fluorescence indicators, the ratio of fluorescence intensities of the donor and acceptor are then determined as a function of changes in analyte concentration or pH, which helps in eliminating the illumination variability, photobleaching effect of a fluctuating excitation source, and other artifacts associated with fluorescence measurements. This is because the two fluorescence intensities are measured simultaneously, and hence photon path length and volume factors are eliminated from the ratio.

In ratiometric fluorescent indicators, functional changes in fluorescent yields are often small, the signal to noise ratio is on the order of unity or less. A small change in either the denominator or numerator leads to a large change in the ratiometric signal. Because fluorescence measurements are very sensitive to small changes in analyte concentration, ratiometric fluorescence indicators have an advantage over the normal fluorescence measurements because of its increased sensitivity. The Cu^{2+} ion indicators have high sensitivity, low detection limit, and high selectivity due to strong binding affinity between Cu^{2+} and many common ligands. In this thesis, a ratiometric fluorescence sensor for Cu^{2+} ions was designed. The

selectivity of the sensor was tested using other transition metal ions such as Zn^{2+}, Pb^{2+}, and Ni^{2+}.

1.5. Glucose Sensor Based on Swellable Molecularly Imprinted Polymers

Glucose is an essential carbohydrate in the human body which is used by the living cells as a source of energy and metabolic intermediate. High blood sugar levels (hyperglycemia) in the human body are caused by a low insulin level resulting in diabetes, a syndrome of disordered metabolism. It is because of this danger that determination of glucose in human blood is of great importance. Our bodies desire blood glucose to be maintained between 0.70mg/mL and 1.10mg/mL.

Glucose exists either in the cyclic or open chain form. Cyclic forms of glucose are the result of formation of a covalent bond between the aldehyde carbon with the hydroxyl group forming a six membered cyclic hemiacetal. In the solid phase, the glucose assumes a cyclic form called glucopyranose while in solution, it can exist in an open-chain (acyclic) form and a ring (cyclic) form in equilibrium. Since carbohydrates contain alcohol and aldehyde or ketone functional groups, the open-chain form is easily converted into the cyclic structure. At pH 7, the cyclic form is the dominant form and exists to a level of about 0.02%, while in acidic medium, the open-chain is the dominant. The equilibrium constant *K* between the cyclic and the open-chain form at pH 7 is represented by the equation:

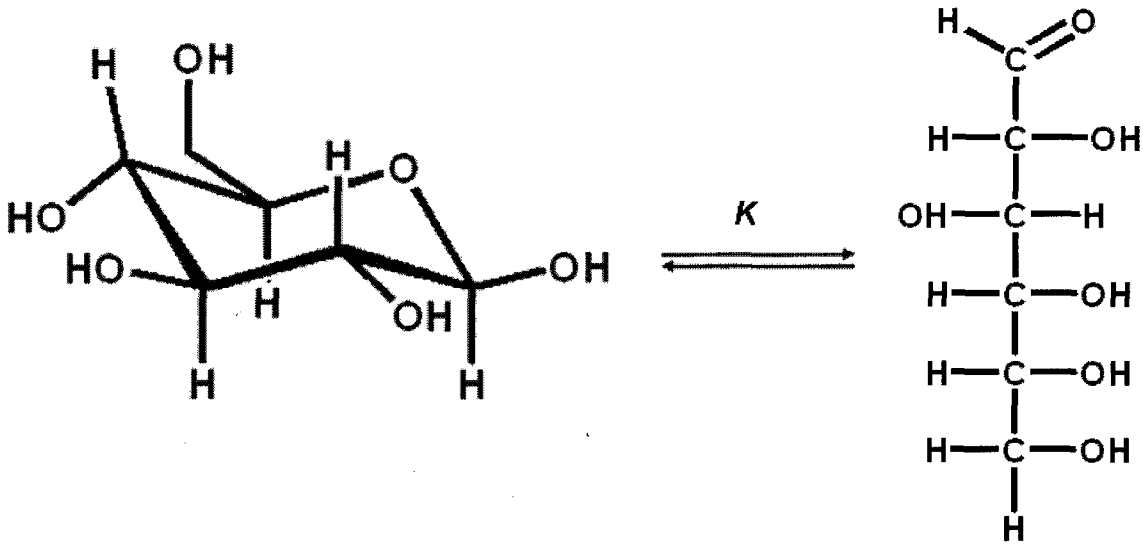

Figure 1.3: An equilibrium representation between cyclic form of β-D-glucose (β-D-glucopyranose) and straight chain form in aqueous medium.

Detection of glucose in human samples, especially blood, has presented a great challenge due to the complex nature of the sample matrix. Because direct absorbance measurements cannot be done on colored samples like blood, extensive sample preparation is required before any glucose analysis is performed on such samples. Common methods of glucose detection involve electrochemical, chemiluminescence, and electrochemiluminescence. Even though the electrochemical method is the most commonly used method because of its inherent high sensitivity and simplicity of the needed instrumentation, its major shortfall is sample degradation.

In 2004, Yan Du and co-workers from Jilin University, Changchun, China developed an electrochemical detector on a hybrid chip for determination of glucose in human plasma. They used a poly (dimethylsiloxane) (PDMS) layer containing separation, injection channels, and a copper microelectrode fabricated by selective electrode deposition [48]. One of the objectives of this thesis is to develop a glucose sensor based on molecularly imprinted polymer that responds to glucose and modify it

to monitor glucose levels in human blood. This is clinically relevant because of its application in monitoring glucose levels in diabetes patients especially patients with type II diabetes.

1.6. Some Important Features of Chemical Sensors

All the various types of chemical sensors discussed above need to address the following key features; selectivity, sensitivity, reliability, accuracy, dynamic response range, limit of detection, response time, and lifetime.

1.6.1 Selectivity

The selectivity of a chemical sensor is the most important parameter. It is defined as the ability of the sensor to respond to the target analyte in a sample containing other interfering species. A sensor designed for a particular analyte (ion or molecule) should only respond to that particular analyte in a sample containing a mixture of that analyte and other substances. It is expressed in terms of a dimension that compares the concentration of the corresponding interfering substance with that of the analyte concentration producing the same signal [49]. This factor is the ratio of the sensitivity of the sensor towards the interfering substance to its sensitivity towards the target analyte.

1.6.2. Limit of Detection for Analyte

Limit of detection is the minimum amount of analyte that an instrument is able to detect. Analyte concentrations less than the detection limit cannot be detected by the instrument. For an analyte to be detected, it should be able to produce a signal that is greater than the noise level of the instrument. For analytical chemistry, this is possible when the signal produced by the analyte is at least three times the general noise level of the instrument. At very low but detectable analyte concentrations, no quantitative analysis of the sample can be performed and for any quantitative analysis to be performed, the signal must be at least ten times the noise level.

1.6.3. Sensitivity

Sensitivity is how large the signal of a sensor is for a given concentration of target analyte. An instrument that is very sensitive to the target analyte produces a large signal for a small concentration of the target analyte. Sensitivity corresponds to the slope of the calibration curve of signal vs. concentration. The sensitivity of an instrument may depend on other parameters such as sample matrix, temperature, pressure and, humidity. It is, therefore, important and necessary to take precautionary measures to ensure that all of these parameters are kept constant both during calibration of the instrument and during sample analysis.

1.6.4. Stability

Stability is the ability of the sensor to produce a consistent output when a constant input is applied. A stable sensor should be able to resist any signal variations due to external factors such as environmental effects. Stability of a sensor can also depend on the sensor's aging conditions. Some other factors that may contribute to the sensor losing stability are electrical and mechanical faults within the functioning sections of the sensor.

1.6.5. Response Time

The response time of a sensor is the time the sensor takes to produce a signal after interacting with the target analyte. In analytical chemistry, response time is defined by the manufacturer as the time interval over which a signal reaches a particular percentage of the expected final value. This expected percentage is not constant and varies from different manufacturers. For most manufacturers, the percentage is between 90-99% [49]. Typical response times for chemical sensors are in the range of seconds but some biosensors have response times in the range of minutes. The response time of the sensor may be affected by factors such as; sample matrix, surface roughness of the sensor and also dead volume of the measuring cell. Because the interaction between the target analyte and the recognition phase of the sensor is what results in a signal, the response time depends on the rate of this interaction. The response time of a sensor is therefore dependent on the kinetics of the interaction between the recognition phase and the target analyte, which in many cases is a chemical reaction.

1.6.6. Dynamic Response Range

Dynamic response range is defined as the concentration range over which a calibration curve can be described by a single mathematical equation. For example, Beer-Lambert's law is the mathematical equation relating the absorbance of a substance to its concentration in the sample. In this case the dynamic response range is the range of concentrations of the absorbing substance in which the Beer-Lambert's law is obeyed.

At very low analyte concentrations, the measurement range is limited by the detection limit of the sensor and experiences deviation from Beer-Lambert's law. Also at very high analyte concentrations, the measurement range is limited by saturation effects and again a deviation from Beer-Lambert's law is experienced. A good sensor is one with a high dynamic response range although such sensors are not commonly found.

1.7. Polymers used in Sensor Applications

Most sensor applications that use polymeric materials use copolymers that are functionalized with groups that interact with the target analyte. The polymeric material is designed to interact with the analyte with both high selectivity and sensitivity. In this thesis, poly (N-Isopropylscrylamide) poly (NIPAAm) was used as the swellable polymer component. The NIPAAm was copolymerized with the fluorophore pairs; 2-naphthylmethacrylate and 9-vinylanthracene, methacryloxethyl thiocarbonyl rhodamine-B and fluorescein o-acrylate for fluorescence ratiometric measurements resulting from Förster resonance energy transfer (FRET) between the fluorophore pairs.

The polymer was also copolymerized with ligands that interact with the target analytes like copper (II) ions. The ligands used are listed in later chapters of this thesis.

1.8. Objectives

The first goal of my research was to develop improved ratiometric fluorescent indicators for sensing transition metal ions, particularly copper (II) ions. To achieve this, swellable polymer microparticles which produce large FRET efficiency with respect to small changes in analyte concentrations were used. The large FRET efficiency is a clear indication of significant swelling and shrinking of the polymer microparticles with respect to small changes in the analyte concentration. The first part of this research focused mainly on the preparation of fluorescently labeled polymer microparticles. In the research, N-Isopropylacrylamide (NIPAAm) was used as the principal monomer and copolymerized with both polymerizable ligands and fluorescent monomers listed in Chapter 3 of this thesis. The microparticles were synthesized by dispersion polymerization.

The second goal was to investigate the effect of polymerization of the ligands on their binding affinity with copper (II) ions, and to determine the formation constants of their complexes with copper (II) ions. To achieve this, suspensions of polymer microparticles containing known amounts of ligands were subjected to potentiometric titrations with standard solutions of copper (II) ions and the titration curves were plotted. Both the potentiometric titration and calibration curves were used to determine the formation constants of the complex formed between the ligands and the copper (II) ions.

The third goal of the research was to develop a chemical sensor based on swellable polymer microparticles for glucose (β-D-glucopyranose) sensing. This project involves synthesis of glucose imprinted polymer microparticles, using NIPAAm, β-D-glucopyranose, and acrylamide as the principal monomer, template molecule, and functional monomer, respectively. The polymer microparticles were immobilized in poly (vinyl alcohol) (PVA) hydrogel membranes. Their swelling-deswelling property with respect to changes in β-D-glucopyranose concentrations were studied using turbidity measurements. The selectivity of the sensor was also determined using galactose (β-D-galactopyranose).

CHAPTER 2

THEORY

2.1 Polymer

A polymer means a long molecule of repeated subunits. It is derived from Greek words *poly* and *mer* meaning "many" and "parts" respectively [50, 51]. Polymers are the result of linking small molecules called "monomers" by polymerization. Polymers vary in their molecular weights depending on the number of subunits linked in the polymer chain. If only a few subunits (less than ten) are linked together, a low molecular weight polymer called an "oligomer" is produced [51]. "Macromolecule" is another term that is used synonymously with polymer [52].

Polymers exist either as natural or artificial polymers. Some examples of natural polymers are RNA, DNA, proteins and cellulose. Artificial polymers include poly (ethylene), nylon, and poly (vinylchloride). Artificial polymers that are employed in chemical sensing will be discussed in greater detail in this dissertation.

On the basis of the structure of the repeated unit, polymers can be classified as either addition or condensation polymer. Addition polymerization involves molecules with double bonds that polymerize by addition of monomer units to growing chains. The polymer formed consists of only carbon atoms in the main chain [53]. The molecular weight of an addition polymer equals the sum of the molecular weights of its monomers since there are no by-products resulting from the polymerization process. Figure 2.1 shows the addition polymerization of styrene monomer.

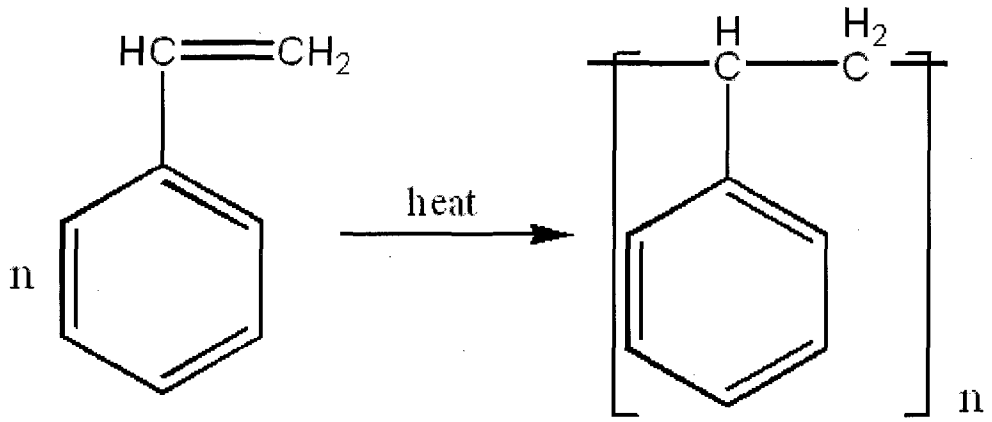

Figure 2.1: Addition polymerization of styrene

Condensation polymerization involves a reaction between molecules with multiple functionality in which small molecules, usually water or hydrogen halide is eliminated to form the polymeric chain. In this polymerization process, the molecular weight of the resulting polymer is less than the sum of molecular weights of the original monomer units and the repeating units contains fewer atoms than the sum of the atoms in the monomers. Figure 2.2 represents the condensation polymerization process.

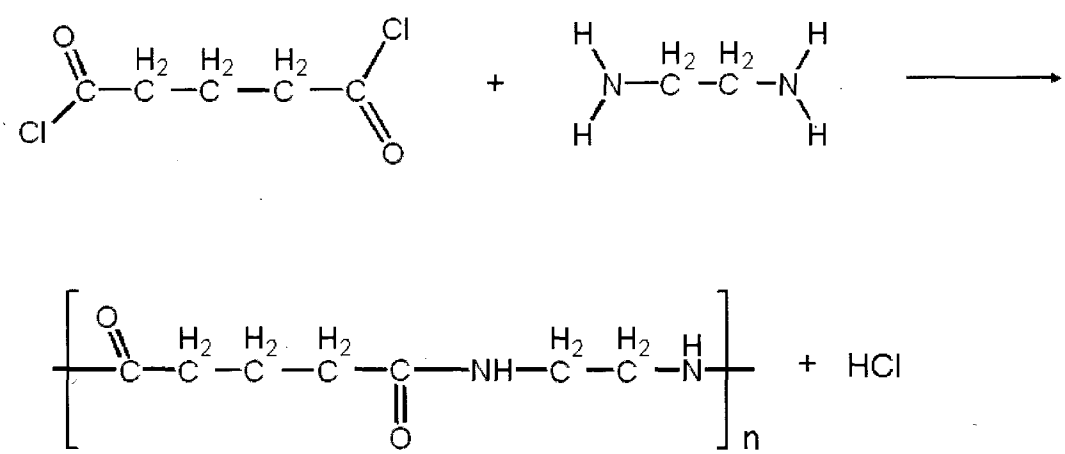

Figure 2.2: Condensation polymerization

Another classification of polymers is in terms of the types of monomers used in the polymerization process. In this type of classification, polymers are classified into either homopolymers or copolymers. Homopolymers are formed by polymerizing molecules of one monomer while copolymers are formed from mixture of monomers. There are four types of copolymers: random, alternating, graft, and block, which correspond to four possible different arrangements of monomer units within the polymer structure. These different arrangements are shown in figure 2.3 where A and B represents the two different monomer units.

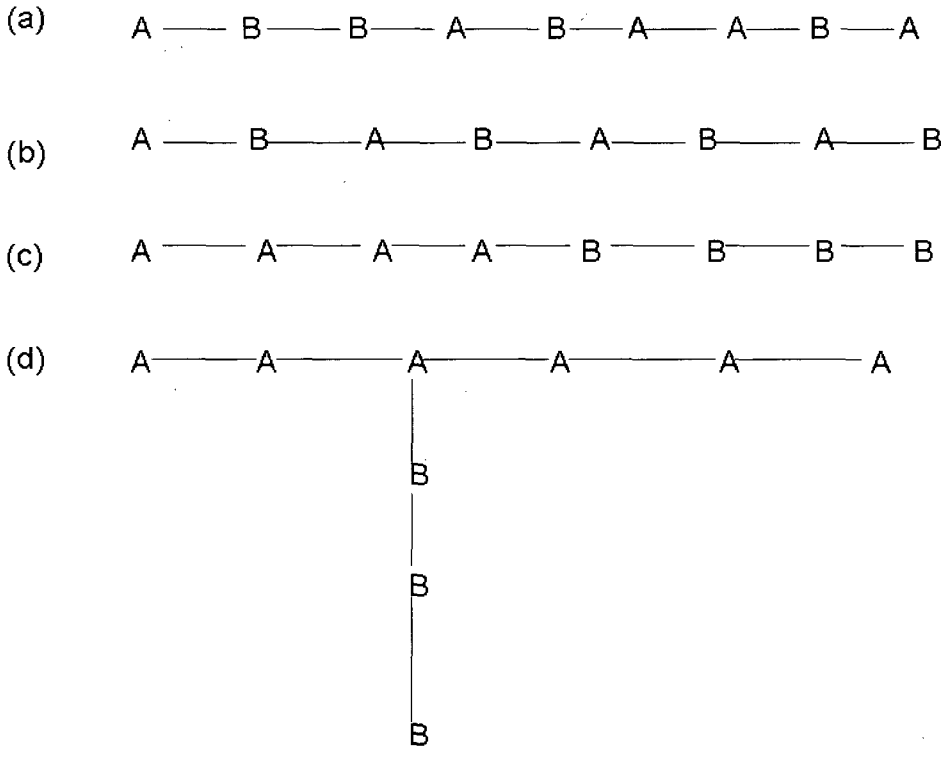

Figure 2.3: A representation of copolymer types: (a) random, (b) alternating, (c) block, and (d) Graft formed from monomers A and B.

In the polymer, the repeating or monomeric units have two or more available binding sites and are linked together by covalent bonds forming either linear, branched, or network polymers. Linear polymers are polymers in which the molecules form long chains without branches or cross-linked structures. The molecular chains of a linear polymer can be intertwined, but the forces holding the molecules together are physical rather than chemical and thus can be weakened by heat (thermoplastic). Branched polymers have side chains extending from the main polymer backbone. Network polymers are formed from monomer molecules with multiple functionalities and are chemically able to bind with their neighboring units using more than two binding sites. Crosslinked polymers have high mechanical stability and are therefore rigid in nature as compared to uncrosslinked polymers, however, the rigidity level of such polymers depend on the percentage of cross-linkers used in the polymerization process. Figure 2.4 shows linear, branched, and network polymers.

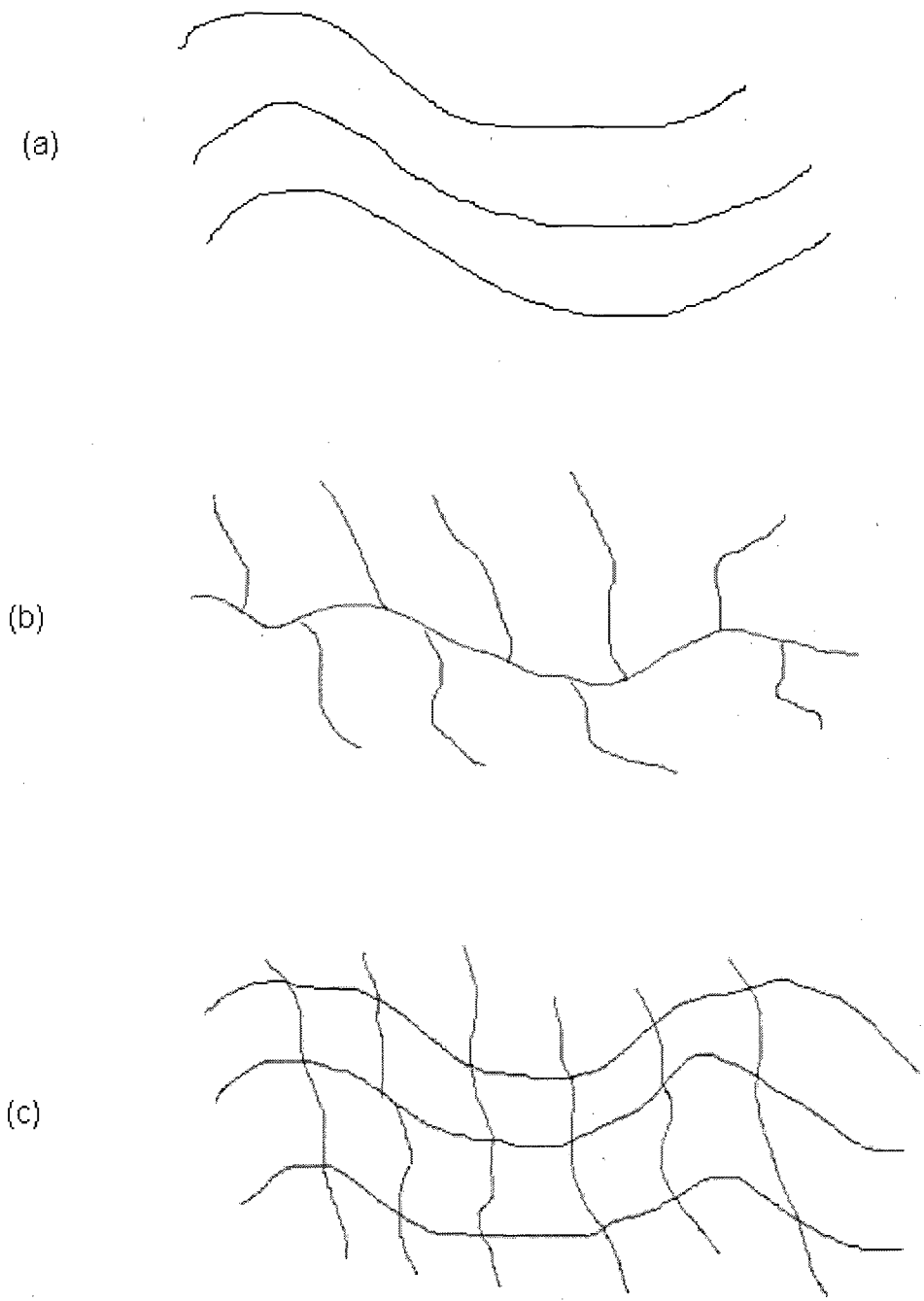

Figure 2.4: (a) Linear, (b) branched, and (c) network polymers

2.2 Free Radical Polymerization

Free radical polymerization is an addition polymerization process involving linkage of mostly vinyl monomers to form long chain polymer molecules. It is the most common type of polymerization. There are two forms of free radical polymerization; homogeneous and heterogeneous [54]. In homogeneous free radical polymerization, the monomer(s), initiator and the resulting polymer are all soluble in the solvent used. Examples of homogeneous polymerization are bulk and solution polymerization. Bulk polymerization is associated with the following problems: (a) can be potentially explosive due to poor heat transfer as the viscosity of the mixture increases during the polymerization process, (b) difficulty in removal of unreacted monomers and initiator, (c) difficulty in controlling the arrangement of the monomer units within the polymer chains.

The problems associated with bulk polymerization are easily avoided by solution polymerization where the solvent decreases the viscosity of the system and removes excess heat from the reaction chamber. But the difficulty of removing solvent molecules presents another problem.

In free radical polymerization, the reaction proceeds via free radicals that are generated by the initiator. The free radicals are extremely reactive and react with monomers containing double bonds forming active centers which react further with more monomer molecules during the chain propagation step of the polymerization process. The process requires that radicals generated by breaking up of the initiator molecules should be stable enough and stay for a long time in order for them to react with the monomer molecules and form an active center [54]. Vinyl monomers

have double bonds that add up in the polymer chains as the polymerization progresses. The figure below represents a free radical attack on the double bond of an ethane molecule to form an active center.

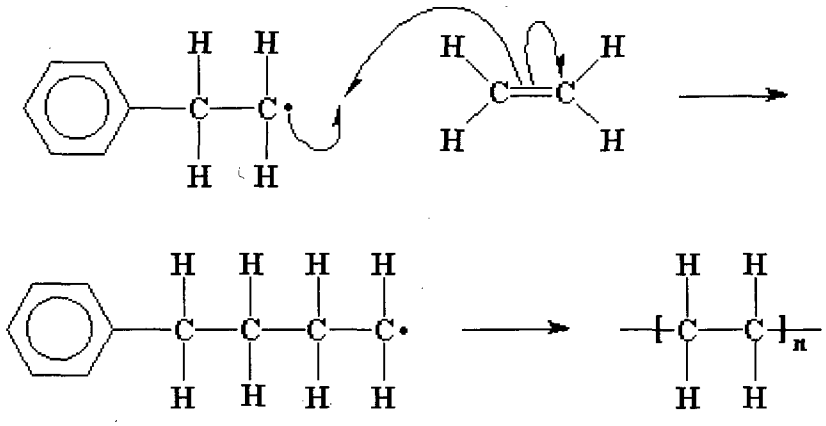

Figure 2.5: Free radical polymerization process.
Figure source: http;//pslc.ws/macrog/radical.htm.

The polymerization process is governed by thermodynamic factors such as the *Gibbs free energy* (ΔG), *enthalpy* (ΔH), and *entropy* (ΔS). Thermodynamics of polymerization determines the position of equilibrium between the polymers and the monomer(s). For most monomers with π-electron systems e.g. olefins, the polymerization process is favored because of the exothermic nature of converting the π bonds into σ bonds. Polymerization is thermodynamically favored if $\Delta G < 0$, and $\Delta H < 0$. Since polymerization is an association reaction involving monomers associating to produce the polymers, $\Delta S < 0$ for almost all polymerization reactions. This results in a large loss of the total number of rotational and translational degrees of freedom in the system as the monomers associate, regardless of the mechanisms

involved in the reaction. At equilibrium, the standard Gibbs free energy of polymerization is given by equation below;

$$\Delta G_p^{\theta} = -RTLn\ K_p \qquad (1)$$

Where ΔG_p^{θ} is the standard Gibbs free energy for propagation and K_p is the equilibrium constant. For the reaction represented by Figure 2.5, K_p is given by,

$K_p =$ 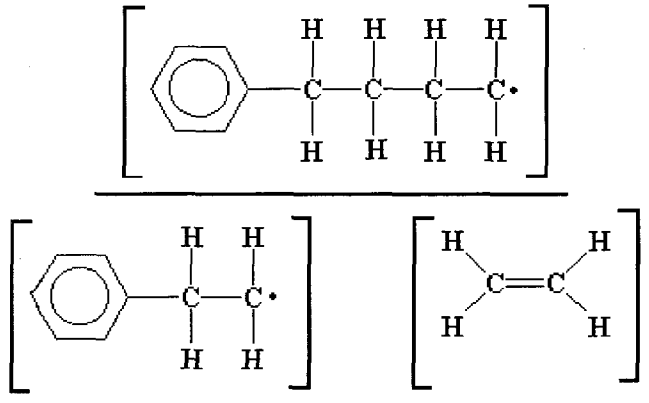

The free radical polymerization process is divided into three distinct stages: initiation, propagation, and termination.

2.2.1 Initiation

Initiation of free radical polymerization involves two steps. The first step is the formation of free radicals by either thermal or photolytic decomposition of an initiator and the second is the attack on the monomer molecules by the free radicals, producing other radicals. There are two ways in which the free radicals can be generated by the initiator. One is homolytic scission (homolysis) and the other is single electron transfer. Homolysis is the breakage of a single bond within the initiator to form radicals. The radical then reacts with the monomer by replacing the double bond in the monomer with a single bond forming a new bond and a new

radical. Commonly used initiators contain the azo (-N=N-), the peroxide (-O-O-), and the persulfate groups. Examples of initiators with azo, peroxide, and persulfate groups are; 2, 2'-azo-bis-isobutyronitrile (AIBN), benzoyl peroxide (BPO), and potassium persulfate (KPS) respectively. In this work, AIBN and KPS were used as initiators because of their ability to initiate polymerization in acetonitrile, and water, respectively. Figure 2.6 shows the dissociation of the initiators to form radicals.

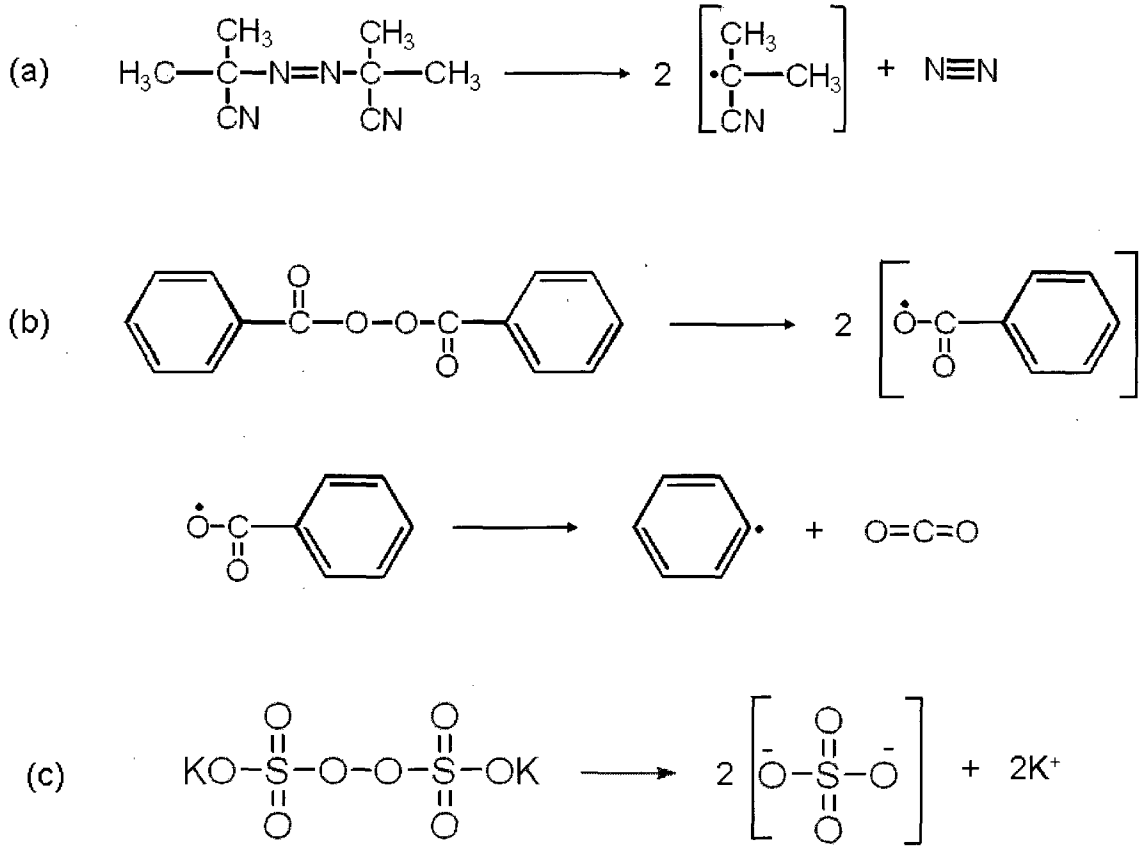

Figure 2.6: Dissociation of initiators, (a) AIBN, (b) BPO, (c) KPS
Figure source: http;//pslc.ws/macrog/radical.htm.

The persulfate initiators e.g. ammonium and potassium persulfates are ionic compounds which dissolve in polar solvents and are commonly used in polymerization processes in polar solvents. The azo and the peroxide based initiators are preferred because they undergo thermolysis at relatively low

temperature (≈50 ° C). This is important in free radical polymerization because it is advantageous to polymerize at lower temperatures. This is because polymerizing at high temperatures produces many free radicals which terminates the polymerization. The choice of initiator to be employed in any free radical polymerization depends on the monomers and the reaction medium.

2.2.2 Propagation

Propagation is the stage in which the polymer grows by addition of monomer molecules to the radical end of the growing polymer chain. It involves free radical attack on the double bond of the monomer molecules. There are two possible propagation linkages: head-to-head, and head-to-tail. Addition polymerization typically prefers head-to-tail linkage. Propagation proceeds until termination by either combination or disproportionation occurs. Most polymerization processes are characterized by an exothermic propagation reaction step. The equation below shows the propagation process of polyethylene.

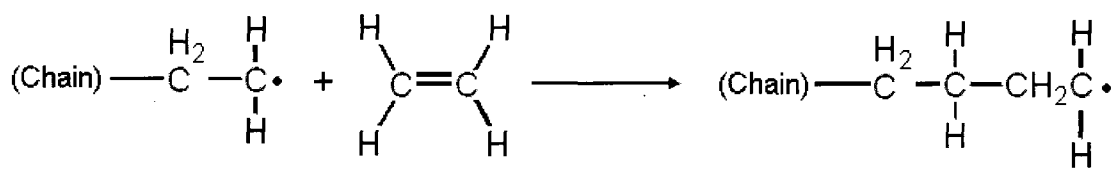

Figure 2.7: Propagation process of polyethylene
Figure source: http;//pslc.ws/macrog/radical.htm.

2.2.3 Termination

Termination involves a reaction between two radicals to form non radicals. The termination process can take place by either combination or disproportionation. Combination takes place when two oligomer radicals react while disproportionation

occurs when a proton is transferred within the ends of the polymer chain radicals producing both saturated and unsaturated compounds. Figure 2.8 shows termination by both combination and disproportionation of poly (ethylene)

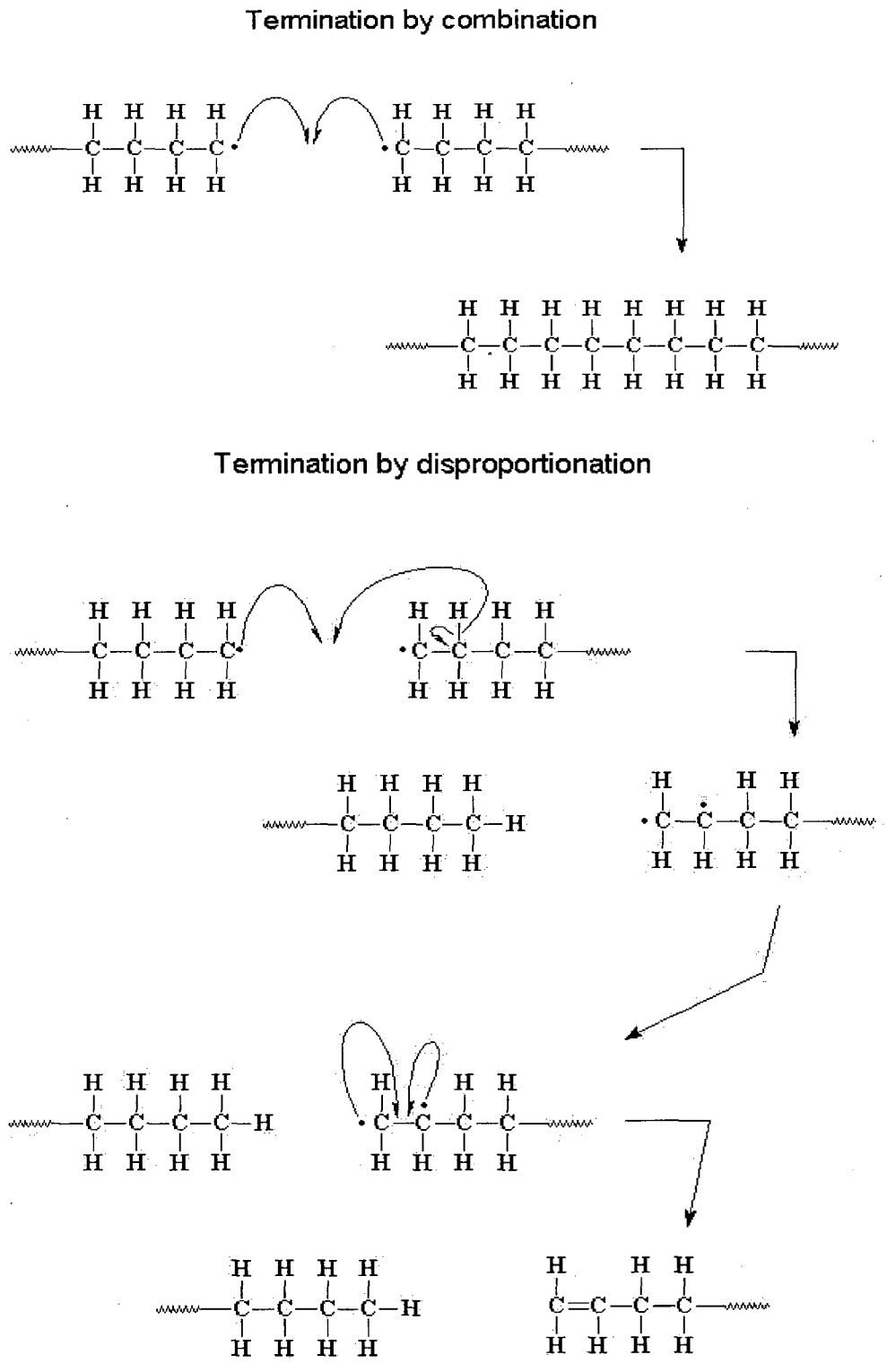

Figure 2.8: Termination process by combination and disproportionation. Figure source: http;//pslc.ws/macrog/radical.htm.

2.2.4. Free Radical Copolymerization

Copolymers are formed by simultaneous polymerization of two or more monomers. The reaction kinetics for the copolymerization processes is more complicated than that of homopolymerization due to the inclusion of other monomers. The copolymer composition and the sequence distribution of the different repeat units in the copolymer molecules formed are affected by the differences in monomer reactivity and their concentrations [55]. During the copolymerization process, the most reactive monomer is incorporated preferentially into the copolymer chains and high molecular mass molecules are formed at low overall conversions of the co-monomers. This effect can result in the formation of copolymer molecules having compositions different form the composition of the original monomer mixture [55- 59].

In the *terminal model,* which is the simplest kinetic model for free-radical copolymerization, the principal assumption is that the reactivity of an active center depends only upon the terminal monomer unit in which it is located. The copolymerization kinetic model also assumes that the amount of monomer consumed in the polymerization reaction steps other than propagation is negligible resulting in formation of copolymer molecules with high molecular mass. A terminal model representing the free radical copolymerization reactions of monomers A and B is given in the equations below in which only two types of active centers are considered. The active centers are; ~~~~~~~~~~ A• and ~~~~~~~~~~B•

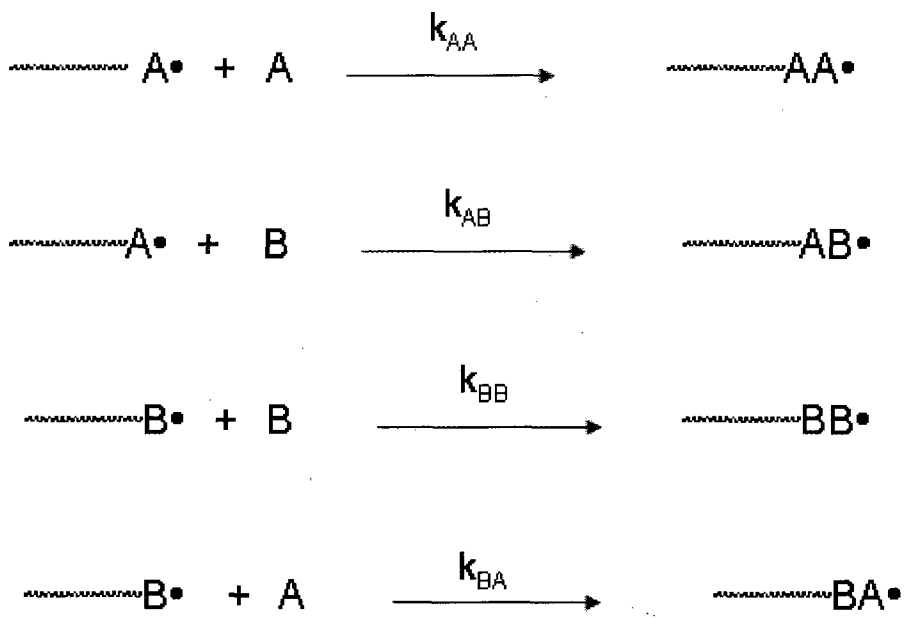

Source: Emulsion Polymerization and Emulsion Polymers, John Wiley and Sons, New York, **1997**.

Where: k_{AA} and k_{BB} are the rate coefficients for homopropagation

k_{AB} and k_{BA} are the rate coefficients for the cross-propagation reactions.

The copolymer formed can either be alternating, or block depending on both the reactivities and concentrations of the two monomers. The difference in monomer reactivities causes a drift in copolymer composition with the more reactive monomer being preferentially consumed. In batch copolymerization reactions, the total quantity of each monomer is added at the beginning of the reaction process and there is no control over this drift in copolymer composition. Therefore batch copolymerization sometimes produces broad composition distributions.

In the reaction equations above, the rate at which monomer A is being consumed during the polymerization process is given by the equation;

$$\frac{-d[A]}{dt} = k_{AA}[A^{\bullet}][A] + k_{BA}[B^{\bullet}][A] \qquad (2)$$

where $[A^{\bullet}]$ and $[B^{\bullet}]$ are the total concentrations of propagating chains with terminals A-type and B-type active centers respectively.

Also the rate at which monomer B is being consumed is given by the equation;

$$\frac{-d[B]}{dt} = k_{BB}[B^{\bullet}][B] + k_{AB}[A^{\bullet}][B] \qquad (3)$$

At any time during the polymerization reaction, the ratio of the amounts of monomers A and B being incorporated into the polymer chains is given by dividing equation 1 by equation 2.

$$\frac{d[A]}{d[B]} = \left[\frac{[A]}{[B]} \; \frac{k_{AA}\{[A^{\bullet}]/[B]\} + k_{BA}}{k_{BB} + k_{AB}\{[A^{\bullet}]/[B^{\bullet}]\}}\right] \qquad (4)$$

The reactivity of a monomer depends upon the ability of its substituent groups to stabilize the corresponding polymer radical. More reactive monomers have substituent groups which stabilize the polymer radical by delocalization of unpaired electrons (resonance). Therefore highly reactive monomers produce low reactive polymer radicals and vise versa. The additive nature of resonance effects of substituent vinyl monomers decrease their reactivity and produce very reactive secondary radicals with low stability. The 1, 2–disubstituted monomers

($CHR_1=CHR_2$) have low reactivity due to steric hindrance of the propagation step by the 2-substituent in the monomer.

2.3 Dispersion Polymerization

Dispersion polymerization is a technique for preparing polymer particles with diameters in the range of 1-15 μm. The method was first described by Osmond et.al. and has been reviewed by Barrett up to 1975 [57]. It is precipitation polymerization modified by inclusion of a stabilizer that prevents coagulation of the growing particles. In this method, the continuous phase is chosen to be a solvent for the monomer and a non-solvent for the resultant polymer. The monomer(s), initiator, and steric stabilizer are dissolved in a solvent, resulting in a homogeneous mixture, and then polymerized. As polymerization proceeds, the polymer particles precipitate from the solvent. The components of dispersion polymerization include; monomers, initiators, stabilizers and also solvents.

2.3.1. Monomers

Monomers are the molecules combining together to form the polymer during the polymerization process. A wide range of monomers has been used in dispersion polymerization. These monomers are either oil-soluble or water-soluble. Monomers commonly used are; styrene, vinyl chloride, methylmethacrylate, vinyl acetate, acrylic acid, acrylamide, and acrylonitrile [60]. Dispersion polymerization can be done by polymerizing either one type of monomer forming a homopolymer or more than one group of monomer forming a copolymer.

2.3.2. Initiators

An important requirement for an initiator in a dispersion polymerization is that it should be soluble in the dispersion medium. The initiator should also be able to produce free radicals in the solvent that are capable of initiating the polymerization process. The production of free radicals by the initiators depends on the temperature at which the polymerization process is carried out. The initiator must be used in very little quantity to avoid excess production of free radicals which may interfere with the polymerization process. The thermal dissociation of initiators has been discussed in section 2.2.1.

2.3.3. Solvent

A very important aspect of dispersion polymerization is the choice of the dispersion medium. A suitable solvent for dispersion polymerization is one that dissolves the monomers, initiators, and the stabilizers but does not dissolve the resulting polymer. The type of stabilizer and initiator used for polymerization depends on the solvent used. Some stabilizers do not offer good stabilizing ability in some solvents and some initiators do not dissociate in some solvents. The composition of the solvent also affects the size of polymer particles produced.

Both polar and non-polar solvents can be used for dispersion polymerization. Earlier work on dispersion polymerization involved the use of non-polar solvents but recent studies have shown the use of polar solvents such as water, methanol, and ethanol [61]. Very few cases of dispersion polymerization have used water as the sole solvent. There are many cases where water is added to

alcohol in order to fine-tune the solubility and to manipulate the particle size and size distribution of the product. In this work, acetonitrile, water, and sometimes a mixed solvent of acetonitrile and water were used as the dispersion medium.

2.3.4. Stabilizers

Stabilizers are important in both particle formation and production of stable and non-coagulated dispersed polymer particles. Stabilizers prevent the particles from growing to uncontrolled macroscopic size. They stabilize the polymer colloids by developing sufficient electrostatic and or steric repulsion to resist aggregation.

Steric stabilizers are preferred because the usual electrostatic stabilizers (used in emulsion and suspension polymerizations) are not suitable for dispersion polymerization due to the low dielectric constant of the solvents used. Most steric stabilizers are amphipathic in nature i.e. contain both an "anchor" segment, with an affinity for the polymer particles and a solvent soluble segment. Stabilizers can be classified into three groups; homopolymers, block and graft copolymers, and macromonomers. The first two groups of stabilizers already have the two chemically distinct segments and are common and effective stabilizers [62]. The macromonomers can copolymerize with the principle monomer forming a graft copolymer.

2.4. Steric Stabilization Mechanism in Dispersion Polymerization

When two particles with adsorbed layers approach each other at a distance of less than twice the thickness of the adsorbed layer, interaction of the layers takes place. Polymer particles in a dispersion medium always show Brownian motion and are continuously colliding with each other. The stability of the particles is determined by the interaction between the particles during such collisions. These interactions are both attractive and repulsive [62].

When attraction dominates, the particles tend to adhere to each other and the entire dispersion coalesces. When repulsion dominates, the system is stable and the particles remain dispersed in the solvent. Van der Waals forces are the primary source of attraction between the polymer particles except for the charged particles. Colloidal dispersions are said to be stable only when a sufficiently strong repulsive force counteracts the van der Waals attraction. The degree of stabilization depends on the energy change occurring upon the interaction of the adsorbed layers and can be determined by the Gibbs free energy equation;

$$\Delta G = \Delta H - T\Delta S \qquad (5)$$

G = Gibbs free energy involved in the interaction

H = Enthalpy of interaction

S = Entropy of the interacting particles

T = Temperature of the system

If ΔG is negative, then the attractive force between the particles is greater than the repulsive force and the polymer particles coagulate. A positive ΔG means a greater stabilization effect and the particles disperse in the medium.

Steric stabilization, which occurs due to adsorbed layers on the dispersed or colloidal polymer particles, is achieved by attaching the grafted or chemisorbed copolymer macromolecules to the surface of the particles. For polymerization in a non-aqueous medium, steric stabilization is preferred to electrostatic or depletion stabilization because it is effective in both aqueous and non-aqueous media [62]. Figure 2.9 shows steric stabilization of colloidal polymer particles.

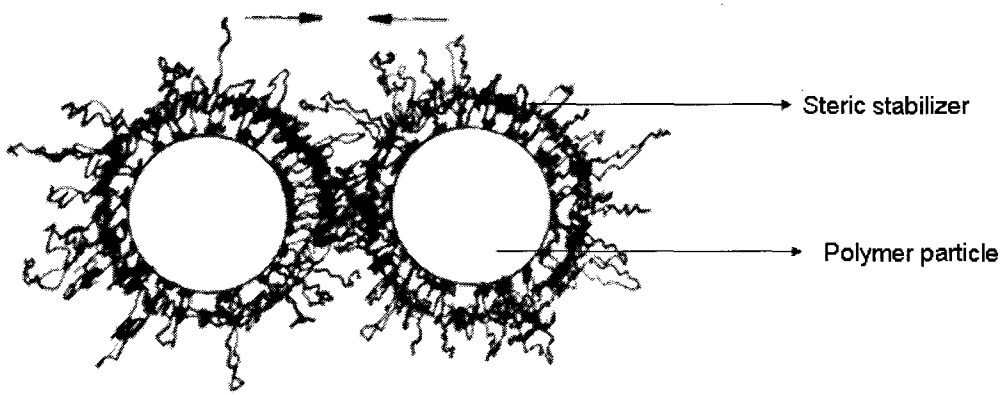

Figure 2.9: Steric stabilization
Figure source: http://www.matseng.ohiostate.edu/ims/LR_ stericstabilizationpdf.

2.5. Mechanism of Particle Formation in Dispersion Polymerization

The first step in a dispersion polymerization is to dissolve the monomers, initiator, and stabilizer in a solvent and stir to form a homogeneous solution. This is followed by thermal decomposition of the initiator forming free radicals, which add to molecules of the monomer, one by one, to form other radicals. The reaction between monomers and radicals continues until oligomers appear and grow to a critical length. After initiation of the reaction, the solution remains transparent for a period of

time then, as nucleation occurs, the reaction mixture turns cloudy. The nuclei are stabilized against coagulation and continue growing by capturing more oligomers and monomers until termination occurs [56]. The mechanism of particle formation is shown in figure 2.10.

(a) All reagents are dissolved in the solvent first.

Polymerization initiated by heating.

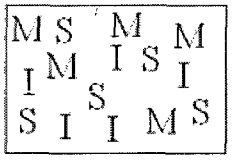

(b) Oligomers form and the polymer chains grow.

Solution stays clear.

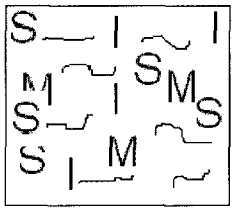

(c) Phase separation begins at the nucleation stage.

Solution becomes tubird.

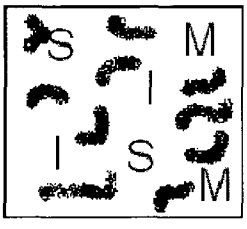

(d) Particles grow by capturing other oligomers and monomers.

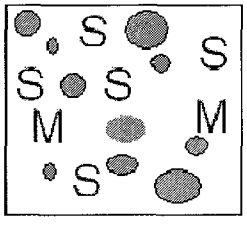

(e) Particles reach maximum size and stay suspended by stabilizer.

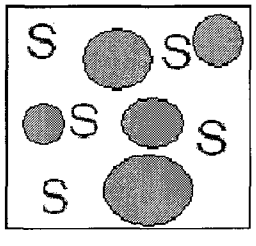

Figure 2.10: Mechanism of particle formation in dispersion polymerization. Figure source: Kaval, N.; PhD. Dissertation, University of New Hampshire, Durham, NH, **2002**.

2.6. Theory of Polymer Swelling

The swelling of polymers has been the subject of debate for the past 60 years, mainly because of the applications of swellable polymers in the biomedical fields. A crosslinked polymer when placed in a good solvent will absorb some of the solvent and subsequently swell to an equilibrium volume instead of dissolving. The extent to which the polymer swells depends on the solvent affinity of the polymer. This solvent affinity depends on the percentage of cross-linker in the polymer, charges within the polymer microspheres, and also hydrophilic or hydrophobic nature of the polymer. As the percentage of the cross-linker increases, the swelling ability of the polymer decreases. The repulsion of charged groups within the polymer network increases the swelling ability of the polymer, while increasing the hydrophilic groups of the polymer increases its swelling ability in a hydrophilic solvent but decreases its swelling ability in a hydrophobic medium.

Our research group has been developing chemical sensors based on the principle of polymer swelling. The focus of this research is to synthesize swellable polymer microparticles, and utilizing polymer swelling to cause changes in optical properties of the microparticles for analysis of the target analytes. The original design of our sensor was based on a swellable polymer bead that was coupled to a moving diaphragm that changed the amount of light on an optical fiber [61].

2.6.1 Non Ionic Polymer Swelling

Cross-linked polymers, when placed in an environment which is similar in structure to itself, will swell. Linear polymers dissolve when placed in compatible solvents. Flory described the polymer swelling process for non-ionic polymers by the equation below [63];

$$q_m^{5/3} \approx \left[\frac{(\bar{u}M_c)\,\frac{(M-2M_c)^{-1}}{M}\,\frac{(2-X_1)}{2}}{V_1} \right] \qquad 6$$

Where:

q_m = Equilibrium swelling ratio
$\bar{u}$ = specific volume of the polymer
M_c = Molecular weight per crosslinking unit
M = Molecular weight of the polymer network
X_1 = Interaction parameter- first neighbor free energy divided by kT for solvent with polymer
V_1 = Molar volume of the solvent

The equilibrium swelling ratio, q_m, is the volume of the swollen polymer (V) divided by the volume of the unswollen polymer (V_0). Equation 6 above describes the dependence of the non-ionic polymer swelling ratio (q_m) with both the degree of cross-linking ((M_c), and the solvent quality (X_1).

2.6.2. Ionic Polymer Swelling

For a charged polymer network, the swelling behavior is introduced in to the polymer by the repulsion of charged sites within the polymer network. Ionic polymer swelling can be explained in terms of either an osmotic pressure or an electrostatic effect. The electrostatic explanation suggests that the electrostatic charges within the polymer particles maximize the distance between the fixed sites. According to Flory's equation (equation 6), the degree of polymer swelling increases with the number of electronic charges on the polymer backbone [63]. The osmotic pressure explanation suggests that polymers with ionizable groups have some fixed charge density. If the charge density of the polymer is greater than that of the solvent, then the solvent will diffuse into the polymer to equalize the charge difference. The uptake of solvent molecules by the polymer results in an increase in the diameter of the polymer particles. But if the charge density of the polymer particles is less than that of the solvent, then the solvent molecules within the polymer particles are released into the surrounding solvent causing the polymer to shrink.

When the polymer swells, the free energy of mixing will cause the solvent to penetrate and dilute the polymer solution. As the polymer chains in the crosslinked polymer network begin to elongate due to absorption of solvent molecules, they generate an elastic retractive force due to this deformation. The volumetric swelling reaches a steady state when the two forces balance each other. The forces depend largely on the properties of the solvent such as the hydrophobic or hydrophilic nature of the solvent.

The degree of swelling increases with the presence of fixed charges. The equilibrium swelling ratio of ionic polymer is given by Flory's equation [63];

$$q_m^{5/3} = \frac{\left(\frac{i}{2V_u\sqrt{S}}\right) + \left(\frac{\frac{1}{2} - X_1}{V_1}\right)}{\frac{V_e}{V_o}} \qquad 7$$

Where:

i = number of polymer electronic charges per polymer units,
q_m = equilibrium swelling ratio,
V_o = volume of expanded polymer network,
V_1 = molecular volume of solvent,
V_u =molecular volume of polymer repeating unit,
S = molar ionic strength,
X_1 = interaction parameter,
V_e = Effective number of chains in the network,

The swelling ratio depends on the interaction between the solvent and the swollen polymer (gel) and can be influenced by factors such as pH, temperature, solvent composition, hydrostatic pressure and also electric and magnetic fields. The swollen polymer is elastic and can be characterized as a solution. The swelling property of cross-linked polymers has contributed to their widespread applications in molecular imprinting, molecular separation, drug delivery systems, and in the development of biomedical services such as contact lenses, and actuators.

2.7. Optical Measurements of Particles Embedded in Hydrogel Membranes

Our group has developed membranes containing swellable polymer microparticles designed for optical sensing of various analytes [27]. The polymer microparticles are immobilized in hydrogel membranes and placed in a pH controlled environment. The microparticles swell or shrink depending on the environmental conditions around them induced by either a change in pH, temperature, or target analyte concentration. As the microparticles swell due to absorption of water, their refractive indices decrease and become closer to that of the hydrogel. Both the size and refractive index of the particles change with changes in analyte concentration. The refractive index of the membrane remains constant and is not sensitive to the analyte concentration.

When light passes through a membrane embedded with polymer particles, the light is reflected, scattered, or absorbed. Scattering is caused by the polymer microspheres if the refractive index of the membrane and the particles differ. Reflection occurs at the phase boundaries if there is difference in refractive index between the medium and the surroundings. The optical properties of light directed at particles embedded in hydrogel membranes were studied extensively by Fresnel [64, 65, 66]. The Fresnel equation (equation 8) gives the amount of reflected light $R_{(\lambda)}$ at a particular wavelength λ, occurring at the phase boundary of medium 1 and medium 2.

$$R_{(\lambda)} = \frac{(n_2 - n_1)^2}{(n_2 + n_1)^2} \qquad 8$$

Where,

n_1 = refractive index of medium 1

n_2 = refractive index of medium 2

For polymer microparticles embedded in a hydrogel membrane, the two media are the microparticles and the membrane. The larger the refractive indices difference between the two media, the larger the reflection. This reflection can be measured as a change in turbidity of the membranes containing swellable polymer particles. Swelling of the particles causes a decrease in the difference in refractive index between the microparticles and the membrane. This in effect causes a decrease in reflectance or scattering and hence a decrease in the turbidity of the microparticles. Conversely, shrinking of the particles increases the refractive index of the particles and thus results in an increase in reflectance. Both reflection and scattering of light result in a decrease in the transmitted light. In our system, the difference in refractive index is the main contributor to the changing turbidity. Turbidity is therefore directly proportional to the absorbance and can be represented by the equation below for light passing through a 1cm path length [64];

$$\tau = 2.303A \qquad (9)$$

Where,

τ = membrane turbidity

A = absorbance

2.8. Temperature Responsive Polymers

Thermal responsive polymers form a three-dimensional polymer network that swells and shrinks with changes in temperatures. They are macromolecules which undergo physical changes with changes in temperature. These physical changes can be exploited for analytical purposes especially in chemical separations and drug delivery systems [67, 68, 69]. An example of a temperature responsive gel is poly (N-Isopropylacrylamide) (poly (NIPAAm)). At lower temperatures, the polymer particles dissolve in aqueous solution and at temperatures above its lower critical solution temperature (LCST), the polymer particles phase separate out of solution. Because the polymer microparticles undergo a phase change at the LCST, this temperature is also referred to as the phase transition temperature [70-76].

2.9. Molecular Imprinting

Molecular recognition is an important aspect of many biological processes [28]. A major emphasis in biotechnology is the development of synthetic recognition molecules and systems which are specific for a template molecule or analyte of interest. Molecular imprinting is the process of designing materials with specific stereochemical structures for selective interaction and recognition with a particular target analyte. The selective recognition property of a molecular imprinted material is achieved by having the imprint molecule itself directing the desired structure during the imprinting process.

The concept of molecular imprinting was developed from Pauling's theory of antigen-antibody interactions and has since led to the development of molecularly

imprinted polymers for use in chromatographic separations, biomimetic sensors, and for *in situ* product removal during biotransformation processes [77, 78]. In his theory, an antigen was used as a template in synthesizing antibody polypeptide chains, which produced complementary binding sites to the imprint molecules after the extraction of the antigen [79, 80].

In 1894, Fischer presented his famous "lock-and-key" analogy of the way a substrate interacts with an enzyme and since then, a wide variety of imprinting processes have been developed. Several molecules have been used as imprint molecules either in their existing form or derivatized to introduce some functionality to enable them to be imprinted [80]. Compounds such as amino acids, carbohydrates, proteins, nucleotide bases, hormones, pesticides, and co-enzymes have been successfully used as templates for selective recognition matrices [81].

The molecular imprinting process involves pre-organization of polymerizable monomers around an imprint molecule. Following polymerization and extraction of the imprint molecule, the solid polymer contains binding sites which are complementary in size, shape, and functionality to the template [82-84]. The created cavity can be used for both selective recognition and also separation of either the template molecule or another molecule with a similar size, shape, and functionality as the imprint molecule [85]. Figure 2.11 shows the imprinting process.

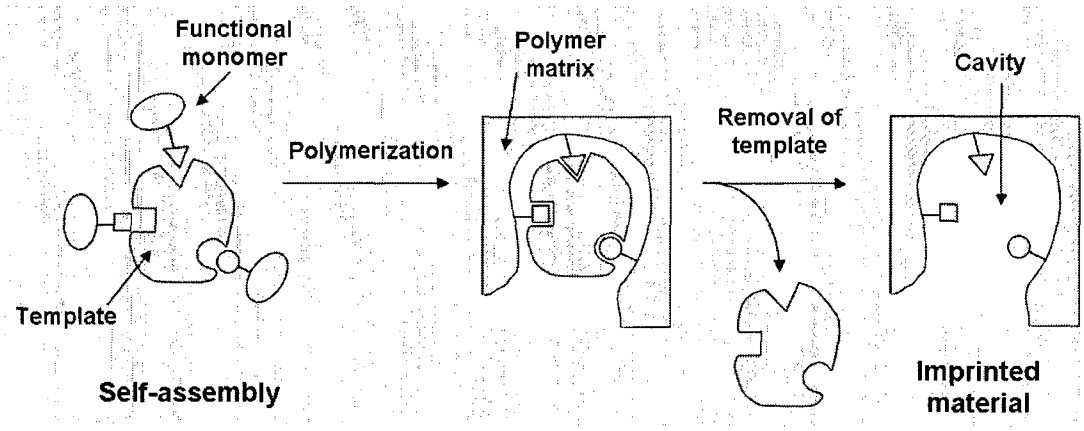

Figure 2.11: Molecular Imprinting Process
Figure source: http://en.wikipedia.org/wiki/molecular_imprinting

2.10. Classification of Molecular Imprinting

Molecular imprinting can be classified into two classes, namely; covalent and non-covalent imprinting depending on the type of interaction involved in the imprinting process [79, 86, 87].

2.10.1. Covalent Imprinting

Covalent imprinting involves formation of reversible covalent bonds between the guest and host molecules [88]. The method was first studied by Wulff and co-workers in 1977 and it has led to the development of novel molecular imprinting systems that are applicable for both chemical separation and chemical sensing [89]. They synthesized the 2:1 covalent conjugate of *p*-vinylbenzeneboronic acid with 4-nitrophenyl-α-D-mannopyranoside (template), and copolymerized this conjugate with methylmethacrylate and ethylene dimethacrylate (a cross-linking monomer). After polymerization, the boronic acid ester in the polymer was cleaved

and the template was removed. The resulting polymer strongly and selectively bound to the sugar [89, 90].

In the imprinting process, the binding sites of the functional monomers covalently bond with the binding sites of the template in either a reversible or non-reversible manner. The types of covalent bonds involved include: ester, Schiff-base, metal coordination, and acetal or ketal. The bonds are strong enough to keep the template-monomer complexes stable during the imprinting process.

2.10.2. Non-covalent imprinting

Non-covalent imprinting is a common imprinting process for drugs, insecticides, and small biomolecules. It involves mainly hydrogen bond interactions between templates and functional monomers in the polymer network. The molecules which exhibit hydrogen bonding are polar molecules containing groups such as; organic acids, alcohols, and amines. Other non-polar compounds containing polar bonds may also exhibit hydrogen bonding. Compounds containing thiol groups have non-polar S-H bonds. The electronegativity difference between the sulfur and hydrogen atoms is very small. Such compounds have insignificant or very weak hydrogen bonding.

Mosbach and coworkers showed that molecular imprinting can be achieved by non-covalent interactions between functional monomers and imprint molecules. By simply mixing the template and functional monomers together in the reaction chamber, their non-covalent adducts are spontaneously formed and satisfactory imprinting effects are obtained [87]. Wenzhe Fan prepared a

norephedrine-imprinted polymer by copolymerizing NIPAAm and acrylic acid (functional monomer) [27].

2.11. Theoretical Background of Metal Complexation

Metal complexes, also known as coordination compounds, consist of all metal compounds including vapors and alloys. Mineralogy, material science and solid state chemistry all involve coordination chemistry since the metals are surrounded by ligands [91]. Coordination complexes had been known for years but were not clearly understood until Alfred Werner proposed that Co (III) bears six ligands in an octahedral geometry. He developed a theory which allows one to understand the difference between coordinated and ionic chlorides in cobalt amine chlorides [92]. He also overthrew the theory that chirality was only associated with carbon compounds by resolving the first coordination complex into optical isomers. In aqueous solutions, transition metal ions are bound to water molecules and exist as hydrated ions [93]. A common example is hexaaquacopper (II) ion with the formula, $[Cu(H_2O)_6]^{2+}$. The structure is shown in figure 2.12.

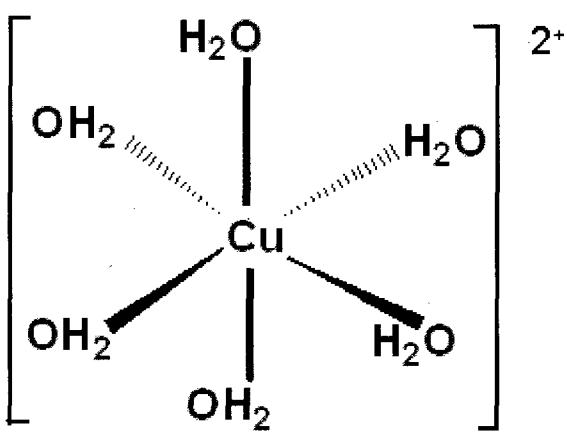

Figure 2.12: Hydrated Cu^{2+} ion.

Metal complexation involves reactions between aqueous solutions of compounds or metal ions, mainly transition metal ions, with atoms having lone pairs of electrons. The concept is derived from *Lewis Acid-Base theory* [94]. According to Lewis, metal ions with *d* and *f* orbitals can readily accept electrons from groups of atoms with lone pairs of electrons and are thus referred to as "Lewis acids" or "electron acceptors". The species that donate the lone pairs of electrons to the metal ions are termed as "Lewis bases" or "ligands". Ligands or electron donors can be classified as either monodentate or polydentate (chelating) ligands.

The reaction between the metal ions and the ligands can be predicted by the *Hard-Soft Acid-Base (HSAB) principle* [94]. In this principle, a complex ion is readily formed if one reactant contains a hard acid and a hard base and the other contains a soft acid and a soft base. The reaction is favored if the product formed contains either a soft acid and a soft base or a hard acid and a hard base. A simplified form of classification of metal ions as either soft or hard acids depends on their ability to accept the donated pair(s) of electrons which also depends on their ionic radius. Also Lewis acids and bases are classified as either soft or hard depending on their ability to accept or donate the electrons respectively. According to Pearson's hard-soft Lewis acid-base principle, hard Lewis acids have high positive charge, high energy (lowest unoccupied molecular orbitals (LUMOs)), and are weakly polarizable, while soft acids have large ionic radii, low or partial positive charge, low energy LUMOs, and are strongly polarizable [94].

The characteristics of hard and soft bases are similar to those of hard and soft acids except that hard bases have high energy highest occupied molecular

orbitals (HOMOs), while soft bases have low energy HOMOs. Hard Lewis acids prefer to bind to hard Lewis bases, while soft Lewis acids prefer to bind to soft Lewis bases. Lewis bases contain donor atoms such as oxygen, nitrogen, sulfur, chlorine, bromine, etc. In the product, the metal ion and the atom from the Lewis base are held together by a shared pair of electrons forming a coordinate or dative covalent bond [94].

The association of metal ions with ligands forms either weak reversible coordinate covalent bonds or strong irreversible bonds. The bonds are mainly sigma (σ) bonds formed by overlap between the s and p atomic orbitals of the ligands and the d (or f) orbitals of the metal ions. Phosphorus- and carbon- donor ligands have empty orbitals of π-type symmetry and act as π-acceptor ligands. They can form π-bonds by accepting electrons from the π-symmetry set of the central metal ion *d*-orbitals which stabilize the complex further. The structure of the complex is determined by the coordination number which is normally between two and nine except for large metal ions which have more than nine. Also the ratio of size of ligand to that of metal ion determines the coordination number of the complex. The number of bonds in a metal ion complex depends on the charge, size, and electron configuration of the metal ions.

The transition metal ion complexes are useful especially in the medical fields. For example, complexes of radioactive technetium are used as imaging agents and the complex *cis*-$[PtCl_2(NH_3)_2]$, cisplatin, is widely used as chemotherapeutic agent. Some of the complexes with low lying excited states are used as photosensitizers while some are used in electro-oxidation reactions as

electrocatalysts. An example is the electrocatalysis for olefin oxidation where metal oxo-catalysts such as ruthenium bipyridine complexes are used because they are strong oxidizing agents. In these reactions, the metal oxo-catalysts are reduced to metal-aqua complexes after reacting with the olefins [94].

2.11.1 Chelating Ligands

Chelating ligands have more than one electron donating atom per ligand molecule or ion and have geometries that enable them to form more than one coordinate bond to the same metal ion. They are thus termed as *"many toothed"* or polydentate ligands [95]. They form more stable metal complexes than the ones formed by monodentate ligands.

There are two major requirements that favor the binding of these chelating ligands with the metal ions. First, the ligand should be flexible and non-linear. The other is that the bond angles of the complex formed should be such that the different donor atoms should be reasonably far apart in the ligand to form *five-* or *six-membered rings* including the metal ion. The favorable angle is usually 90° or 109.5° [94]. An example is the binding of ethylenediamine with Ni^{2+} ions from aqueous solution represented by the scheme below.

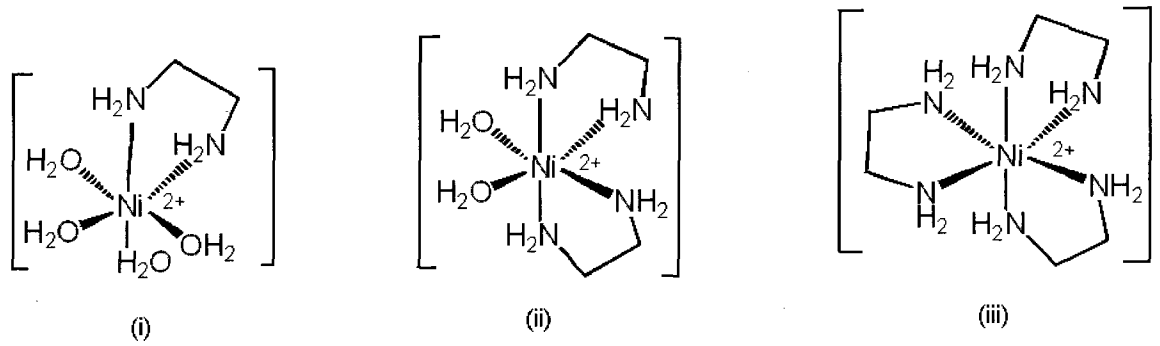

Figure 2.13: Co-ordination of ethylenediamine with Ni^{2+} ions.

The Ni^{2+}-ethylenediamine complex formed has a favored *five-membered ring structure* as shown in figure 2.13. The simple complex ions like hydrated ions in aqueous solutions are easily substituted by more electron donating and chelating ligands, a process that is thermodynamically favored because it is accompanied by an increase in entropy. Equation (10) below represents the substitution of water molecules in hexaaquanickel (II) ions with ethylene diamine (en). In the reaction process, a total of four moles of reacting species form seven moles of products indicating an increase in entropy (+ΔS). Each of the three ethylenediamine molecules form a *five membered ring* structure with bond angles of 108° when complexed with the hydrated Ni^{2+} ions.

$$[Ni(H_2O)_6]^{2+}_{(aq)} + 3\,(CH_2NH_2)_2 \rightarrow [Ni(CH_2NH_2)_3]^{2+}_{(aq)} + 6H_2O_{(l)} \qquad (10)$$

The binding of ligands to metal ions results in formation of complexes with low lying excited π^* molecular orbitals. These complexes experience charge transfer transitions of electrons between the metal like and ligand like molecular orbitals and are called "charge transfer complexes". There are two forms of charge transfers; metal to ligand charge transfer (MLCT) and ligand to metal charge transfer (LMCT)

[91]. The MLCT is the transfer of electrons from the molecular orbitals with metal like characteristics to those with ligand like characteristics. MLCT is common in aromatic ligands such as 2, 2'-bipyridine (bipy) and 1,10-phenanthroline (phen) due to the presence of π^* orbitals in the ligand. LMCT involves the transfer of electrons from the molecular orbitals with ligand like characteristics to those of metal like characteristics. MLCT and LMCT result in oxidation and reduction of the central metal ions respectively. The charge transfer process results in changes in spectroscopic properties of the solutions of the central metal ions such as molar absorptivities. Charge transfer absorption bands have high intensities and usually absorb in the ultraviolet or visible region. The charge transfer complexes have high molar absorptivities because the charge transfer processes are not spin forbidden [96-9100]. In this research project, a number of chelating ligands were used.

2.11.2. Formation Constants of Metal Ion Complexes

For monodentate ligands, there is only one atom per ligand that binds directly to the metal ion. This one atom can donate a maximum of only one lone pair of electrons for the formation of a dative covalent bond between the metal ion and the ligand. This leaves the empty orbitals from the metal ion still unfilled and according to the octet rule, more ligands need to bind to the metal ion to fill these orbitals [94]. This leads to successive binding of the metal ions to the ligands forming a series of complexes with each binding process having a different formation constant. The formation constants for the successive complexes are called

"stepwise formation constants". In general, a metal complexation reaction can be represented by the equations shown.

$$M + L \longrightarrow ML \quad (11)$$

$$\beta_1 = \frac{[ML]}{[M][L]}$$

$$ML + L \longrightarrow ML_2 \quad (12)$$

$$\beta_2 = \frac{[ML_2]}{[ML][L]}$$

$$ML_2 + L \longrightarrow ML_3 \quad (13)$$

$$\beta_3 = \frac{[ML_3]}{[ML_2][L]}$$

$$ML_3 + L \longrightarrow ML_4 \quad (14)$$

$$\beta_4 = \frac{[ML_4]}{[ML_3][L]}$$

Where, M, L, and ML_i represent the metal ion, ligand and complex respectively. β_1, β_2, β_3, and β_4 are the stepwise formation constants for the complexes ML, ML_2, ML_3 and ML_4 respectively. For ligands whose complexing abilities are pH dependent, the formation constants are called "conditional formation constants" [95].

2.12. Fluorescence Spectroscopy

Fluorescence spectroscopy is widely used in both chemical and biochemical research. Many biological substances such as colored proteins and chlorophyll from leaves emit characteristic fluorescence [101]. In biotechnology, fluorescence assays are commonly used instead of radioactive assays because they are considered safer. Enzymes, antibodies and membranes have been labeled with fluorescent dyes by either equilibrium binding or covalent attachment [102].

Fluorescence is the emission of radiation by either a molecule or atom after absorption of photons. If a molecule is irradiated with light whose energy corresponds to the energy difference between its excited and ground states, absorption of photons occurs and rearrangement of electronic distribution of the molecule occurs as it reaches the excited state. The excited electronic state has the excited electron in an anti-bonding orbital, and the bonded atoms are stretched out further than in the ground state, resulting in a shift of the minimum of potential well for the excited electronic state. The excited molecule can subsequently return to the ground state by losing its energy in fluorescence, phosphorescence, or radiationless emission. The radiationless transitions are also called internal conversions. For most molecules, internal conversion is the predominant mechanism of de-excitation. These molecules are therefore non-fluorescent [103, 104, 105].

Fluorescence always occurs from the lowest (singlet) excited state of the molecule because the processes of internal conversion of the higher states (thermal deactivation from higher electronic states to the lowest excited state) are so rapid [105]. Figure 2.14 shows the diagrammatic representation of fluorescence.

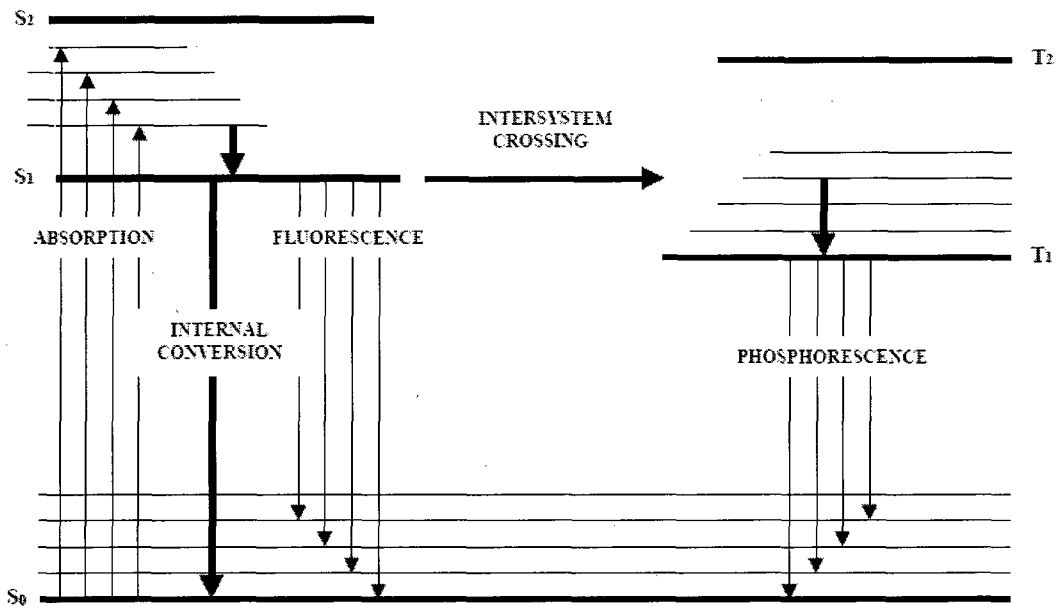

Figure 2.14: Emission of fluorescence, phosphorescence, and radiationless transition.
Figure source: http://www.oswego.edu/~kadina/CHEM425L/ FLUORESCENCE_ SPECTROSCOPY_08.pdf

2.12.1. Excitation Spectrum

A fluorescent molecule has two characteristic spectra; the excitation and emission spectra. The excitation spectrum should be identical to the absorption spectrum of the molecule although this is usually not the case mainly due to instrumental artifacts. Some of the reasons why the excitation and the absorption spectra may not overlap include changes in sensitivity of the radiation source, detector sensitivity, and changes in monochromator throughput with wavelength [104]. The excitation spectrum should indicate the relative positions of the absorptions giving rise to the fluorescence emission.

2.12.2. Emission Spectrum and Inner Filter Effect on Fluorescence

The emission spectrum is obtained from the reemission of radiation absorbed by the molecule. The shape of the emission spectrum and the quantum efficiency do not depend on the wavelength of the exciting radiation. The emitted intensity is lower if the excitation wavelength differs from the absorption maximum. Any portion of the spectrum where absorption occurs can produce an emission since emission almost always takes place from the lowest vibrational level of the first excited singlet state in solution regardless of the energy level to which the molecule was originally excited. The emission or fluorescent peak will be at the same wavelength regardless of the excitation wavelength but the intensity of the emission peak will vary according to the relative strength of absorption. Because the energy differences between the bands in the emission spectrum are similar to those in the absorption spectrum, the emission spectrum is approximately a mirror image of the absorption spectrum.

For steady state fluorescence measurements at low analyte concentrations, the intensity is linearly dependent on concentration. At low concentration, the emission of light is uniform from the front to the back of sample cuvette. At high concentration, more light is emitted from the front than the back of the sample cuvette. This is called the fluorescence inner filter effect. Because only light emitted from the middle of the cuvette is detected, the concentration must be low enough to ensure accurate intensity measurements. For polymer particles suspended in liquids, it is important to have very few solid particles distributed

uniformly within the liquid to reduce scattering of the incident light by the solid particles. The amount of scattered light depends on both the size and number of particles within the light path.

2.12.3. Förster Resonance Energy Transfer (FRET) Spectroscopy

Förster resonance energy transfer (FRET) is the transfer of excitation from one chromophore to another. The word "*resonance*" in FRET can be metaphorically referred to as a coupled pendulum as shown in figure 2.15 (a). In a coupled pendulum system with a spring connecting them, setting one of the pendulums to oscillate will set the other pendulum also to oscillate. This phenomenon is similar to the absorption of energy by the donor and emission of a photon by the acceptor in the FRET system shown in figure 2.15 (b). FRET is most applicable in analysis of biochemical compounds.

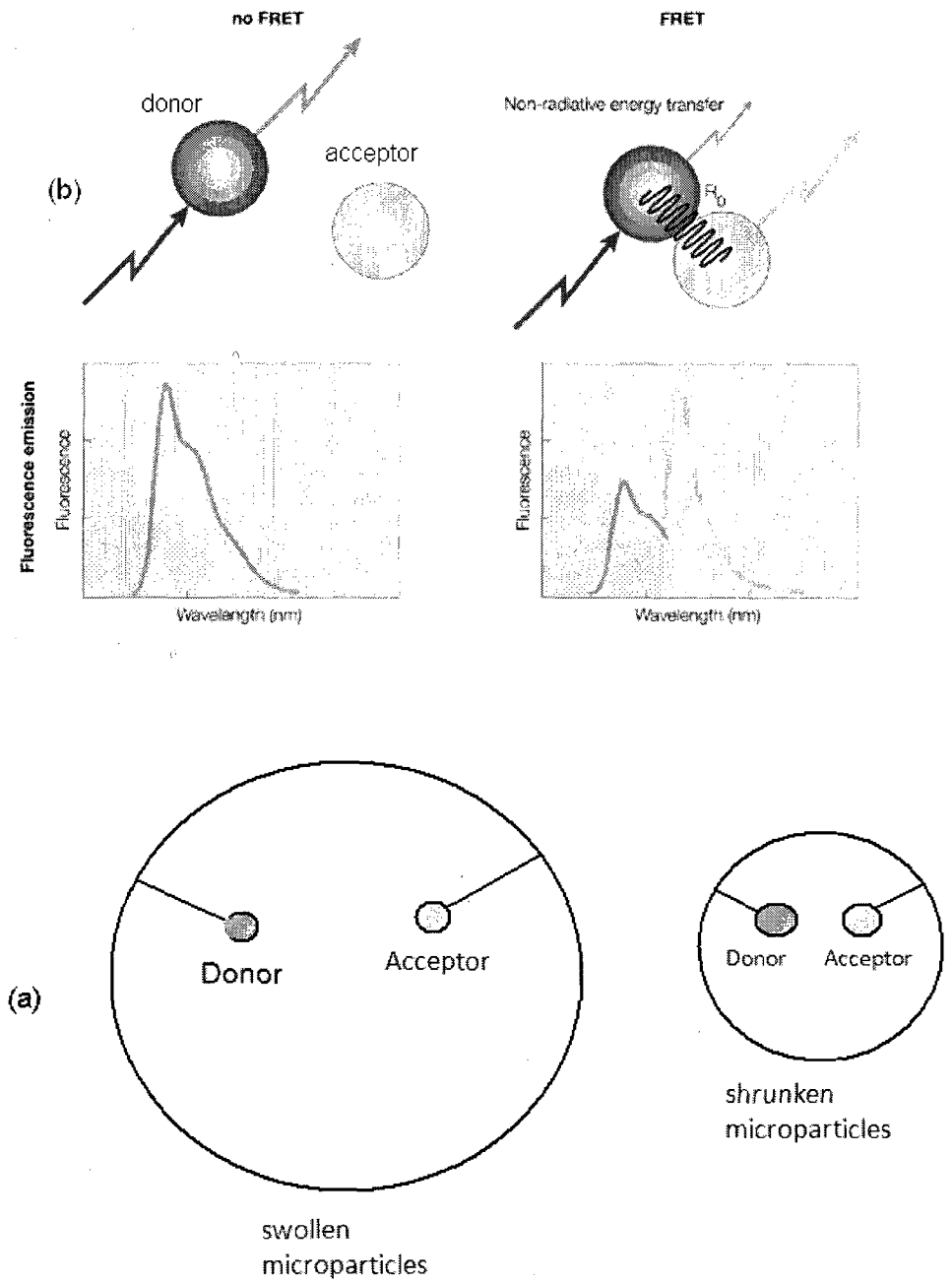

Figure 2.15: Energy transfer process in swollen and shrunken polymer microparticles.
Figure source: Nature Reviews Molecular Cell Biology.

FRET is a physical process by which energy is transferred non-radiatively from one excited molecular fluorophore (donor) to another molecule (acceptor) by means of intermolecular, long range, dipole-dipole interaction [106]. In this process,

the quantum, or excitation, is transferred which raises the electron in the acceptor to a higher energy state as the excited donor electron returns to the ground state. Transfer of excitation causes a decrease in quantum yield or fluorescence emission of the donor, increase in the fluorescence emission of the acceptor, and a decrease in the fluorescence lifetime of the donor [107]. The equations below represent the processes involved in fluorescence resonance energy transfer.

$$D + h\nu \rightarrow D^* \quad \text{(donor absorption)} \quad (15)$$

$$D^* \rightarrow D + h\nu \quad \text{(donor fluorescence)} \quad (16)$$

$$D^* + A \rightarrow D + A^* \quad \text{(excitation transfer)} \quad (17)$$

$$A^* \rightarrow A + h\nu \quad \text{(acceptor fluorescence)} \quad (18)$$

FRET spectroscopy depends strongly on the distance between the two chromophores. It is most efficient when the donor and acceptor fluorophores are positioned within the distance at which half of the energy of the donor is transferred to the acceptor which is between 3-6nm [108]. This distance is known as the Förster radius. Because FRET is highly dependent on the distance between the two fluorophores, it is often referred to as a molecular ruler and is used in determining the distance between two fluorescent molecules within a system. The FRET efficiency (F) depends on the inverse sixth power of intermolecular separation as given in the equation below which makes it a sensitive technique for investigating variety of biological phenomena that produce changes in molecular proximity.

Other factors determining FRET efficiency are presence of considerable spectral overlap between the emission and the absorption spectra of the donor and acceptor fluorophores respectively, and also near parallel relative orientations of the

donor emission and the acceptor absorption dipole moments. FRET efficiency can be obtained by measuring the fluorescence intensities of the donor with and without the acceptor. The FRET efficiency (E) is given by: [109].

$$E = 1 - F_{da} / F_d \qquad (19)$$

Where E_{da} = FRET efficiency

F_{da} = fluorescence intensity of the donor with the acceptor

F_d = fluorescence intensity of the donor without the acceptor

The efficiency can also be determined by using the lifetime of the donor in the presence and the absence of the acceptor. This can be represented by:

$$E = 1 - T_{da} / T_d \qquad (20)$$

Where T_{da} = fluorescence lifetime of the donor in the presence of the acceptor

T_d =fluorescence lifetime of the donor in the absence of the acceptor

The relationship between the transfer efficiency and the distance between the donor and the acceptor, is given by:

$$E = \frac{1}{1 + (r / R_0)^6} \qquad 21$$

Where r = distance between the donor and the acceptor

R_o = Forster distance, distance at which the energy transfer Is 50% efficient.

2.12.4. Fluorescence Quantum Efficiency

The fluorescence quantum efficiency, Φ, is the total energy emitted per quantum of energy absorbed. Its mathematical expression is;

$$\Phi = \frac{\text{Number of quanta emitted}}{\text{Number of quanta absorbed}} \qquad 22$$

The fluorescence quantum yield can also be defined as the fraction of absorbed photons that are emitted as fluorescence photons of the appropriate wavelength. This fraction is equivalent to the probability that an atom excited by absorption will undergo the appropriate transition and emit a fluorescence photon.

2.12.5. Fluorescence Quenching

This is a decrease in fluorescence emission intensity or quantum yield caused by collision of the fluorescent molecules with other molecules that are non fluorescent, energy transfer to nonfluorescent molecules, chemical reactions producing nonfluorescent compounds, and reabsorption or self-absorption of the fluorescent intensity [110, 111, 112].

Oxygen is a good fluorescent quencher because oxygen molecules in the ground triplet electronic state collide with fluorescent molecules producing non-fluorescent oxygen molecules in the excited singlet state. The excited oxygen molecules return to the ground triplet state after subsequent collisions or interactions with solvents [113, 114]. The equations below represent the relevant chemical processes taking place during fluorescence emission.

$$A + h\nu \rightarrow A^* \quad \text{(excitation)} \quad (23)$$

$$A^* \rightarrow A + h\nu \quad \text{(fluorescence)} \quad (24)$$

$$A^* + Q \rightarrow A + Q \quad \text{(quenching)} \quad (25)$$

2.12.6. Effect of Light Scattering on Fluorescence

Light scattering signals often coexist with fluorescence and interfere with fluorescence measurements [115]. When incident light is directed at a suspension, some of the light is absorbed, scattered, and also transmitted as shown in figure 2.16.

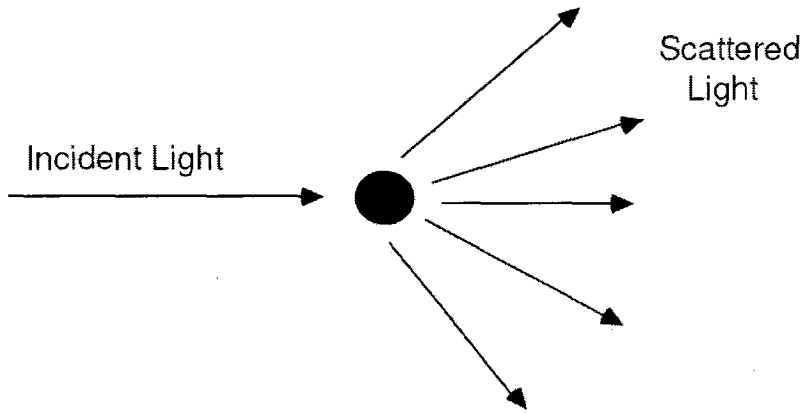

Figure 2.16: Scattering of light by a particle in solution.

According to Mie's theory, scattering of light by particles in suspension depends on particle size, number of particles, shape of the particles, particle composition, composition of the surrounding medium, wavelength of incident light, and refractive index of the particles relative to the medium in which the particle is suspended [116-118]. There are different types of light scattering namely; Rayleigh scattering, Tyndall scattering, and Raman scattering. Rayleigh scattering is the

scattering of light by particles much smaller in size than the wavelength of the incident light being scattered [119, 120]. Scattering of light from larger spherical particles is explained by Mie's Theory. Mie's theory gives the scattering cross-section (σ_s) which is proportional to the amount of light scattered by the particles in the suspension. In this case the Mie's theory for spherical particles with diameters larger than the wavelength of incident light reduces to the Rayleigh approximation given by the equation below;

$$\sigma_s = \frac{2\pi^5 d^6}{3\lambda^4}\left(\frac{n^2-1}{n^2+2}\right)^2 \qquad 26$$

σ_s = Rayleigh scattering cross section

n = particle refractive index

d = particle diameter

λ = wavelength of light

Rayleigh scattering applies to particles much smaller than the wavelength of incident light and accounts for why the sky appears blue. The smaller particles in the atmosphere like oxygen and nitrogen scatter shorter wavelength light much more effectively than the longer wavelength light. Rayleigh scattering also occurs when light travels in transparent liquids such as solvents. In a suspension containing many uniformly spherical particles, Rayleigh scattering increases with the increase in concentration of particles [119]. Tyndall Scattering occurs in colloidal systems such as suspensions or emulsions and is best explained by Mie's theory because the particle size is much greater than the wavelength of incident light. In this case, larger particles (about 25μm) scatter all wavelengths of light in the visible region equally. It

is useful in determining the difference between various types of mixtures such as solutions, colloids, and suspensions, and also in determining the particle size of the colloids because these mixtures contain different sizes of particles.

Raman scattering depends on the polarizability of the molecule. The incident light can excite the vibrational modes of the polarizable molecules producing scattered photons of less energy than the incident photons and thus appear at wavelengths longer than that of the incident radiation. It occurs in both sample and solvent used since it is a physical property of the compounds radiated by the incident light.

During fluorescence measurements, all the above mentioned scattering processes affect the fluorescence intensity. At all sensitivities, all types of scattering appear, but Rayleigh and Tyndall scattering are more intense than Raman scattering. For polymer particles suspended in a solvent, the difference in refractive indices between the polymer particles and solvent causes polarizability which depends on the molecular weight of the polymer particles. In this thesis, turbid suspensions were used which had low concentrations of microparticles. The sizes of the microparticles were also changing with either changes in analyte concentration or temperature which results in changes in amount of scattered light.

2.12.7. Effect of Photodissociation on Fluorescence

Photodissociation is the chemical destruction of fluorescent molecules due to absorption of energy. It is also called photodecomposition or photobleaching. It is usually experienced when a fluorescent substance is excited with light of higher energy or shorter wavelength. Photodissociation results in a decrease in fluorescence intensity of the sample. The more energetic photons are likely to cause photodecomposition rather than electronic transitions hence the decrease in fluorescence intensity of the sample [113]. To reduce photodecomposition, fluorescence measurements are made at longer wavelengths and exposure times are minimized.

2.12.8. Effect of Viscosity of the Medium on Fluorescence

Fluorescence is also affected by the viscosity of the medium. The intensity of fluorescence increases with increasing viscosity of the medium. This is due to the fact that an increase in molecular collisions increases energy transfer and hence increases the fluorescence intensity [113].

CHAPTER 3

EXPERIMENTAL

3.1 Reagents

The following reagents were purchased from Aldrich Chemical Company, Milwaukee, WI 53233:

N-Isopropylacrylamide (NIPAm), 97%, F.W. 113.16, m.p. 60-63°C, b.p. 89-92°C

Methacrylic acid (MAA), 99% F.W. 86.09, b.p 163°C

2,2'-Azobisisobutyronitrile (AIBN), 98%, F.W. 164.21, m.p. 103-105°C

N-methylenebisacrylamide (MBA), 99%, F. W. 154.17

Acetonitrile,anhydrous, 99.8% , F.W. 41.05, b.p. 81-82°C

Methanol, 99%, F.W. 32.04, b.p. 64.7°C

Acetic acid, 99.9%, F.W. 60.05, b.p. 117-118°C

Poly (vinyl alcohol) (PVA), 100% hydrolyzed, average MW 14,000

Poly (vinyl alcohol) (PVA), 87-89% hydrolyzed, average MW 85,000-146,000

Poly (vinylpyrrolidone) (PVP), 98%, M.W. 70,000

Polystyrene-*co*-acrylonitrile, 32% acrylonitrile

Sodium hydroxide, 97%, F.W. 40.00

Sodium nitrate, 99%, F.W 84.99

Hydrochloric acid, 36.5-38.0%, F.W. 36.46

Theophylline, 99%, F.W. 180.2

Caffeine, 99%, F.W. 194.19

Potassium persulfate (KPS), 99.2%, F.W. 270.33

Ethylene glycol dimethacrylate, (EGDMA), 98%. F.W. 198.22, b.p. 98-100°C

Acrylamide, 97%, F. W. 71.08

β-D-glucopyranose, 97%, F.W. 180.2

β-D-galactopyranose, 99%, F.W.180.2

Glutaraldehyde, 50% solution in water, F.W. 100.12

Acetone, HPLC grade, F.W. 58.08, b.p. 56.01°C

Copper (II) nitrate anhydrous, 99.5%, F.W. 187.56

Zinc (II) nitrate anhydrous, 99%, F.W. 189.36

Nickel (II) nitrate anhydrous, 98%, F.W. 182.7

Lead (II) nitrate, 99.8%, F.W. 331.2

3-(N-Morpholino)-propanesulfonic acid (MOP) buffer, 99.5%, F.W. 209.3

The following chemicals were purchased from Polyscience Inc, Fair Lawn, NJ 07410:

9-Vinyanthracene (9-VA), 97%, F.W. 204.27

2-Naphthylmethacrylate (2-NMA), F.W. 212.24

Fluorescein o-acrylate, 97%, F.W. 400.38

Methacryloxethyl thiocarbonyl rhodamine-B, F.W. 683.24

The following Chemicals were synthesized by Daniel Kennedy of Prof.

Planalp's research group at University of New Hampshire:

2,2'-acrylamidodiacetic acid (AIDA), M.W. 187.15

Dibutyl 2,2'-(3-vinylphenylazanediyl)diacetate (DVPAA), M.W. 347.45

N,N-bis (pyridin-2-ylmethyl)prop-2-en-1-amine (NBPMPA),

M.W. 239.32

N-((4'-methyl-2,2'-bipyridin-4-yl) methyl)-N-propylacrylamide

(NMPPAAm), M.W. 295.38 was provided by Prof. Shawn Barnett of

the University of Connecticut

All buffers were prepared at 0.1M concentration and adjusted to 0.1M ionic strength with potassium chloride. Aqueous solutions were prepared from doubly deionized distilled water from a corning Mega-Pure distillation apparatus.

Figures 3.1-3.3 illustrates the structures of the major reagents used for preparation of the polymer microparticles.

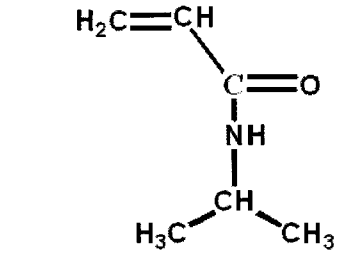

N-Isopropylacrylamide (NIPAAm)

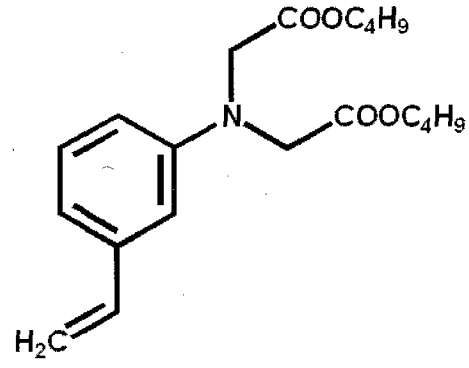

dibutyl 2,2'-(3-vinylphenylazanediyl)diacetate (DVPAA)

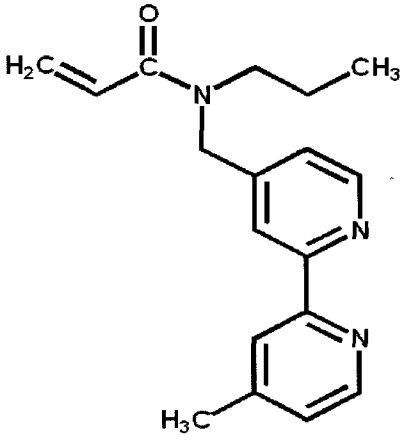

N-((4'-methyl-2,2'-bipyridin-4-yl) methyl)-N-propylacrylamide (NMPPAAm)

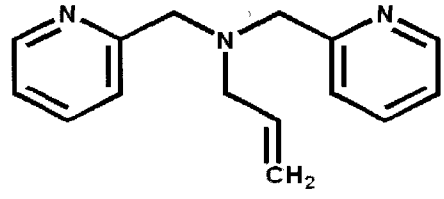

N,N-bis(pyridin-2-ylmethyl)prop-2-en-1-amine (NBPMPA)

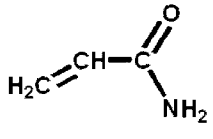

Acrylamide

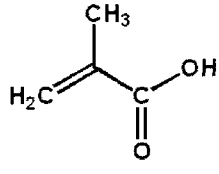

Methacrylic acid (MAA)

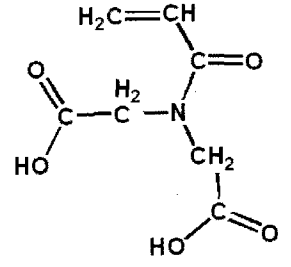

2,2'-acrylamidodiacetic acid (AIDA)

Figure 3.1: Structures of monomers.

Stabilizers

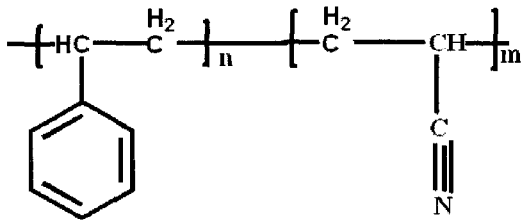

Poly (styrene-co-acrylonitrile)

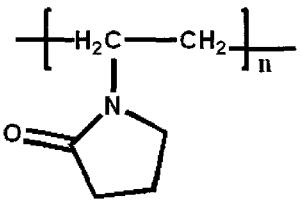

Polyvinyl pyrrolidone (PVP)

Cross-linkers

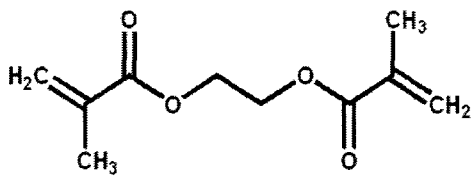

Ethylene glycol dimethacrylate
(EGDMA)

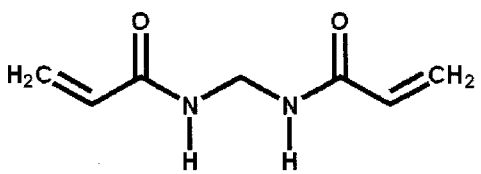

N,N'Methylenebisacrylamide
(MBA)

Initiators

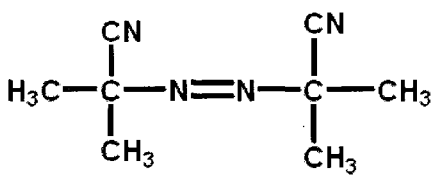

Azobis (isobutyronitrile) (AIBN)

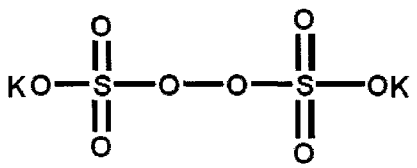

Potassium persulfate (KPS)

Figure 3.2: Molecular structures of stabilizers, cross-linkers, and initiators.

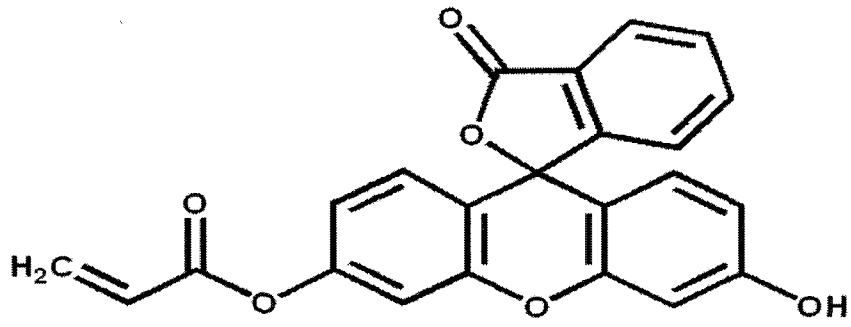

Fluorescein o-acrylate

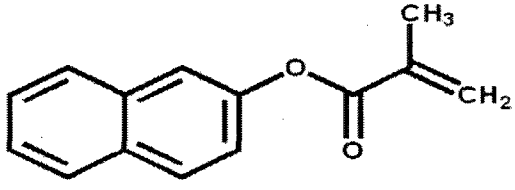

2-Naphthyl methacrylate
(2-NMA)

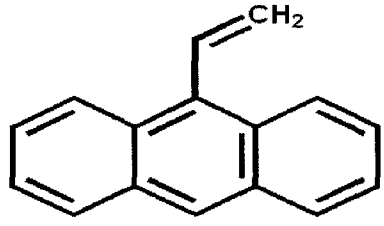

9-Vinylanthracene (9-VA)

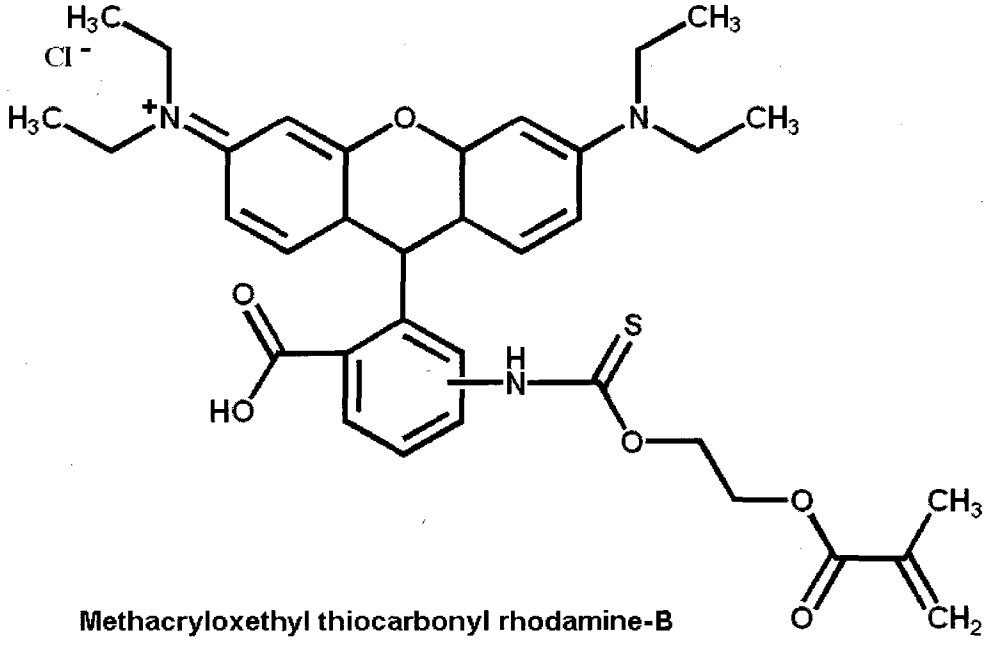

Methacryloxethyl thiocarbonyl rhodamine-B

Figure 3.3: Molecular structures of fluorescent monomers.

Template Molecules

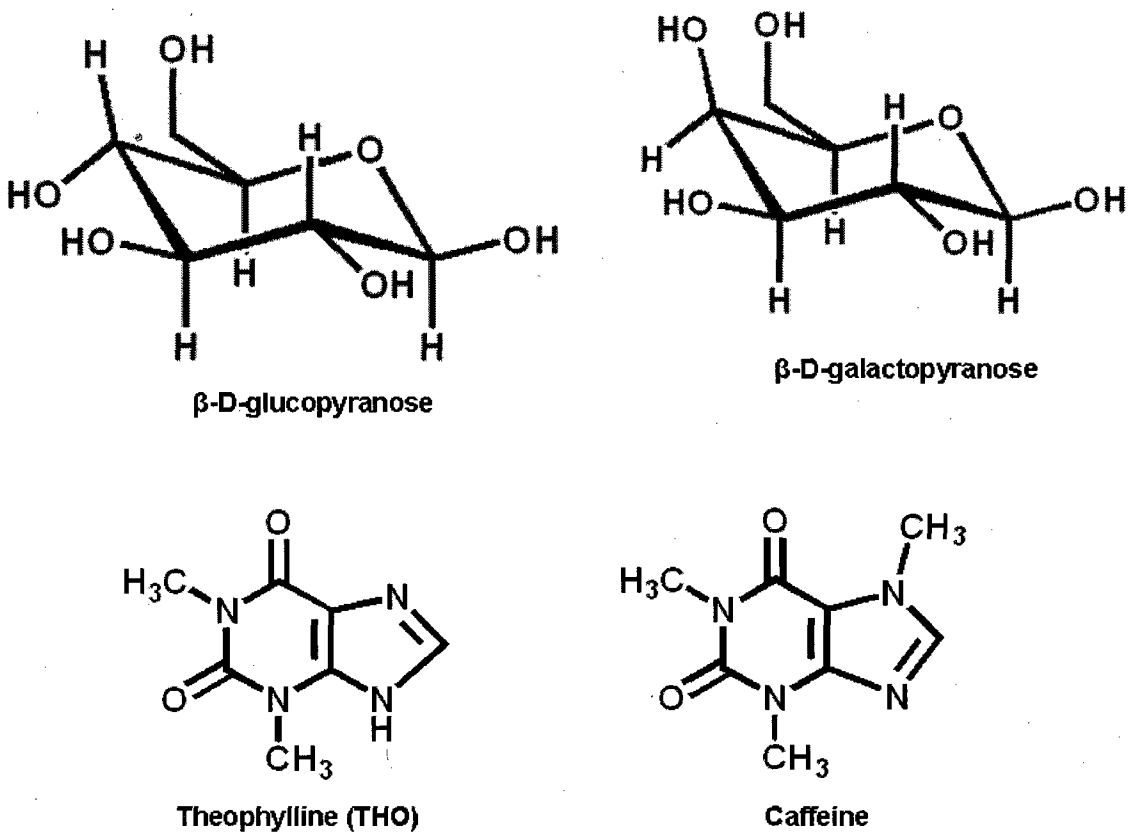

Figure 3.4: Molecular structures of template molecules.

3.2 Apparatus

A Cary 50 Bio UV/Vis/NIR spectrophotometer was used for turbidity measurements. A Cary Eclipse fluorescence spectrophotometer was used for fluorescence measurements, and acquiring second order light scattering data. A Branson model 1210 sonicator was used both for dissolving, and also resuspension of the microparticles in the solvent after centrifugation. A Fisher laboratory centrifuge (3400rpm) was used to remove particles from suspension.

An Amray model (3300FE) scanning electron microscope from the University of New Hampshire Instrumentation Center was used to determine both polymer morphology, particle size and size distribution. An Orion 901 digital analyzer with an Orion 91/55 combination pH electrode was used for buffer preparation. A copper ion selective electrode was used for potentiometric titrations of the polymer suspensions. 100ml single-neck, round bottom flasks were used for synthesis of the polymer microparticles.

3.3 Procedures

3.3.1 Preparation of Temperature Responsive Poly (NIPAAm) Polymer Microparticles by Dispersion Polymerization

NIPAAm, MBA, and PVP were dissolved in 50mL of distilled water in a single neck, round bottom flask and stirred using a magnetic stirrer for about 30minutes. KPS was added to the mixture to initiate the polymerization reaction. The amounts of these reagents are given on table 3.1. The resulting solution was sonicated for 15minutes to obtain a homogeneous mixture. A rubber stopper was then fitted tightly on the flask. The mixture was purged with nitrogen at a pressure of 1psi for 20 minutes to remove all of the oxygen in the flask and then inserted in a temperature controlled water bath with temperature maintained at 60°C. The resulting mixture was polymerized for 16 hrs. The resulting polymer microparticles were then cleaned with repetitive centrifugations in distilled water to remove excess unreacted water soluble monomers and initiator. Figure 3.5 gives the polymerization reaction.

Poly (NIPAAm) microparticles were also prepared in acetonitrile using AIBN and poly (styrene-co-acrylonitrile) as the initiator and stabilizer respectively. MBA was used as the cross-inker. The percentage of cross-linker was varied in all formulations to obtain the optimum mechanical strength of the polymer microparticles. The concentration of the steric stabilizer was also varied to improve the morphology of the polymer microparticles. The microparticles were centrifuged and resuspended in additional acetonitrile to dissolve any unreacted monomers.

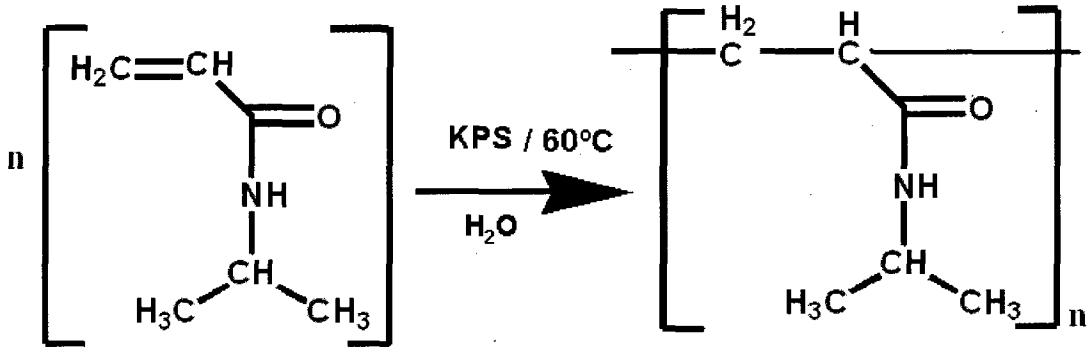

Figure 3.5: Polymerization of NIPAAm in water.

Reagent	Quantity
NIPAAm	1.018g
KPS	0.040g
MBA	0.077g
Poly(vinylpyrrolidone)	0.224g
water	50mL

Table 3.1: A typical formulation for preparation of poly (NIPAAm) microparticles in water.

3.3.2 Preparation of Swellable Poly (NIPAAm) Labeled with 2-NMA and 9-VA Fluorophores.

The objective of this section was to investigate the possibility of using 2-Naphthylmethacrylate (2-NMA), and 9-Vinylanthracene (9-VA) as a suitable fluorophore pair for studying polymer swelling properties using fluorescent ratiometric measurements. Since 2-NMA has peak excitation and emission wavelengths of 280nm and 345nm respectively, while 9-VA has peak excitation and emission wavelengths of 350nm and 420nm respectively, there is spectral overlap of the emission and absorption spectra of 2-NMA and 9-VA respectively. This spectral overlap combined with induced dipole moments of the two fluorophores resulting from relative orientations and distance between them make the two fluorophores suitable candidates for the fluorescence study of the swelling and shrinking of the polymer microparticles.

Temperature sensitive poly (NIPAAm) microparticles were prepared in a 100mL single neck round bottom flask according to the formulation table 3.2.

Reagent	Quantity
NIPAAm	1.01800g (9.000mmol)
AIBN	0.03280g (0.200mmol)
MBA	0.07710 (0.500mmol)
Poly(styrene-co-acrylonitrile)	0.22400g (5.600 x 10^{-3}mmol)
2-NMA	0.00410g (0.020mmol)
9-VA	0.00085g (0.004mmol)
Acetonitrile	50mL

Table 3.2: A typical formulation for the dispersion polymerization of Poly (NIPAAm) labeled with 2-NMA and 9-VA fluorophores.

The mixture of NIPAAm, MBA, 2-NMA, 9-VA, poly (styrene-co-acrylonitrile) copolymer was dissolved in 50ml acetonitrile and sonicated for 30minutes. After sonication, the initiator, AIBN, was added to the reaction mixture. The mixture was purged with nitrogen for 20 minutes to remove oxygen, and then inserted in a temperature controlled water bath with temperature maintained at 60°C. The resulting mixture was polymerized for 16 hrs.

3.3.3 Preparation of Swellable Poly (NIPAAm) Labeled with Fluorecein o-acrylate and Methacryloxethyl thiocarbonyl rhodamine-B Fluorophores

In this section, fluorescein o-acrylate and methacryloxethyl thiocarbonyl rhodamine-B fluorophores were being investigated as a suitable fluorophore pair for the intended fluorometric analysis of polymer swelling and shrinking. The formulation of this polymerization was similar to the one shown in Table 3.2 except fluorecein o-acrylate and methacryloxethyl thiocarbonyl rhodamine-B fluorophores were used instead of 2-NMA and 9-VA. Fluorescein o-acrylate has peak excitation and emission wavelengths of 494nm and 521nm respectively, while methacryloxethyl thiocarbonyl rhodamine-B has peak excitation and emission wavelengths of 548nm and 580nm respectively. Polymerization process was carried out according to the procedure already described in section 3.3.1 of this chapter.

3.3.4 Polymer Cleaning

After polymerization, the resulting polymer particles were cleaned and isolated by centrifugation. The particles were suspended in acetonitrile and centrifuged several times to remove all the unreacted monomers. Scanning electron micrographs were used to evaluate the size of particles including the size distribution.

3.3.5 Preparation of Hydrogel Membranes with Polymer Microparticles

Our research group has used various hydrogel materials for preparing membranes to immobilize the polymer microparticles for convenient spectroscopic measurements. In this research project, poly (vinyl alcohol) (PVA) was used to prepare hydrogel membranes to immobilize the polymer microparticles for turbidity measurements. PVA was considered suitable because of its hydrophilic nature which makes it soluble in water. Its advantages include solubility in water, non toxicity, excellent film forming, high adhesive and tensile strengths, and also, flexibility [121].

The PVA membranes with and without polymer microparticles were prepared according to a procedure described in the literature [27]. A 10% aqueous solution of PVA was prepared by dissolving 10g of PVA (MW 14,000) in 90g of water and stirring while heating until all the PVA dissolved. This was used as stock solution during the process of immobilization of the polymer microparticles in the PVA membranes. A 10 % aqueous solution of glutaraldehyde was also prepared from a 25% stock solution. Accurately weighed polymer microparticles were immobilized in a PVA membrane by suspending them in the prepared 10% w/w aqueous PVA solution in a vial. The resulting mixture was sonicated for homogeneous mixing for 10 minutes followed by addition of 10% aqueous solution of glutaraldehyde. The mixture was again sonicated for 10 minutes and a known amount of 4M HCL was finally added and stirred for 30 seconds.

In this polymerization process, glutaraldehyde was used as the cross-linking agent and the polymerization process was initiated by 4M hydrochloric acid. The

suspension was applied on to the surface of a microscope slide with a 76µm thick Teflon spacer applied around the edges. The microscope slide was then covered with another slide and secured with a binder clip. The solution was then allowed to polymerize for 20 minutes after which the membranes were carefully removed to avoid ripping them. The membranes were then washed several times with de-ionized water and stored in a vial containing water. The thickness of the Teflon spacer controls the thickness of the membranes containing the polymer particles. Table 3.3 gives the formulation of the reagents used in the immobilization of the particles on PVA membrane.

Reagent	Amount
Poly(NIPAAm)	0.1g
10% aqueous PVA solution	1.0g
10% aqueous Glutaraldehyde solution	100µL
4M aqueous HCL solution	50µL

Table 3.3: A formulation of PVA membrane preparation.

3.4 Characterization of Polymer Microparticles

3.4.1 Scanning Electron Microscopy (SEM)

An Amray 3300FE Scanning electron microscope (SEM) was used to obtain morphology, size, and also size distribution of the microparticles. The samples were vacuum coated with about 300-350Å thick gold/palladium alloy. Before the microparticles were taken for SEM scanning, the microparticles were observed using a light microscope in the lab (magnification 15x). Small portions of dry samples were dropped on the surface of a glass substrate which was glued on the sample stub of the microscope and viewed for coagulation or estimation of particle size.

3.4.2 Determination of Microarticle Size and Size Distribution

The exact particle size was measured from the SEM pictures and the average particle size was also estimated by summing up the size of a few particles and dividing by the number of particles. This method was also used in determining the particle size distribution. A good tool that gives a statistical analysis of size distribution is the Carl Zeiss Microscope coupled with KS200 software.

3.4.3 Turbidity Measurements

There are two ways of determining turbidity of the polymer microparticles; using either absorbance, or second order scattering of either the microparticles suspended in buffer solution or microparticles immobilized in a hydrogel membrane. Turbidity measurements using microparticles immobilized in hydrogel membranes is the

preferred method since it produces more reproducible data than using microparticles suspended in buffer solution.

The major disadvantage of this method is that the hydrogel membranes can restrict the swelling of the microgels and lower the sensitivity of the sensor. This problem can be minimized or eliminated by using less cross-linking during the membrane preparation. Even though determination of turbidity using polymer microparticles suspended in a buffer solution has an advantage in that it does not restrain the microparticle from swelling, its major problem is that there is the possibility of particles coagulating and settling to the bottom of curvette. This settling of microparticles affects the results for both absorbance and second order light scattering.

Poly (NIPAAm) particles were immobilized in PVA membranes prepared according to the procedure described previously in this chapter. The membranes were secured in a homemade plastic membrane holder and fitted into a cuvette containing a buffer solution for turbidity measurements as shown in figure 3.6. Blank membranes without the polymer particles were also prepared and secured in the membrane holder. They were then fitted into a cuvette containing a buffer solution and were used as reference for analysis. The cuvette was then inserted in a cuvette holder of a Cary 50 UV-Visible spectrophotometer for turbidity measurements. Turbidity was measured at various temperatures and pH values by scanning from 200nm to 800nm. All the turbidity data presented here were measured at 500nm, a wavelength at which the polymer microparticles do not absorb. Figure 3.6 shows a picture of the membrane holder used for the measurements.

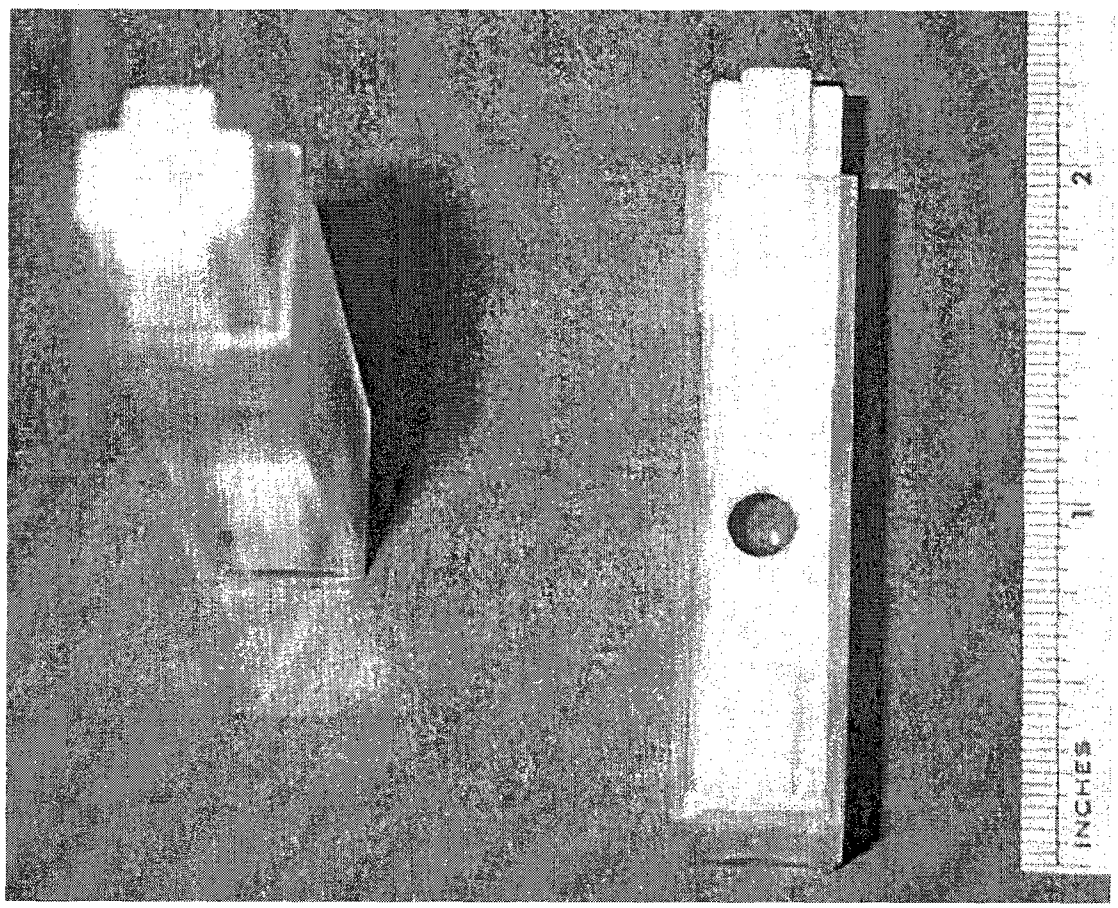

Figure 3.6: Membrane holder for turbidity measurements.

3.4.4 Fluorescence Measurements

A known amount of fluorescent labeled poly (NIPAAm) microparticles were suspended in pH 6 MOP buffer with ionic strength adjusted to 0.1M using aqueous sodium chloride and a portion of the suspension was poured into a cuvette. A Cary Eclipse Spectrofluorometer was used for the measurement of fluorescence intensities of the fluorescent moieties within the polymer network. The emission wavelengths of the two fluorophores (donor and acceptor) were obtained by scanning mode. Because suspensions of microparticles were used instead of solution, the kinetics mode which measures the two fluorescence intensities at the same time was used to obtain the

absolute fluorescence intensities. Scanning within the excitation and emission wavelengths of the two fluorophores was considered unsuitable for obtaining absolute intensities due to non homogeneous nature of the suspension. The movement of the microparticles within the suspension and also the possibility of settling of the microparticles to the bottom of the cuvette could also interfere with the absolute values of the two fluorescence intensities. The fluorophores used were 9-VA, 2-NMA, fluorescein o-acrylate, and methacryloxethyl thiocarbonyl rhodamine-B.

CHAPTER 4

EFFECT OF TEMPERATURE ON LIGHTLY CROSS-LINKED POLY (N-ISPROPYLACRYLAMIDE) POLY (NIPAAm)

4.1 Introduction

Poly (N-Isopropylacrylamide) (poly (NIPAAm)) particles exhibit a reversible phase transition upon changes in temperature in aqueous solutions. The particles undergo reversible swelling and shrinking below and above a lower critical solution temperature (LCST) respectively. The LCST of pure poly (NIPAAm) homopolymer is 32°C but copolymerizing NIPAAm with other monomers causes changes in the LCST. Copolymerizing NIPAAm with hydrophilic monomers increases the LCST, while hydrophobic monomers lower the LCST. At temperatures below its LCST, poly (NIPAAm) microparticles in aqueous solution are hydrophilic and in this hydrated form the particles are swollen. At temperatures above LCST the polymer microparticles are hydrophobic and shrink in the dehydrated form. The swelling and shrinking property of poly (NIPAAm) microparticles can be modified to suit the intended use of the polymer by introducing some functional groups within the polymer network.

In this project, swelling and shrinking of the poly (NIPAAm) microparticles was an important feature in the development of the sensor. The fluorophores were copolymerized with NIPAAm to provide the polymer microparticles with

spectroscopic properties. The sensitivity of the sensor depends on the arrangement and relative positions of the two fluorophores within the polymer network. This arrangement depends on the relative reactivities of the two fluorophores and also NIPAAm. Since the vinyl group is more reactive than the acrylate group, 9-vinylanthracene (9-VA) is expected to be preferentially located in polymer segments that form early and 2-naphthylmethacrylate (2-NMA) will be more evenly distributed within the polymer network during the polymerization. Thus using a lower concentration of 9-VA than 2-NMA eliminates formation of block copolymers of the two fluorophores, but there is a possibility of polymer strands without either 9-VA and 2-NMA fluorophores. For the fluorescein o-acrylate and methacryloxethyl thiocarbonyl rhodamine-B system, both have similar polymerizable acrylate groups and both should be evenly distributed within the polymer network.

In this chapter, fluorescent labeled and lightly cross-linked poly (NIPAm) microparticles were synthesized according to the formulation and procedure described in Chapter 3 of this thesis. Effect of temperature on these polymer networks was investigated using both turbidity and FRET. 2-NMA, 9-VA, fluorescein o-acrylate, and methacryloxethyl thiocarbonyl rhodamine-B were used as the fluorescent monomers. The microparticle size and size distribution were determined. Also the effect of introducing the fluorescent monomers on the LCST of the polymer network was also investigated. Since the experimental procedure involved using immobilized polymer microparticles that could possibly settle to the bottom of cuvette after collapsing, second order light scattering by the microparticles was used to study how settling of the microparticles affects the results.

4.2 Results and Discussion

4.2.1 Particle Size and Size Distribution.

Scanning electron micrographs (SEM) of the poly (NIPAAm) microparticles show that the beads are fairly dispersed and could be suspended in solvent. The microparticles formed stable suspensions without settling rapidly at the bottom of the cuvette enabling thermal response to be evaluated. The average microparticle diameter was found to be 0.47μm and the bead diameters range from 0.40-0.52μm. The SEM pictures of the microparticles are shown in figure 4.1.

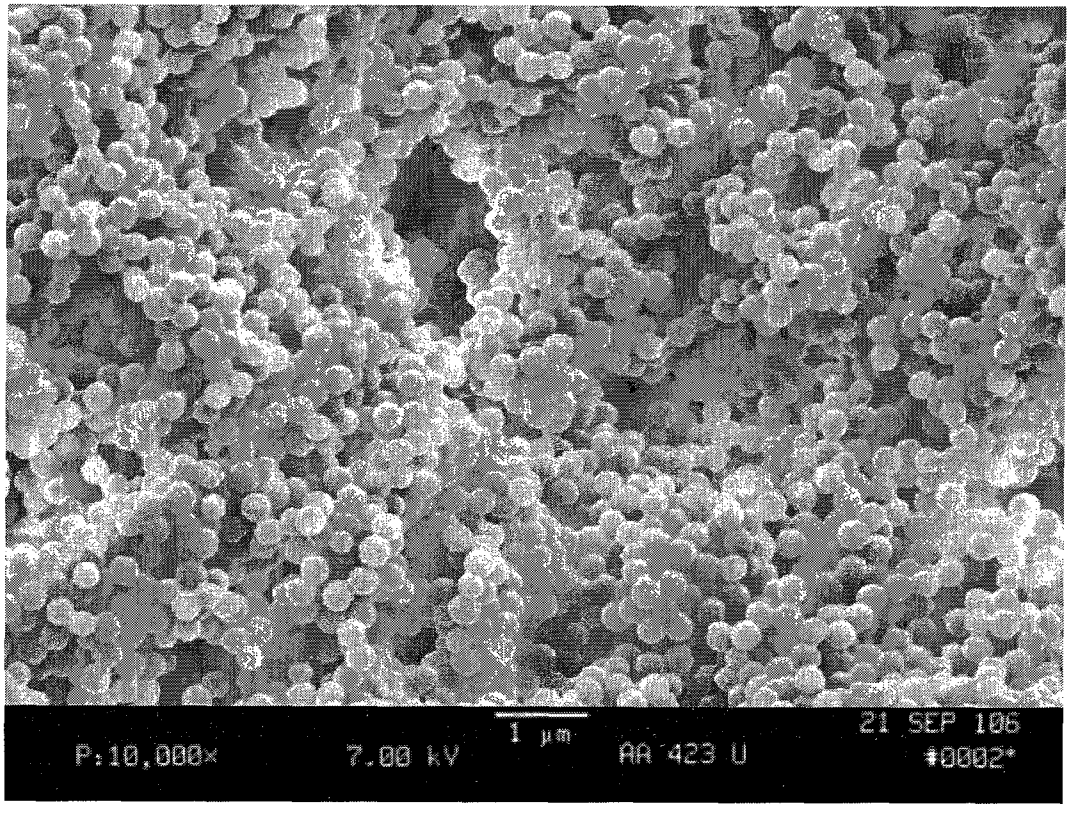

Figure 4.1: Scanning Electron Micrograph of poly (NIPAAm) particles labeled with 9-VA and 2-NMA

4.2.2 Turbidity Measurements and Temperature Response of Poly (NIPAAm) Microparticles.

The temperature response of the poly (NIPAAm) beads was determined by measuring the turbidity of the polymer beads suspended in PVA membranes. The turbidities were measured as absorbance using a conventional spectrophotometer at 500nm. The absorbences were found to increase with increasing temperature. The low turbidity of the microparticles at temperatures below the lower critical solution temperature (LCST) of poly (NIPAAm) and relatively higher turbidity at temperatures above the LCST indicate that the microparticles were swollen at temperatures below the LCST but shrunken at temperatures above the LCST. The refractive index of the microparticles increases with increasing temperature. At temperatures below the LCST, the microparticles are swollen and the refractive index is less than at temperatures above the LCST when the microparticles are shrunken. The LCST of the polymer microparticles was found to be about 33.2°C which is very close to the expected LCST of poly (NIPAAm). The absorbences of the polymer microparticles at the various temperatures were converted to turbidity using the formula discussed in Chapter 2 of this thesis. Figure 4.2 shows the absorbances of the polymer microparticles at different temperatures. A graph of turbidity at 500nm vs. temperature was plotted as shown in figure 4.3.

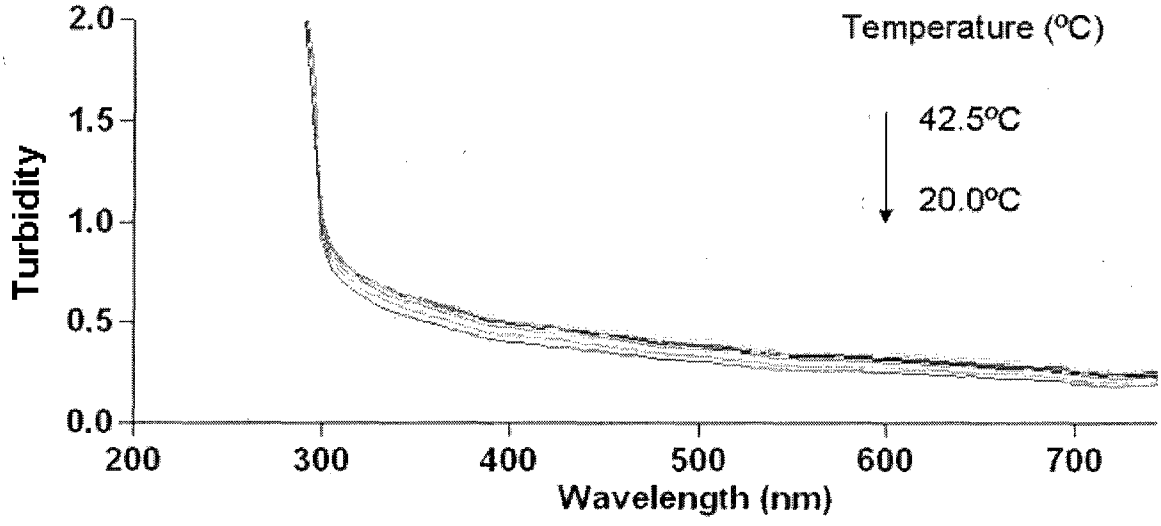

Figure 4.2: Turbidity spectra for lightly cross-linked poly (NIPAAm) embedded in PVA membrane in pH 6 MOP buffer.

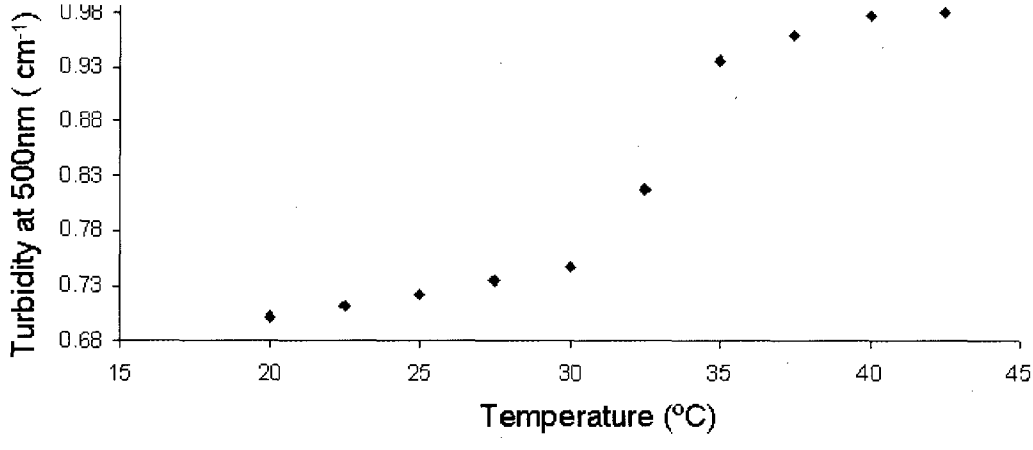

Figure 4.3: Temperature response of poly (NIPAAm)

4.2.3 Temperature Coefficients of Fluorescent Monomers.

Fluorescence intensities are sometimes affected by changes in temperature and therefore an experiment was performed to investigate how the fluorescence intensities and also the intensity ratios of the fluorophore pairs change with changes in temperature. The temperature coefficients of the fluorophore pairs can cause a change in fluorescence intensity ratio, a phenomenon that can be confused with changes in FRET efficiency in this system. The changes in fluorescence intensities of 9-VA and 2-NMA monomers in ethanol were investigated at various temperatures and fluorescence intensity ratios of 9-VA: 2-NMA were calculated. The polymer microparticles were excited at 280nm and fluorescence intensities of the two fluorophores were obtained. A plot of fluorescence intensity ratio vs. temperature was plotted as shown in figure 4.4. The procedure was repeated for fluorescein o-acrylate and methacryloxethyl thiocarbonyl rhodamine-B, but in this case the polymer microparticles were excited at 480nm, and a graph of fluorescence intensity ratio vs. temperature was plotted as shown in figure 4.5. The results show that the 9-VA: 2-NMA fluorescence intensity ratio is constant throughout the temperature range, while that of methacryloxethyl thiocarbonyl rhodamine-B: fluorescein o-acrylate decreases slightly with increasing temperature.

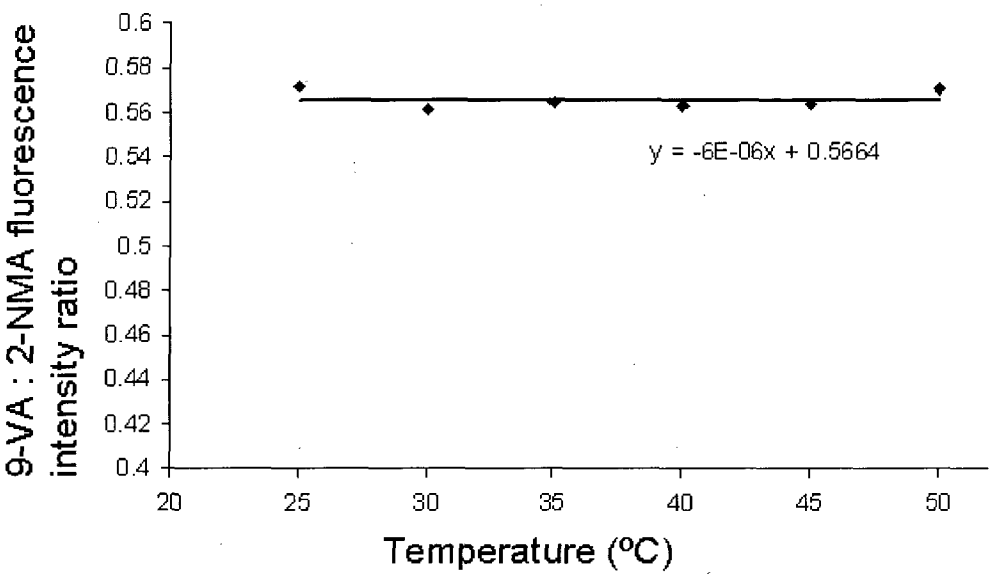

Figure 4.4: 9-VA :2-NMA fluorescence intensity ratio vs. temperature measured in ethanol.

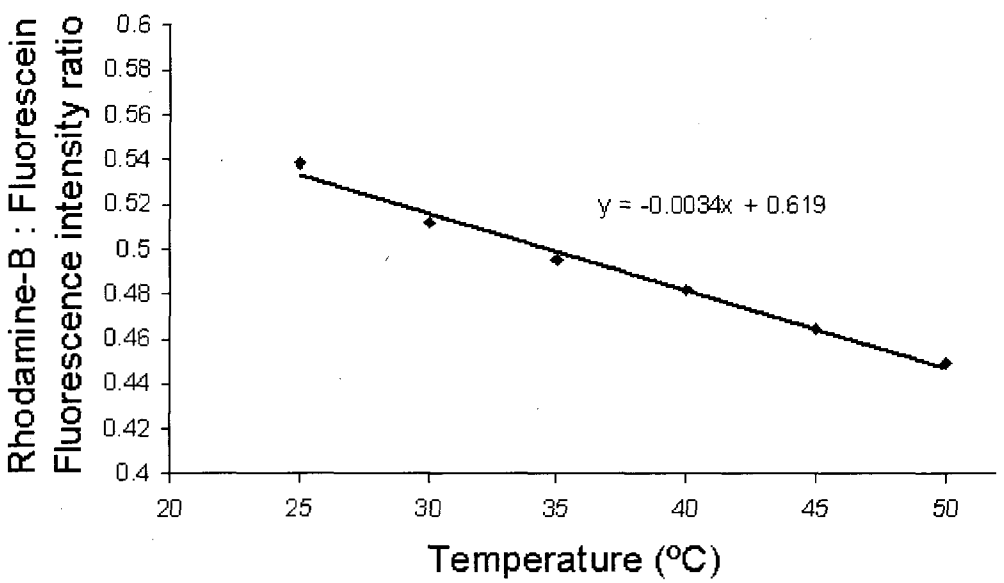

Figure 4.5: Fluorescein o-acrylate and methacryloxethyl thiocarbonyl rhodamine-B fluorescence intensity ratio vs. temperature measured in ethanol.

4.2.4 Fluorescence Measurements and Temperature Response of Poly (NIPAAm) Labeled with 2-NMA and 9-VA.

In this part, changes in the fluorescent intensities of 2-NMA and 9-VA were used in determining the temperature response for the polymer microparticles. The maximum emission wavelengths of the two fluorophores were obtained by spectrofluorometer using the scanning mode, while the absolute intensities were obtained by the kinetic mode. In the kinetic mode, the absolute fluorescence emission intensities of the two fluorophores were obtained simultaneously and hence avoid the decrease in the acceptor emission intensity resulting from settling of the microparticles with time when the scanning mode is used.

In the scanning mode, the shorter emission wavelengths are scanned before the longer wavelengths and therefore, the acceptor emission intensity is bound to decrease especially when the polymer microparticles settle to the bottom of the cuvette with time. 2.5mL of the fluorescent-labeled polymer suspensions in pH 6 MOP buffer were transferred into a cuvette and excited at 280nm. Fluorescent intensities of 2-NMA and 9-VA were measured at 343nm and 421nm respectively. The results show that as the temperature increases, the intensity ratio of 9-VA: 2-NMA increased. A slight decrease in fluorescence intensities of the two fluorophores was also observed.

As the temperature of the polymer microparticles rises, they collapse causing an increase in FRET efficiency. The decrease in fluorescence intensities is caused by polymer microparticles settling down at the bottom of the cuvette at temperatures above the LCST after collapsing. This results in a decrease in the number of fluorescent microparticles interacting with light in the spectrofluorometer. To verify the effect of

temperature changes on the swelling ability of the fluorescent labeled polymer microparticles, turbidity was measured for polymer microparticles immobilized in hydrogel membranes.

Figure 4.6 shows the decrease in fluorescence intensities of 2-NMA and 9-VA. A graph of fluorescence intensity ratio of 9-VA: 2-NMA vs. temperature of the polymer suspension was plotted and an increase in the intensity ratio with increase in temperature of the microparticles was observed. The phase transition temperature of polymer network decreased to about 30.1°C compared to that of Poly (NIPAAm) microparticles not copolymerized with 2-NMA and 9-VA monomers. This decrease in phase transition temperature is due to introduction of hydrophobic fluorescent groups within the polymer network, which causes the polymer microparticles to stay in collapsed form rather than in expanded form.

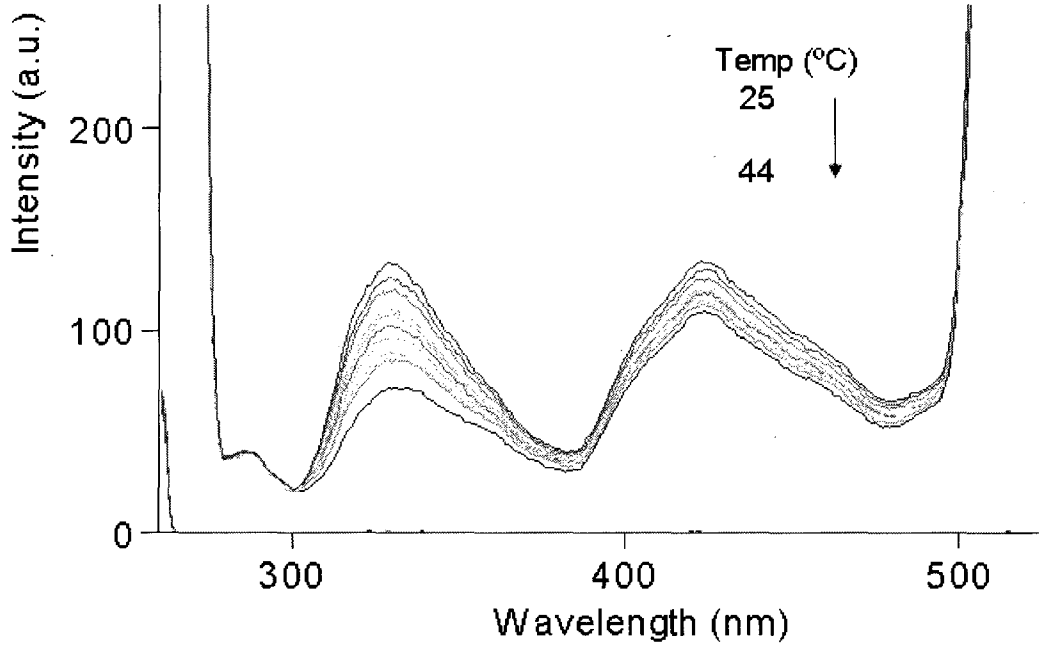

Figure 4.6: Fluorescence spectrum of poly (NIPAAm) labeled with 2-NMA and 9-VA.

A graph of the intensity ratio of 9-VA: 2-NMA was plotted and the results are shown in figure 4.7.

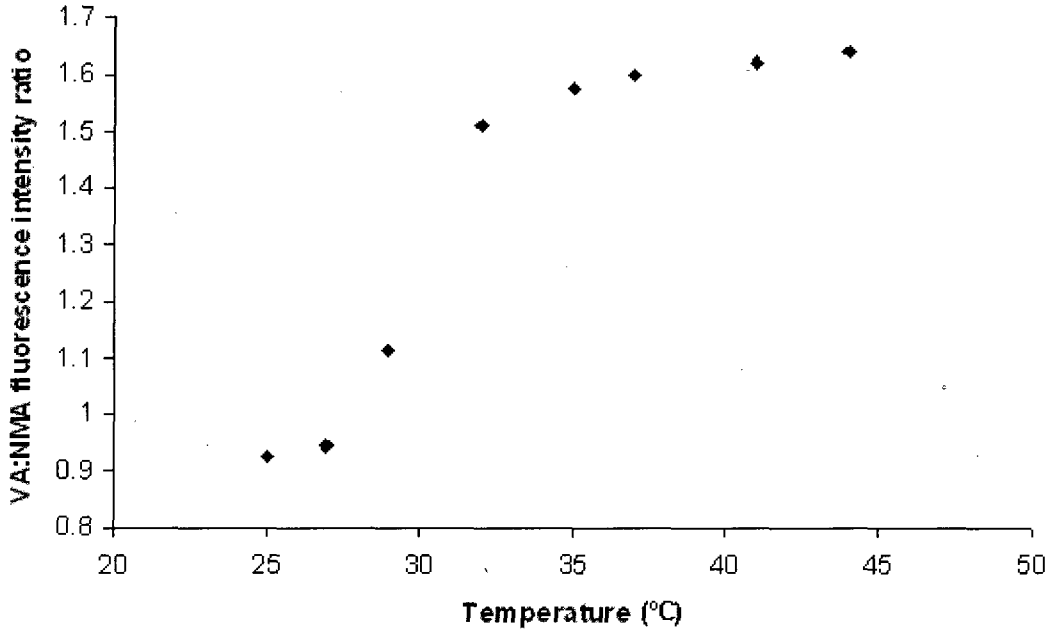

Figure 4.7: Temperature responsive of poly (NIPAAm) labeled with 2-NMA and 9-VA.

4.2.5 Fluorescence Measurements and Temperature Response of Poly (NIPAAm) Labeled with Fluorescein o-acrylate and Methacryloxethyl thiocarbonyl rhodamine-B Fluorophores.

In this part, changes in fluorescent intensities of fluorescein o-acrylate and methacryloxethyl thiocarbonyl rhodamine-B were used in determining the temperature response for the polymer microparticles. The fluorescent-labeled polymer suspensions were excited at 480nm and fluorescent intensities of fluorescein o-acrylate and methacryloxethyl thiocarbonyl rhodamine-B measured at 518nm and 584.5nm respectively at different temperatures. The fluorescence intensities of both fluorescein

o-acrylate and methacryloxethyl thiocarbonyl rhodamine-B decreased slightly with increasing temperature because of the polymer microparticles separating out of solution and setting to the top of the cuvette with time, and also due to thermal quenching.

The fluorescence intensities of fluorescein o-acrylate decreased more than those of methacryloxethyl thiocarbonyl rhodamine-B with increasing temperature. Methacryloxethyl thiocarbonyl rhodamine-B: fluorescein o-acrylate fluorescence intensity ratios were determined at various temperatures and were found to increase with increasing temperature, a confirmation that the FRET effect was more dominant than the thermal coefficients for the two fluorophores. A graph of the fluorescence intensity ratio of methacryloxethyl thiocarbonyl rhodamine-B: fluorescein o-acrylate vs. temperature of the polymer suspension was plotted and shown in Figure 4.8. The LCST of the polymer microparticles was found to be 34.5°C.

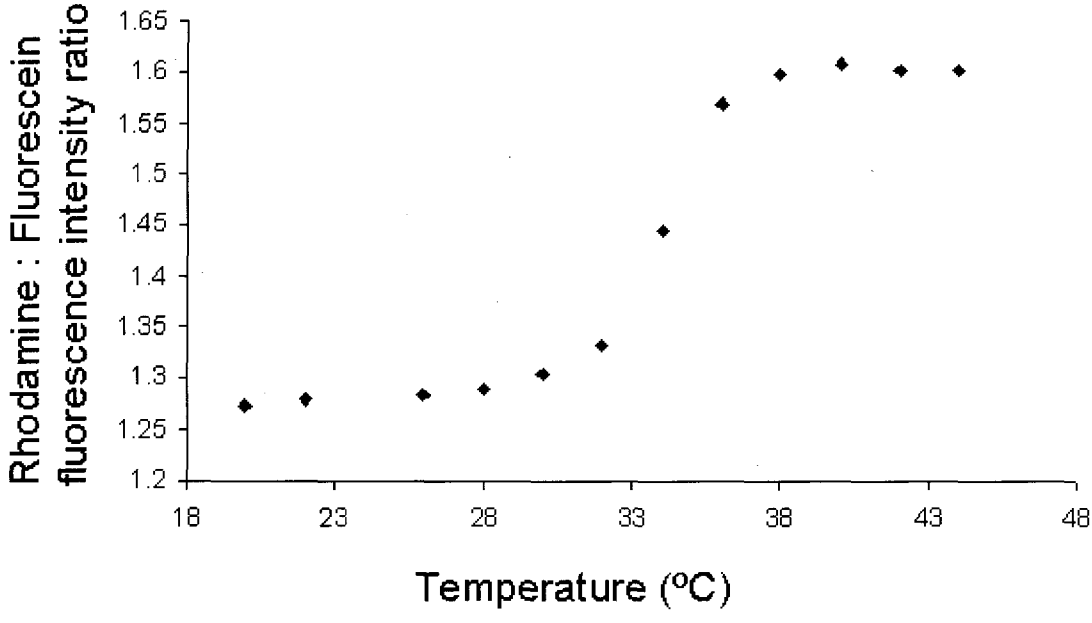

Figure 4.8: Temperature responsive characteristics of poly (NIPAAm) labeled with fluorescein o-acrylate and methacryloxethyl thiocarbonyl rhodamine-B.

4.3 Conclusions

Poly (NIPAAm) particles were prepared by dispersion polymerization in acetonitrile. The lightly cross-linked polymer microparticles were slightly coagulated but showed molecular specific swelling and shrinking properties with changes in temperature. Fluorescent-labeled Poly (NIPAAm) microparticles were also prepared in acetonitrile. The fluorescent-labeled polymer microparticles were also found to be temperature responsive. Copolymerizing NIPAAm with 2-NMA and 9-VA resulted in a slight decrease in the phase transition temperature (30.1°C), while copolymerizing NIPAAm with fluorescein o-acrylate and methacryloxethyl thiocarbonyl rhodamine-B produced a slight increase in the phase transition temperature (34.5°C) of the swellable polymer microparticles.

CHAPTER 5

DETERMINATION OF FORMATION CONSTANTS OF COPPER (II) COMPLEXES BY POTENTIOMETRIC TITRATION

5.1 Introduction.

The formation constants of metal ion complexes depend on factors such as; solvent, pH, charge on the metal ion, and also presence of attached groups to the non binding sites of the ligand which includes polymeric chains within the non-binding sites of the ligand. In Chapter 4, it was established that we could use FRET to show the swelling and shrinking of the polymer microparticles. The next step in the development of the sensor is to establish the strength and the stoichiometry of the binding between the metal ions and the ligands by using the swelling and shrinking property of the polymer microparticles with the ligands. In this chapter, formation constants of the copper (II) ion complexes with polymer microparticles containing ligands; hydrolyzed dibutyl-2,2'-(3-vinylphenylazanedyl) diacetate (DVPAA), N,N-bis (pyridin-2-ylmethyl)prop-2-en-1-amine (NBPMPA), and N-((4'-methyl-2,2'-bipyridin-4-yl) methyl)-N-propylacrylamide (NMPPAAm) were determined by potentiometric titration. The molecular structures of the ligands are shown in figure 5.1. The ligands were copolymerized with NIPAAm and suspensions of the polymer microparticles in pH 6, MOP buffer were used for the determination of formation constants. A copper (II) ion selective electrode was used to determine the concentration of free copper ions in the suspension after some of the copper (II) ions bind with the ligands. The electrode was

first calibrated using standard solutions of Cu^{2+} ions in pH 6, MOP buffer, and a calibration curve was plotted.

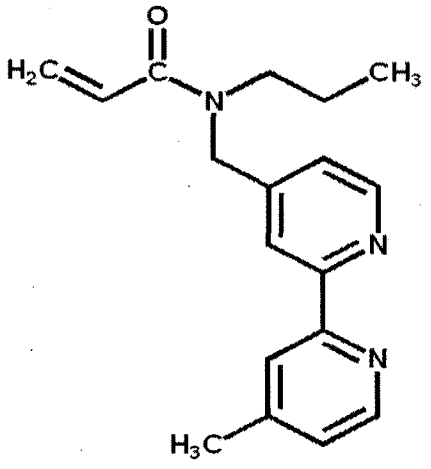

N-((4'-methyl-2,2'-bipyridin-4-yl) methyl)-N-propylacrylamide (NMPPAAm)

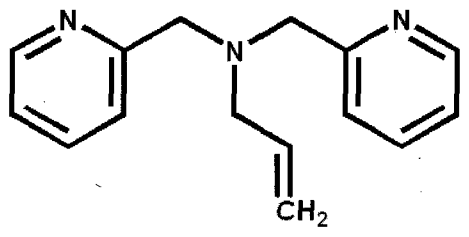

N,N-bis(pyridin-2-ylmethyl)prop-2-en-1-amine (NBPMPA)

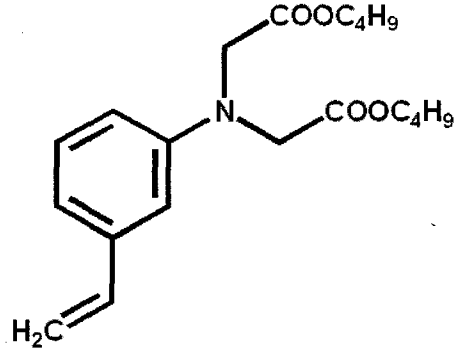

dibutyl 2,2'-(3-vinylphenylazanediyl)diacetate (DVPAA)

Figure 5.1: Molecular structures of the ligands.

5.2. Calibration of Cu^{2+} ion Selective Electrode

Copper (II) nitrate standard solutions with concentrations ranging from 10^{-1}- 10^{-6}M were prepared in pH 6 MOP buffer to calibrate the copper (II) ion selective electrode that was used later for the titration of the polymer microparticles with copper (II) ion. The calibration curve is shown in figure 5.2.

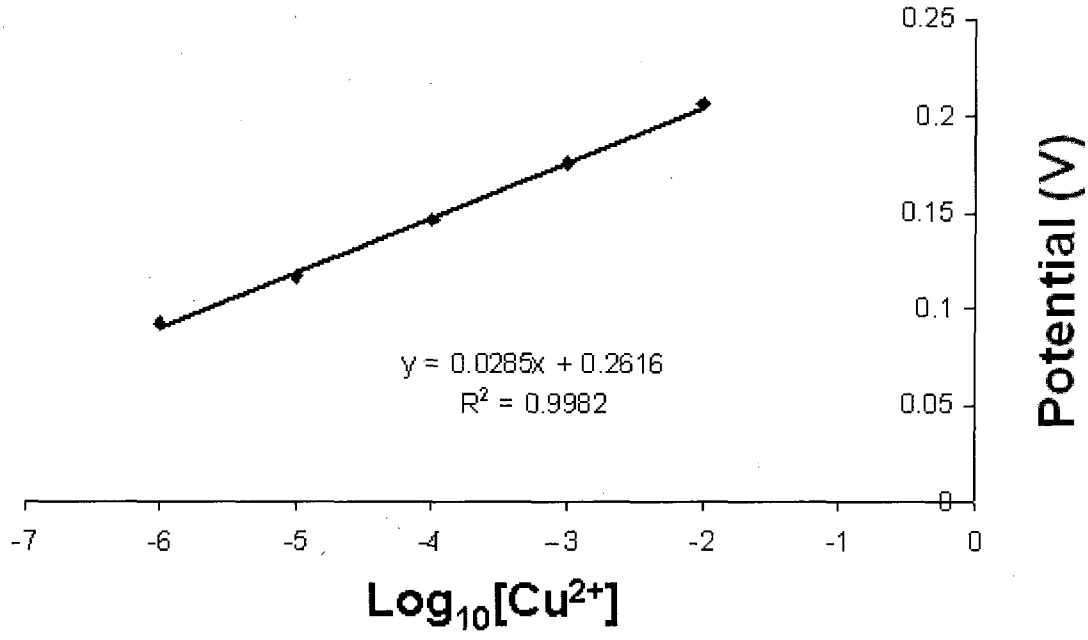

Figure 5.2: Calibration curve for the ion selective electrode.

5.3 Potentiometric Titration of the Hydrolyzed Poly (NIPAAm-co-DVPAA) Microparticles

Poly(NIPAAm-co-DVPAA) microparticles were synthesized by dispersion polymerization in acetonitrile. The microparticles were then isolated, and hydrolyzed. The polymerization formulation used was; 90 mole % NIPAAm, 5mole % DVPAA, 0.1 mole % 2-NMA, 0.05 mole % 9-VA, and 5mole % MBA. The total number of moles of the monomers was 10mmoles. 20%w/w of poly (styrene-co-acrylonitrile) was used as the stabilizer. The microparticles were hydrolyzed by suspending them in 2M sulfuric acid solution in a 100mL round bottom flask. The flask was then submerged in a water bath maintained at 35°C and left for 12 hours for completion of hydrolysis. The hydrolysis equation is shown in the figure below.

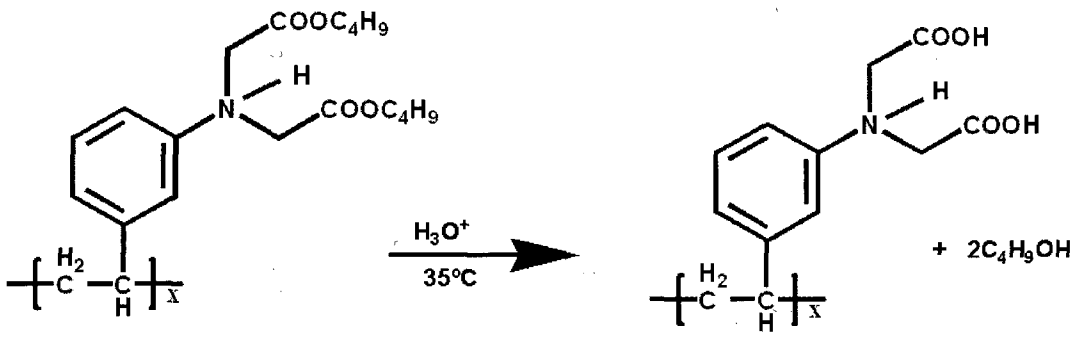

Figure 5.3: Hydrolysis of DVPAA moiety in the polymer network by H_2SO_4 solution.

After hydrolysis, the polymer microparticles were isolated from the acidic solution by centrifugation followed by washing several times with distilled water. 0.050g of the hydrolyzed polymer microparticles containing dibutyl-2, 2'-(3-vinylphenylazanediyl) diacetic acid was suspended in 20mL pH 6 MOP buffer and titrated with 10^{-3} M Cu^{2+} ions also in pH 6 MOP buffer, using the Cu^{2+} ion selective electrode to determine the formation constant of the complex. The ionic strength of the MOP buffer was adjusted to 0.1M using KCl. The potentiometric titration curve was plotted and the formation constant (K_f) of the resulting complex determined.

The formation constant (K_f) of the complex formed between the hydrolyzed polymer microparticles with the DVPAA ligand group and Cu^{2+} ions was determined as indicated in chapter 2 of this thesis and found to be 8.4×10^5. This is comparable to the literature K_{f1} value of the deprotonated phenyliminodiacetate ion ligand which is 2.5×10^6 [122]. The difference could be due to both polymerization and solvent effects. The polymerized ligand seems to have a lower binding constant with copper compared to the unpolymerized ligand although the two formation constants were determined under different solvent conditions. Comparing the formation constant obtained for the sensor to the one found in the literature for unpolymerized ligand, it is reasonable to

conclude that the binding between the polymerized ligand and the Cu^{2+} ions is 1:1 stoichiometry instead of 2:1 for the unpolymerized ligands.

The stoichiometry of the reaction was used to calculate the reacting moles of the ligand in the polymer microparticle suspension. About 88.0% of the ligand moiety reacted with the Cu^{2+} ions in the suspension according to the potentiometric titration curve. Some of the major causes leading to less ligand reacting with the Cu^{2+} ions in the suspension include both an incomplete polymerization process and hydrolysis of the polymer. Figure 5.4 shows the potentiometric titration curve of the polymer suspension.

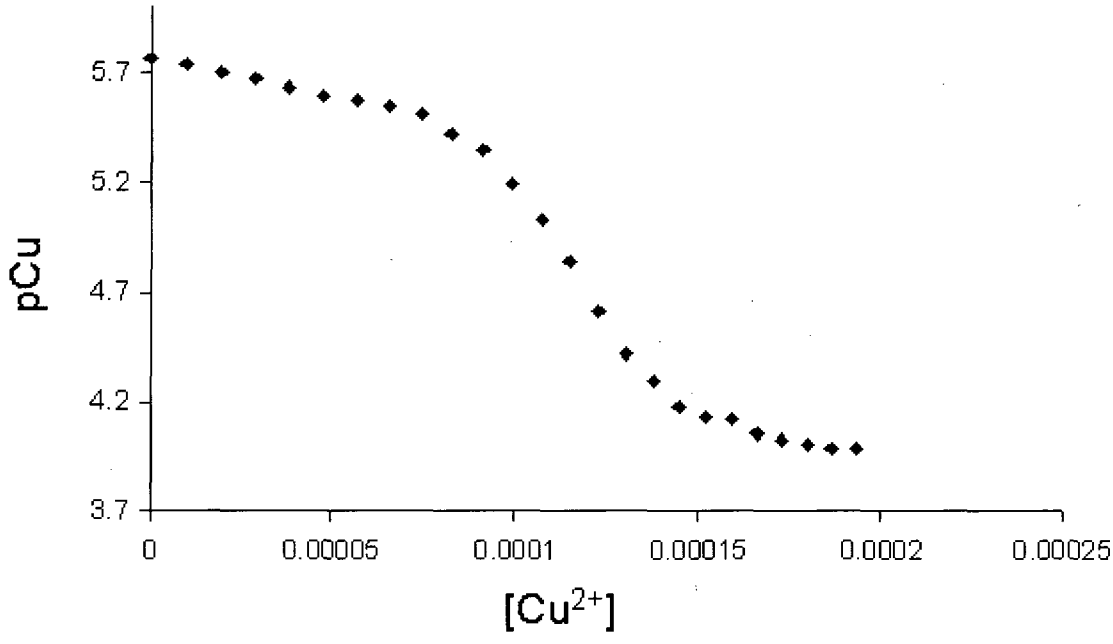

Figure 5.4: Potentiometric titration of poly (NIPAAm-co-DVPAA) microparticles suspended in pH 6 MOP buffer

5.4 Potentiometric Titration of Poly (NIPAAm-co-NMPPAAm) Microparticles

Poly (NIPAAm-co-NMPPAAm) microparticles were prepared by dispersion polymerization in acetonitrile. The polymerization formulation was; 90 mole % NIPAAm, 2 mole % NMPAAm, 0.1 mole % 2-NMA, 0.05 mole % 9-VA and 5mole % MBA. The total number of moles of the monomers was 10mmoles. 20%w/w of poly (styrene-co-acrylonitrile) was used as the stabilizer. 0.012g of the microparticles were suspended in 20mL, MOP buffer pH 6 with the ionic strength adjusted to 0.1M using KCl. The suspension was then titrated with 10^{-4}M Cu^{2+} ions in pH 6 MOP buffer using a Cu^{2+} ion selective electrode. A potentiometric titration curve was plotted and the formation constant for Cu^{2+}-NMPPAAm ligand complex determined. The formation constant (K_f) was determined to be 2.6×10^7.

There was no literature K_{f1} value for NMPPAAm ligand binding with Cu^{2+} ions, but the K_{f1} value obtained from the literature for the bipyridine-Cu^{2+} complex was 1.0×10^8 [123]. The K_{f1} values for bipyridine ligand binding with the metal ions obtained from the literature was found to increase with an increase in number of methyl or ethyl groups attached to the bipyridine ligand [118]. The position of the methyl or ethyl group on the bipyridine ring also affects the K_{f1} values with the groups attached to the para-position having the highest K_{f1} values.

Figure 5.5 is the titration curve obtained when polymer microparticles containing NMPPAAm suspended in MOP buffer pH 6 were titrated with Cu^{2+} ions. The exact equivalence point was determined by plotting the derivative of the potential vs. volume curve (dPotential / volume). The calculated K_f value for the polymerized

NMPPAAm-Cu^{2+} complex is comparable to the literature K_{f1} value for the unpolymerized bipyridyl ligand. This leads to a conclusion that the binding between the NMPPAAm and Cu^{2+} ions is a 1:1 stoichiometry. This stoichiometry was used in calculating the percentage of NMPPAAm ligand that reacted with the Cu^{2+} ions in the polymer microparticle suspension. About 83.7% of the ligand moiety reacted with the Cu^{2+} ions in the suspension according to the potentiometric titration curve. This loss in moles of ligand moiety may be due to incomplete polymerization.

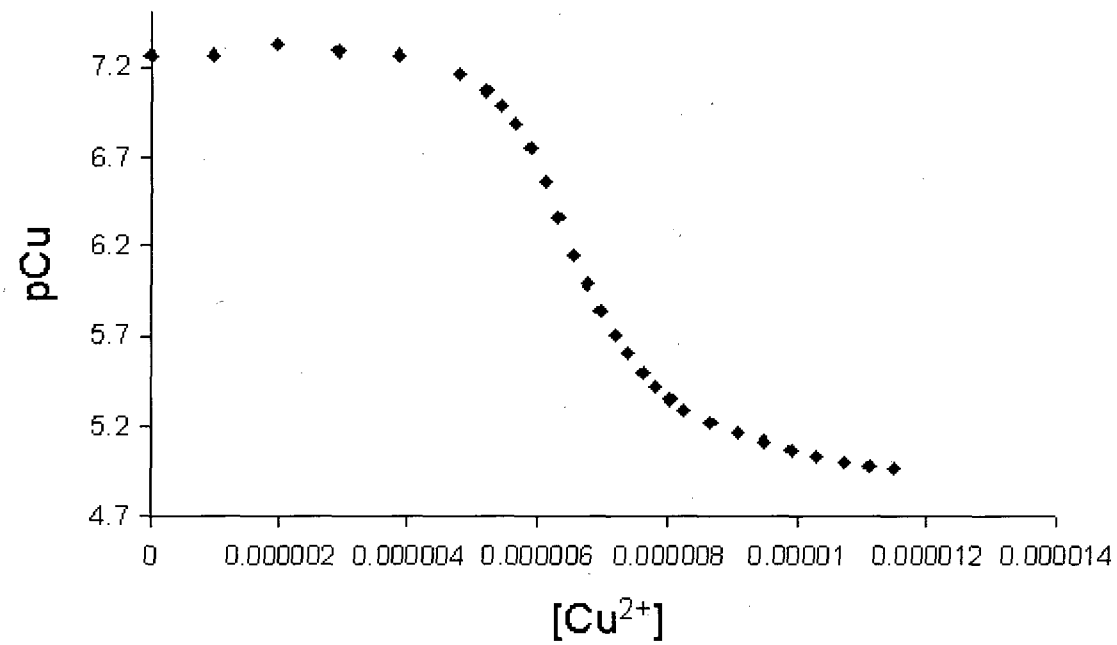

Figure 5.5: Potentiometric titration of poly (NIPAAm-co-NMPPAAm) polymer particles suspended in pH 6 MOP buffer.

5.5 Potentiometric Titration of Poly (NIPAAm-co-NBPMPA) Microparticles

Poly (NIPAAm-co-NBPMPA) microparticles were prepared by dispersion polymerization in acetonitrile. The polymerization formulation was: 90 mole % NIPAAm, 2 mole % NBPMPA, 0.1 mole % 2-NMA, 0.05 mole % 9-VA, and 5mole % MBA. The total number of moles of the monomers was 10mmoles. 20%w/w of poly (styrene-co-acrylonitrile) was used as the stabilizer. 0.015g of the microparticles was suspended in 20mL, pH 6 MOP buffer with the ionic strength adjusted to 0.1M using KCl. The microparticles were then titrated with 10^{-4}M Cu^{2+} ions using a Cu^{2+} ion selective electrode. A potentiometric titration curve was plotted and used in determining the formation constant of the Cu^{2+}-NBPMPA ligand complex. The titration curve has one equivalence point as shown in figure 5.6. The formation constant (K_f) was determined to be 3.1×10^8 which is several orders of magnitude lower than the K_{f1} value for Cu^{2+}-di-2-picolylamine (DPA) complex found in the literature which is 2.5×10^{14} [124]. The formation constant is a conditional formation constant, which depends on the pH of the reaction medium; it decreases with a decrease in pH. At pH 6, the nitrogen forming the imino group is positively charged and weakly bind to the Cu^{2+} ions.

The calculated conditional formation constant for the Cu^{2+}-DPA complex at pH 6 was about 1.6×10^{10} which is almost two orders of magnitude higher than the formation constant for the Cu^{2+}-NBPMPA complex obtained from the sensor. The conclusion that the Cu^{2+}-NBPMPA complex was a 1:1 stoichiometry was drawn from the fact that the conditional formation constant was less than the K_{f1} value found in

the literature and also from the fact that the titration curve has only one equivalence point. This conclusion was used in calculating the percentage of NBPMPA reacted with the Cu^{2+} ions in the solution. About 84.0% of the ligand moiety reacted with the Cu^{2+} ions in the suspension according to the potentiometric titration curve. This could be due to incomplete polymerization or incomplete complexation reaction between Cu^{2+} ions and the NBPMPA ligand groups.

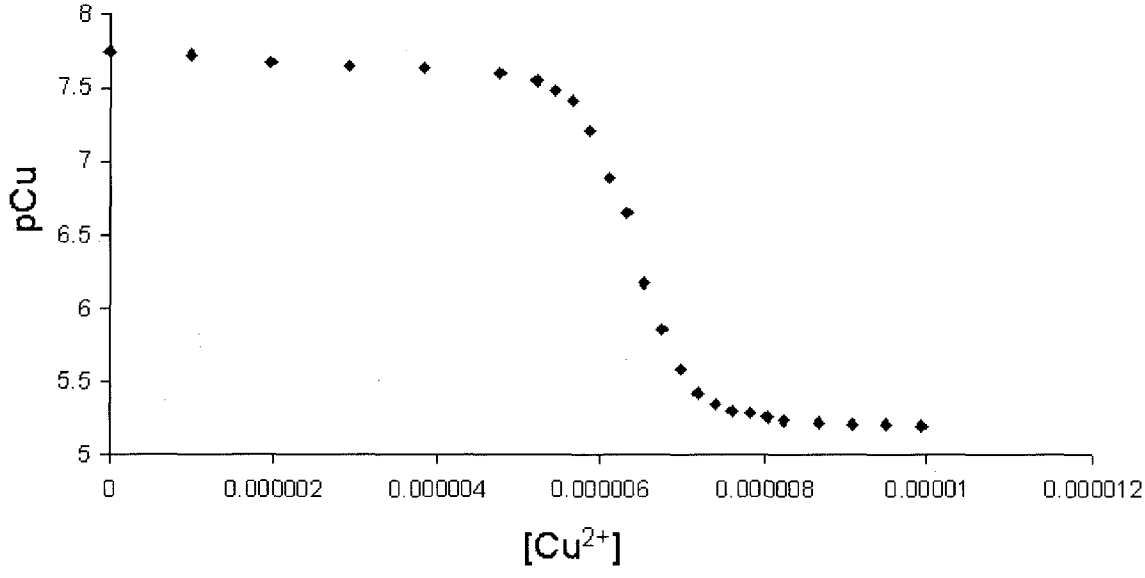

Figure 5.6: Potentiometric titration of poly (NIPAAm-co-NBPMPA) polymer particles suspended in pH 6 MOP buffer.

5.6 Conclusions

The potentiometric titrations of poly (NIPAAm-co-NMPPAAm), poly (NIPAAm-co-NBPMPA), and hydrolyzed poly (NIPAAm-co-DVPAA) microparticles with Cu^{2+} ions confirmed the binding between the ligand moieties within the polymer microparticles and the Cu^{2+} ions. A comparison of the formation constants of the complexes formed by these polymerized ligands and Cu^{2+} ions with the K_{f1} values from literature for unpolymerized ligands with the same binding sites indicates a 1:1 stoichiometric

reaction. This conclusion is further supported by the presence of only one equivalence point in the potentiometric titration curves. Polymerization of the ligands results in weakening the binding between the ligands and Cu^{2+} ions causing a decrease in the formation constants.

CHAPTER 6

PREPARATION OF SWELLABLE FLUORESCENT LABELLED POLY (NIPAAm-co-AIDA) AND POLY(NIPAAm-co-DVPAA) PARTICLES FOR TRANSITION METAL ION SENSING

6.1 Introduction

The application of functionalized swellable polymers is currently among the expanding fields in research. A good number of functionalized swellable polymers have been developed for use in analysis of biomolecules, in molecular imprinting, and also in the analysis of transition metal ions in environmental systems. In the analysis of biomolecules, the functionalized swellable polymer networks are prepared by copolymerizing the monomers which provide the polymer with swelling properties with monomers that interact with the template molecules via either hydrogen bonding or reversible covalent bonds.

For analysis of transition metal ions, the polymers interact with the metal ions via coordination between the metal ions and the binding sites of the chelating ligands within the polymer network. Some of the binding sites of the ligands are charged and produce inter-electrostatic repulsion within the polymer chains, resulting in expansion of the polymer network [40]. In an anionic polymer network containing carboxylic acid groups, ionization of the functional group takes place as the pH of the swelling medium increases above the pKa of the acidic moiety. The polymer network becomes more

hydrophilic as the pH increases above the pKa of the ionizable group. When these charged groups interact with positively charged metal ions, the charges are neutralized, reducing the electrostatic repulsion between the remaining charged groups. This causes shrinking of the polymer microparticles. This swelling and shrinking phenomenon of polymer microparticles when complexing with metal ions can be employed in; analysis of the metal ions, treatment of dilute aqueous effluents to recover precious metals, removal of toxic and radioactive elements from various effluents, and also preconcentration of metals for environmental sample analysis.

In this chapter, FRET was used to investigate the interaction between the metal ions and the ligands within the functionalized swellable poly (NIPAAm) microparticles. The lightly crosslinked polymer microparticles were labeled with two fluorescent monomers. The interaction of these metal ions with the ligands causes a change in the size of the polymer microparticles which is translated in to a change in the fluorescence intensity ratio of the two fluorophores. The monomers; 2, 2'-acrylamidodiacetic acid (AIDA), and dibutyl-2,2'-(3-vinylphenylazanedyl) diacetate (DVPAA) were used as ligands to create binding sites with the transition metal ions. The molecular structure of AIDA is shown in Figure 6.1, and that of DVPAA is given in Figure 5.1 of Chapter 5 of this thesis. The DVPAA groups in the polymer network were acid hydrolyzed producing diacetate groups that bind to metal ions at pH 6. The monomers; 2-NMA, 9- 9-VA, methacryloxethyl thicarbonyl rhodamine-B, and fluorescein o-acrylate were used as fluorescent labels in the co-polymerization process. Because the experimental procedure involves suspending the polymer microparticles in a pH 6 MOP buffer, there is possibility of the microparticles settling at the bottom of cuvette or

at the top part of the pH 6 buffer solutions after shrinking. Second order light scattering by the microparticles was used to study how this affects the response to copper (II) ions.

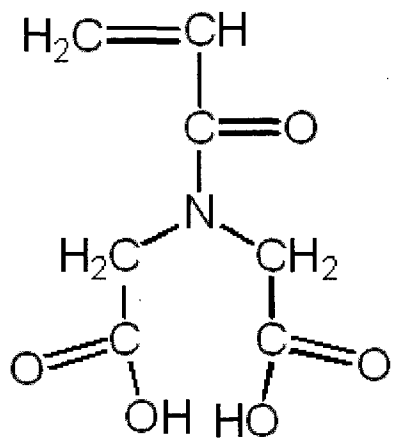

Figure 6.1: Molecular structure of 2, 2'-acrylamidodiacetic acid (AIDA)

Poly (NIPAAm) microparticles are swollen at temperatures below the LCST and shrunken at temperatures above the LCST. The principle can be used in studying the stimuli response especially in thermal responsive systems. In the swollen microparticles, the fluorophores are further apart within the polymer network than in the shrunken microparticles, decreasing the FRET efficiency. The polymer microparticles containing both AIDA and the hydrolyzed DVPAA groups are swollen at pH 6 because the diacetate groups are negatively charged and repel one another. The binding of metal ions to these microparticles is expected to neutralize the negative charges causing the microparticles to shrink, enhancing the energy transfer efficiency.

6.2 Preparation of Poly(NIPAAm-Co-AIDA) Labeled with Methacryloxethyl thiocarbonyl rhodamine-B and Fluorescein o-acrylate

Poly (NIPAAm-co-AIDA) microparticles labeled with methacryloxethyl thiocarbonyl rhodamine-B and fluorescein o-acrylate were prepared by dispersion polymerization in acetonitrile. 5 mole % of the AIDA ligand, 0.1 mole % fluorescein o-acrylate, 0.04 mole % methacryloxethyl thiocarbonyl rhodamine-B, and 5mole % MBA were used in the polymerization formulation. The total moles of monomers used was 10mmoles. The polymerization process was carried out according to the procedure already stated in chapter 3 of this thesis.

6.3 Polymer Microparticle Settling and its Effect on the Fluorescence Intensity Ratio

Because of the possibility of the polymer microparticles in the suspension separating from the solution by settling due to the density difference between the polymer microparticles and the buffer solution, the effect of settling of the microparticles was investigated by measuring fluorescence intensities and second order light scattering. Also the rate of microparticle settling was investigated by measuring the change in fluorescence intensities and second order light scattering with time.

After polymerization, the polymer microparticles were isolated and cleaned as already discussed in chapter 3 of this thesis. 0.15g of the resulting polymer microparticles were suspended in 100.00mL MOP buffer pH 6. 2.50mL of the suspension was transferred to a quartz cuvette and inserted into the cuvette holder in

the spectrofluorometer. The microparticles were then excited at the excitation wavelength of the donor fluorophore. The spectrofluorometer was set to the scanning mode to obtain the maximum emission wavelengths of the two fluorophores and also the second order light scattering peak. The spectrofluorometer was then set to the kinetic mode to determine the changes in both the fluorescence intensities of the two fluorophores, and also the second order light scattering by the microparticles with time.

6.4 Analysis of Transition Metal Ions

2.5mL aliquots of the polymer microparticle suspension prepared according to procedure stated in section 6.3 above were titrated with various standard solutions of 10^{-3} M metal ions. The suspended polymer microparticles were excited at 480nm and the intensity ratios of methacryloxethyl thiocarbonyl rhodamine-B: fluorescein o-acrylate was determined as the concentrations of the metal ions were increased in the polymer suspension. The emission wavelengths of the two fluorophores were obtained by scanning mode while the absolute intensities were obtained by kinetic mode. A graph of methacryloxethyl thiocarbonyl rhodamine-B: fluorescein o-acrylate fluorescence intensity ratio vs. concentration of the various metal ions was plotted. A control experiment was performed by titrating fluorescent labeled poly (NIPAAm) that was not co-polymerized with ligands.

6.5. Results and Discussion

6.5.1. Microparticle Size and Size Distribution

Scanning electron micrograph pictures of the polymer microparticles were taken to determine the size of the polymer microparticles, and also size distribution. The microparticles were found to be coagulated with an average diameter of about 0.95μm. The scanning electron micrographs of the resulting polymer microparticles are shown in Figure 6.2. The microparticles are slightly less dense than the pH 6 MOP buffer solution and hence rise to the top section of the solution in the cuvette.

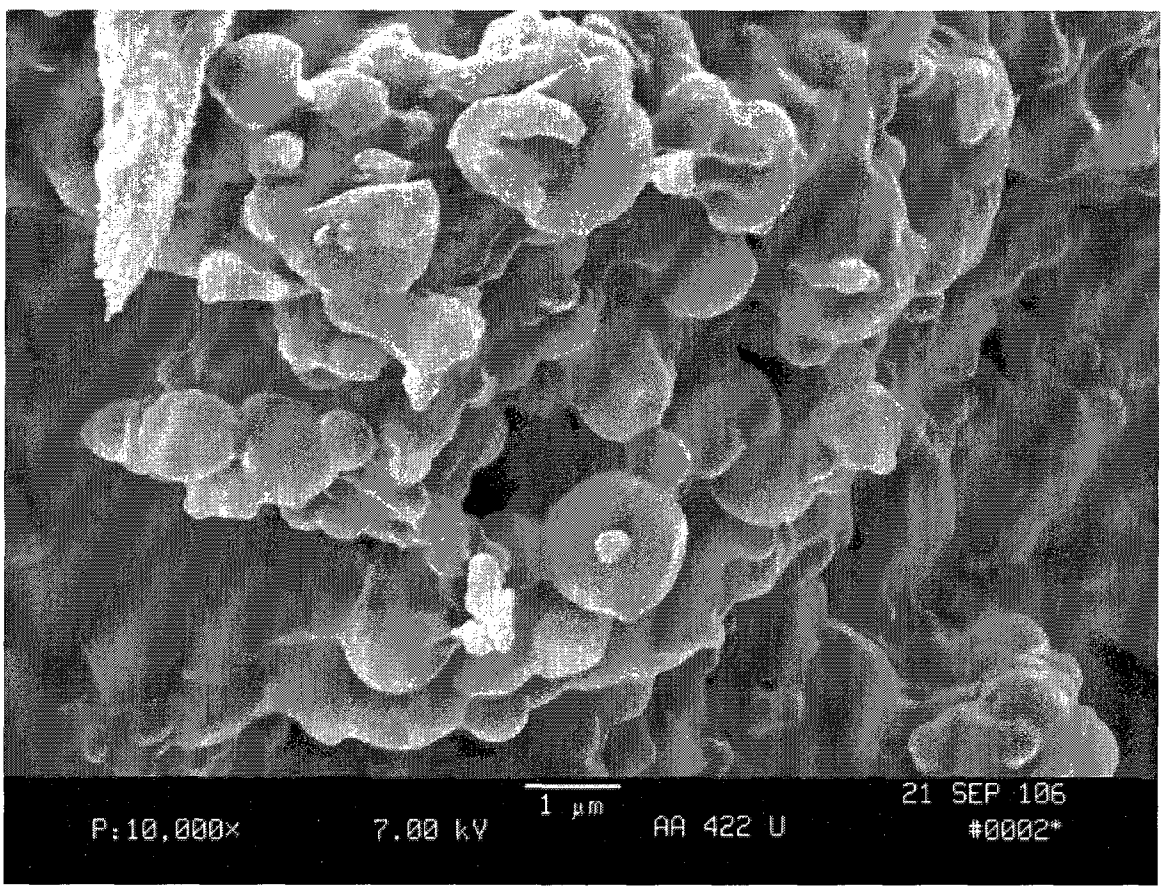

Figure 6.2: Scanning Electron Micrograph of Poly (NIPAAm-co-AIDA) labeled with methacryloxethyl thiocarbonyl rhodamine-B and fluorescein O-acrylate

6.5.2 Investigating Settling of Polymer Microparticles by Fluorescence and Second Order Light Scattering

The microparticles were excited at 480nm and both fluorescence intensities and second order light scattering were measured at 25°C and 40°C. The changes in these measurements were used to determine the settling rate of the polymer microparticles. The settling rate was very slow when the microparticles are left undisturbed. Figure 6.3 shows the change of fluorescence intensities of the two fluorophores with time. The methacryloxethyl thiocarbonyl rhodamine-B: fluorescein o-acrylate fluorescence intensity ratio decreased insignificantly, decreasing by only about 0.005units at both 25°C and 40°C over a period of 40minutes. This confirms that settling of the microparticles does not significantly affect the FRET efficiency between the donor and acceptor fluorophores. Second order light scattering also decreased slightly with time as can be seen in figure 6.4.

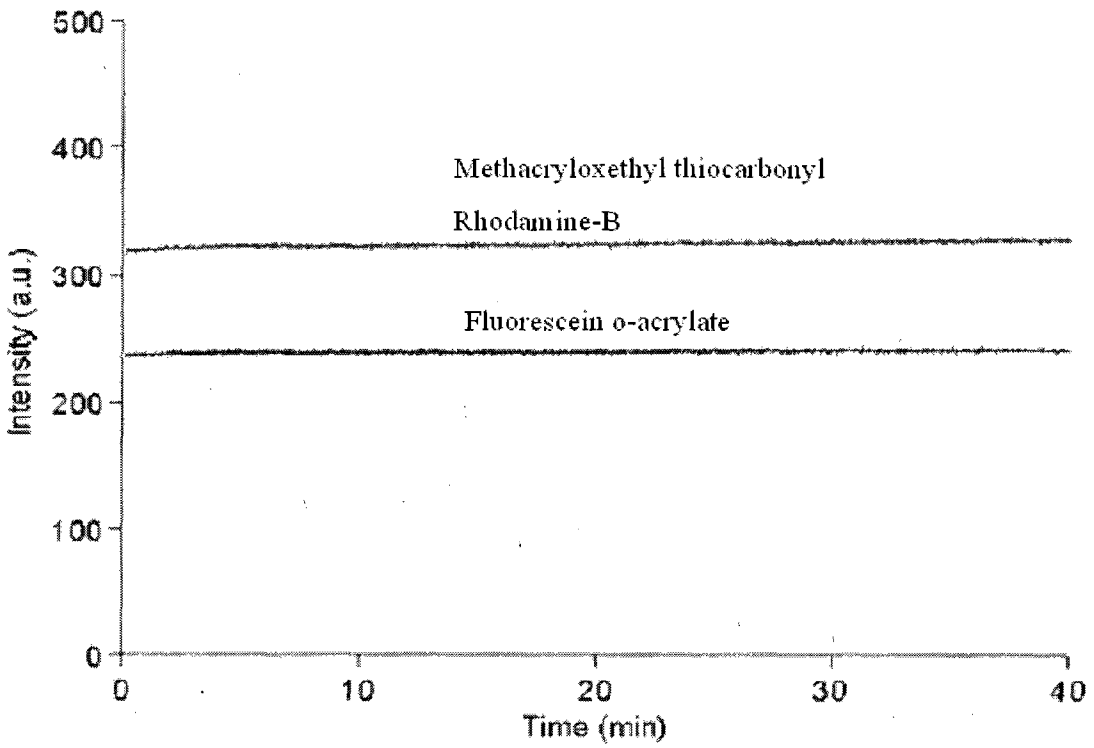

Figure 6.3: Methacryloxethyl thiocarbonyl rhodamine-B and fluorescein o-acrylate fluorescence intensities vs. time at 25°C.

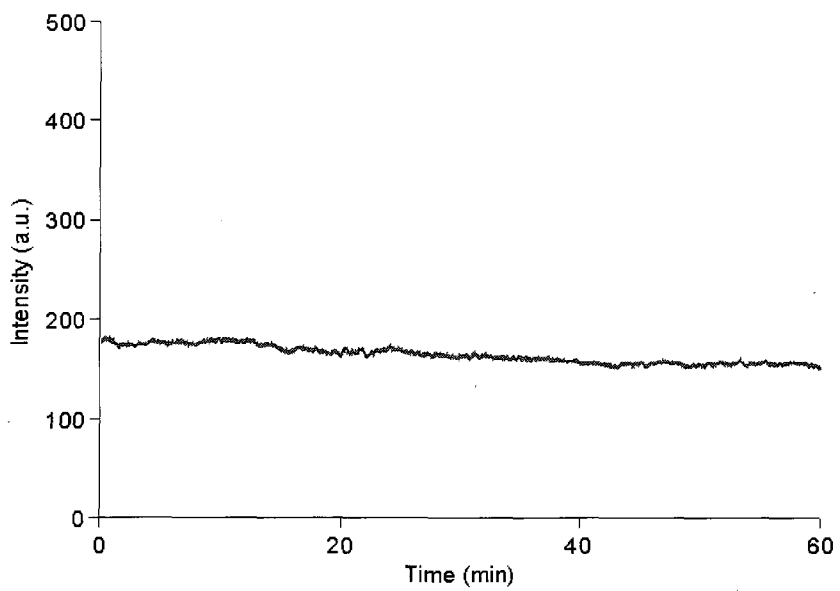

Figure 6.4: Second order light scattering of poly (NIPAAm-Co-AIDA) labeled with 2-NMA and 9-VA fluorophores.

6.5.3. Fluorometric Titration of Poly (NIPAAm-co-AIDA) with Solutions of Metal Ions

There was no change in the fluorescent intensity ratio with increase in concentration of Cu^{2+}, Co^{2+}, Pb^{2+}, and Zn^{2+} ions suggesting that there is no binding between the diacetate ions within the polymer microparticles and the metal ions in the solution. The concentration range of metal ions used were 0-1.6x10^{-4}M. A possible explanation to this is attributed to the small binding constant of AIDA with Cu^{2+} ions. The small binding constant indicates that there is weak binding between the diacetate ions and the metal ions because the nitrogen in acrylamidodiacetate ion is an amide group which does not bind with the metal ion. Figure 6.5 shows methacryloxethyl thiocarbonyl rhodamine-B: fluorescein O-acrylate fluorescence intensity ratio vs Cu^{2+} ions at 25°C and 50°C.

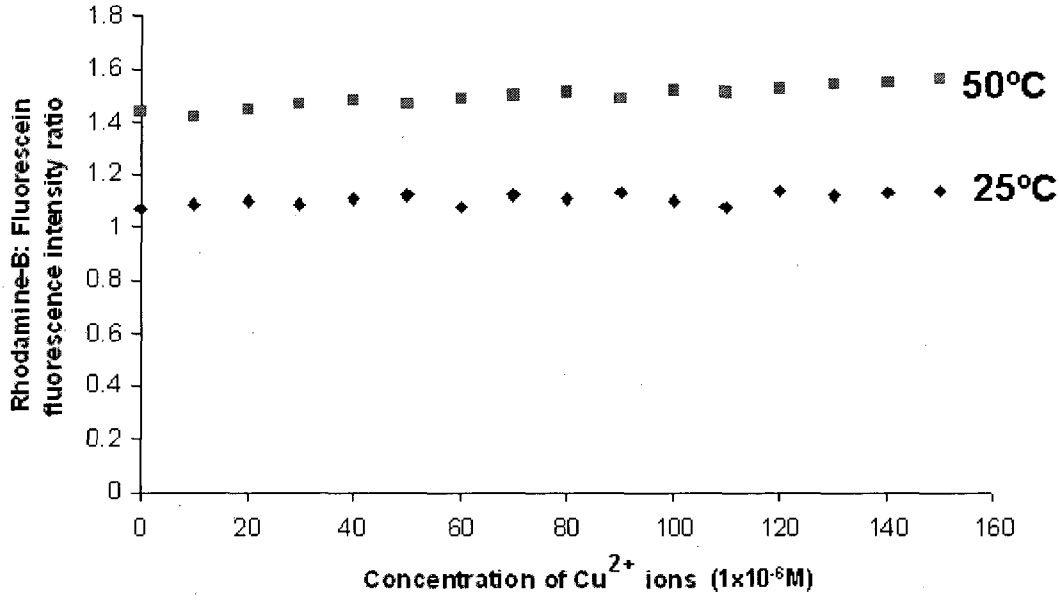

Figure 6.5: Methacryloxethyl thiocarbonyl rhodamine-B: fluorescein o-acrylate intensity ratio vs. concentration of Cu^{2+} ions added to poly (NIPAAm-co-AIDA) suspended in pH 6 MOP buffer.

6.6 Preparation of Poly (NIPAAm-Co-DVPAA) Labeled with 2-NMA and 9-VA Fluorophores.

In this polymer synthesis, dibutyl 2, 2′-(3-vinylphenylazane diyl) diacetate (DVPAA) was copolymerized with NIPAAm. 2-NMA and 9-VA were used as fluorescent monomers. Poly (NIPAAm-co-DVPAA) microparticles labeled with 2-NMA and 9-VA were prepared by dispersion polymerization in acetonitrile. 5 mole % of the DVPAA ligand, 0.1 mole % 2-NMA, 0.05 mole % 9-VA, and 5mole % MBA were used in the polymerization formulation. The total number of moles of monomers used was 10mmoles excluding the 20%w/w of poly (styrene-co-acrylonitrile) stabilizer used. The polymer synthesis was performed according to the procedure already discussed in chapter 3 of this thesis. The resulting polymer particles were then isolated by centrifugation and washed several times with de-ionized water. The polymer microparticles were hydrolyzed in acid medium according to the procedure given in Chapter 5 of this thesis to produce the acid form; 2, 2'-(3-vinylphenylazanediyl) diacetic acid which is a tridentate ligand.

6.7 Analysis of Transition Metal Ions

0.0145g of the hydrolyzed polymer microparticles were suspended in 100.00mL of pH 6 MOP buffer. 2.5mL of this polymer suspension was titrated with various standard solutions of transition metal ions such as Cu^{2+}, Pb^{2+}, Zn^{2+}, and Co^{2+} to investigate its binding with these metal ions. The emission wavelengths of the two fluorophores were obtained by scanning mode while the absolute intensities were obtained by kinetic mode. The fluorescence intensity ratios recorded in this chapter

were corrected by subtracting the effect of intensity ratio caused by settling of microparticles, temperature coefficient, and also fluorescence quenching by copper (II) ions from the observed intensity ratio caused by the concentration changes of Copper (II) ions. A control experiment was also performed by titrating suspensions of the unhydrolyzed polymer particles in pH 6 MOP buffer with various transition metal ions.

6.8. Results and Discussion

6.8.1 Particle Size and Size Distribution

Scanning electron micrograph pictures of the polymer microparticles were taken to determine the microparticle size and also the size distribution. Due to the non-spherical nature of the microparticles, it was difficult to determine the actual size of the microparticles, however, the average diameter of the microparticles was estimated to be about 0.4μm. The microparticles also appeared to be dispersed as can be seen in the scanning electron micrographs of the polymer microparticles in figure 6.6.

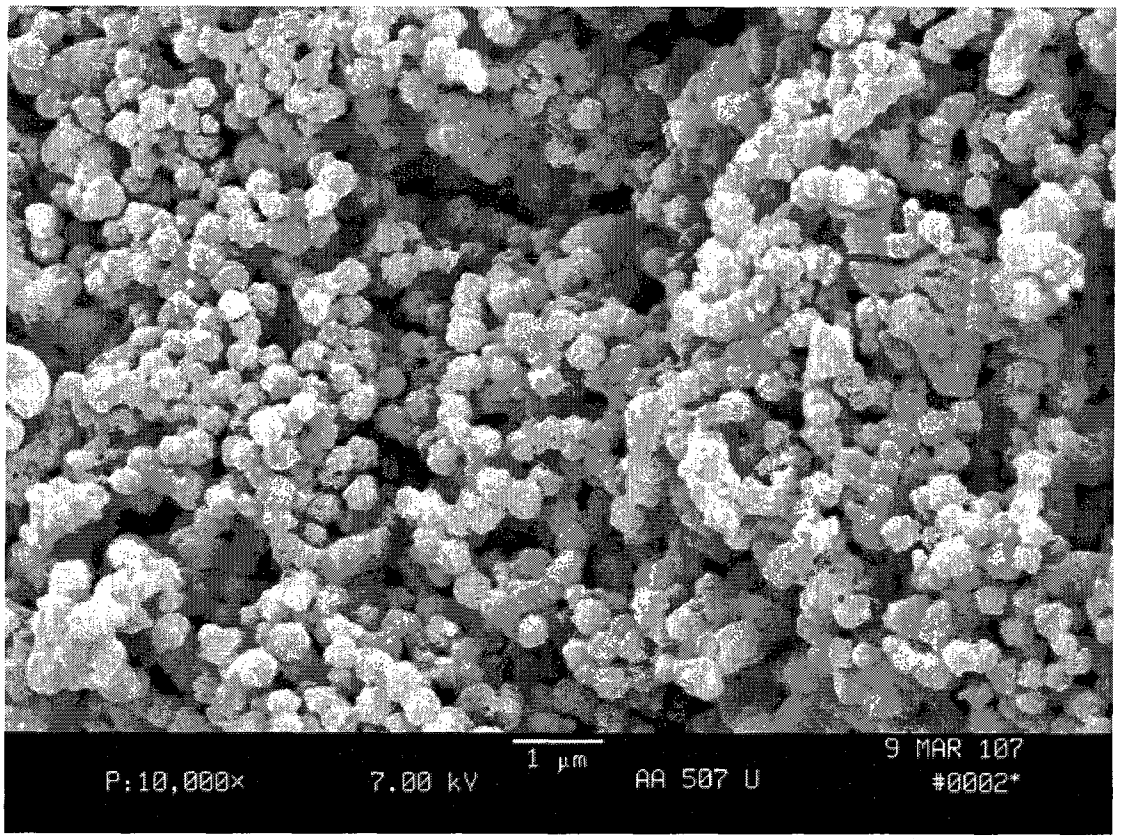

Figure 6.6: Scanning Electron Micrograph of poly (NIPAAm-co-DVPAA) labeled with 2-NMA and 9-VA.

6.8.2 Investigating the Settling of Polymer Microparticles by Fluorescence and Second Order Light Scattering

2.5mL of polymer microparticle suspension prepared according to the procedure stated in section 6.7 of this thesis was transferred to a cuvette, inserted in the cuvette holder in the spectrofluorometer and excited at 260nm. Fluorescence intensities of both 2-NMA and 9-VA, and also second order light scattering were obtained at 25 °C and 40 °C for a period of one hour. The rate of settling of the polymer microparticles was determined from the changes of both fluorescence intensities of the two fluorophores and the second order light scattering. In this case, the microparticles

settled at the bottom of the cuvette instead of settling towards the top part of the cuvette as seen when using methacryloxethyl thicarbonyl rhodamine-B and fluorescein o-acrylate fluorescent monomers.

The settling rate of polymer microparticles was found to be slow as shown in both figures 6.7 and 6.8. A significant decrease in the fluorescence intensities of the two fluorophores was observed, but the 9-VA: 2-NMA fluorescence intensity ratio only increased by about 0.01 within a period of one hour. At 40 °C the fluorescence intensities of both 9-VA and 2-NMA decreased significantly with no significant decrease in the intensity ratio. The second order light scattering also decreased at a faster rate at 40 °C indicating that the microparticles were settling to the bottom of the cuvette much faster because they shrunk in size.

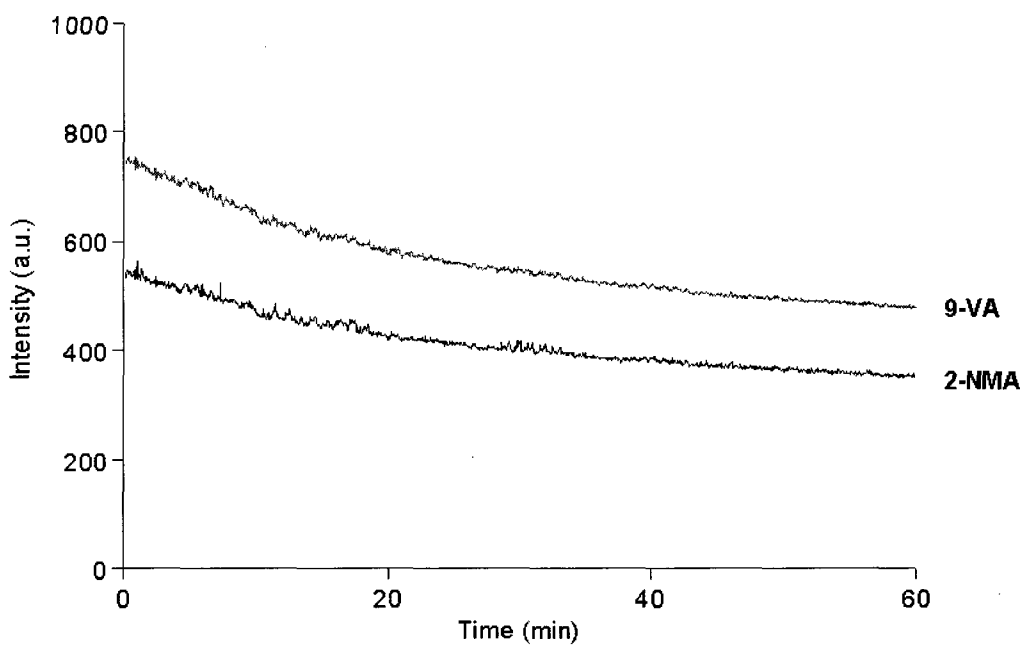

Figure 6.7: 9-VA and 2-NMA fluorescence intensities vs. time at 25°C.

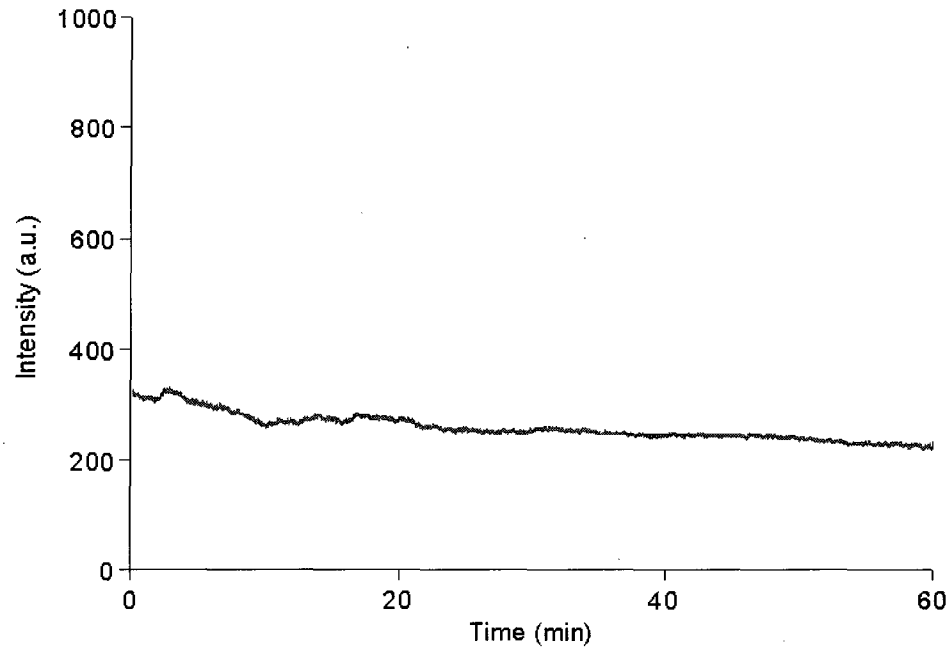

Figure 6.8: Second order light scattering of poly (NIPAAm-Co-DVPAA) labeled with 2-NMA and 9-VA fluorophores.

6.8.3 Thermal Response of Both Hydrolyzed and Unhydrolyzed Poly (NIPAAm-co-DVPAA)

Both hydrolyzed and unhydrolyzed poly (NIPAAm-co-DVPAA) labeled with 9-VA and 2-NMA fluorophores were suspended in pH 6 MOP buffer and the 9-VA: 2-NMA fluorescence intensity ratio was determined for various temperatures. The results are shown in figure 6.9. The results show no increase in fluorescence intensity ratio for the hydrolyzed polymer microparticles because they were swollen even at higher temperature and hence did not undergo phase transition. The unhydrolyzed polymer microparticles underwent phase transition and had a phase transition temperature.

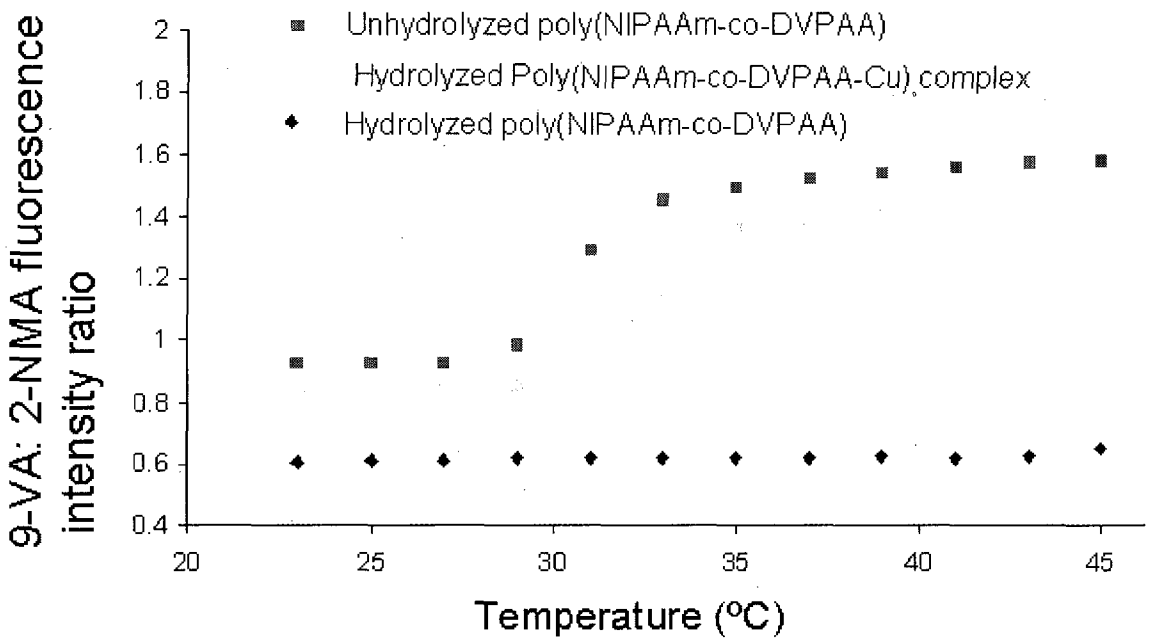

Figure 6.9: 9-VA: 2-NMA fluorescence intensity ratio of poly (NIPAAm-co-DVPAA vs. temperature.

6.8.4 Control Experiment for the Binding of Cu^{2+} Ions to the Poly (NIPAAm) Polymer Particles Suspended in pH 6 MOP Buffer.

Control experiments to determine whether Cu^{2+} ions bind to non-functionalized poly (NIPAAm) microparticles were performed by suspending the fluorescent labeled poly (NIPAAm) microparticles without ligand in pH 6 MOP buffer and adding aliquots of 10^{-3}M Cu^{2+} ions. Figure 6.10 shows the results of the titration of the polymer microparticle suspension with a solution of Cu^{2+} ions. There is no binding of Cu^{2+} ions with the poly (NIPAAm) polymer particles as indicated by no change in 9-VA: 2-NMA fluorescence intensity ratio.

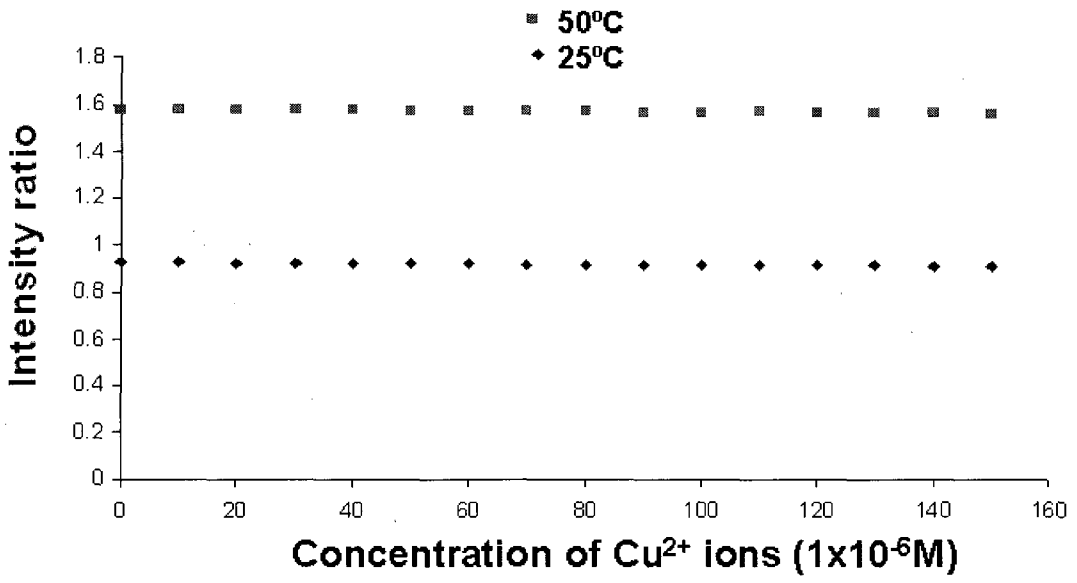

Figure 6.10: 9-VA: 2-NMA fluorescence intensity ratio vs. concentration of Cu^{2+} ions added to poly (NIPAAm) suspended in pH 6 MOP buffer.

6.8.5 Fluorometric Titration of Hydrolyzed Poly (NIPAAM-co-DVPAA) Suspension with Standard Solution of Copper (II) Ions

The hydrolyzed poly (NIPAAm-co-DVPAA) polymer microparticles were titrated with 10^{-3} M Cu^{2+} ions solution in a cuvette according to the procedure described earlier in this chapter. The results show that there was a decrease in the fluorescence intensities of both 9-VA and 2-NMA with increasing concentration of Cu^{2+} ions. The decrease in fluorescence intensity of 2-NMA was much more than that of 9-VA. This decrease in fluorescence intensities is attributed to the settling of the polymer microparticles to the bottom of the cuvette with increasing of concentration of Cu^{2+} ions.

The fluorescence intensity ratio of 9-VA: 2-NMA increased with increasing Cu^{2+} ion concentration indicating binding between the Cu^{2+} ions and the hydrolyzed ligand moiety of the polymer network. The binding of positively charged copper (II) ions

with the 2, 2'-(3-vinylphenylazane diyl) diacetate groups neutralized the negative charges of the DVPAA groups in the polymer microparticles forming a stable complex with a formation constant of 8.4 x 10^5. The formation of the stable complex causes the polymer microparticles to collapse. Figure 6.11 shows the change in fluorescence intensities of 9-VA and 2-NMA within polymer microparticles in pH 6 MOP buffer as titrated with 10^{-3} M Cu^{2+} ions, and figure 6.12 shows the increase in the fluorescence intensity ratio of 9-VA: 2-NMA with increasing concentration of Cu^{2+} ions at 25 °C and at 50 °C.

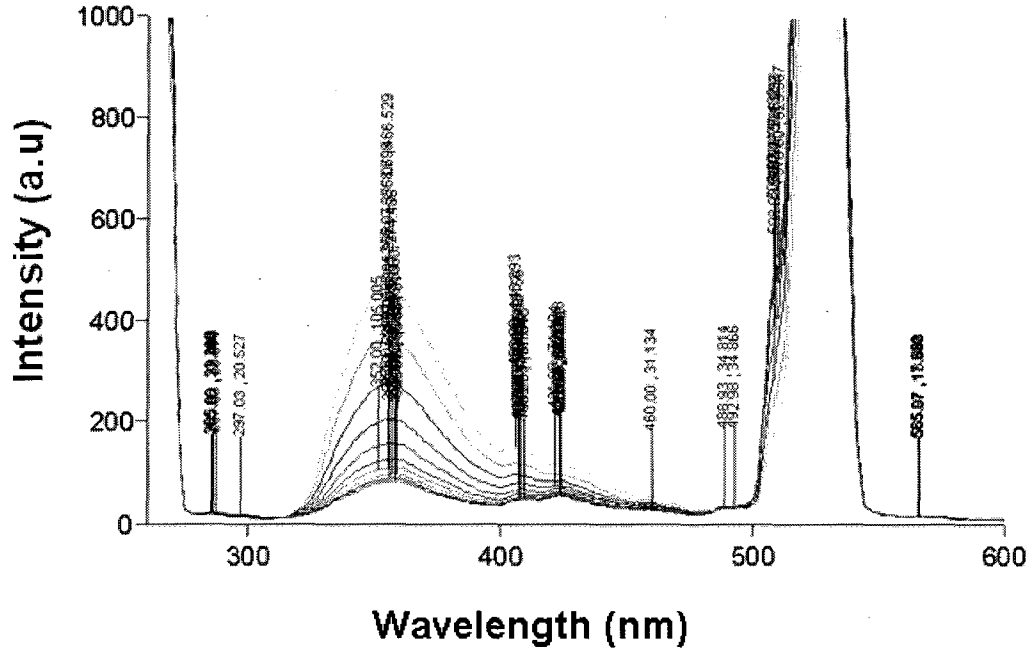

Figure 6.11: Fluorescence spectrum of Poly (NIPAAm-co-DVPAA) labeled with 2-NMA and 9-VA at 25°C.

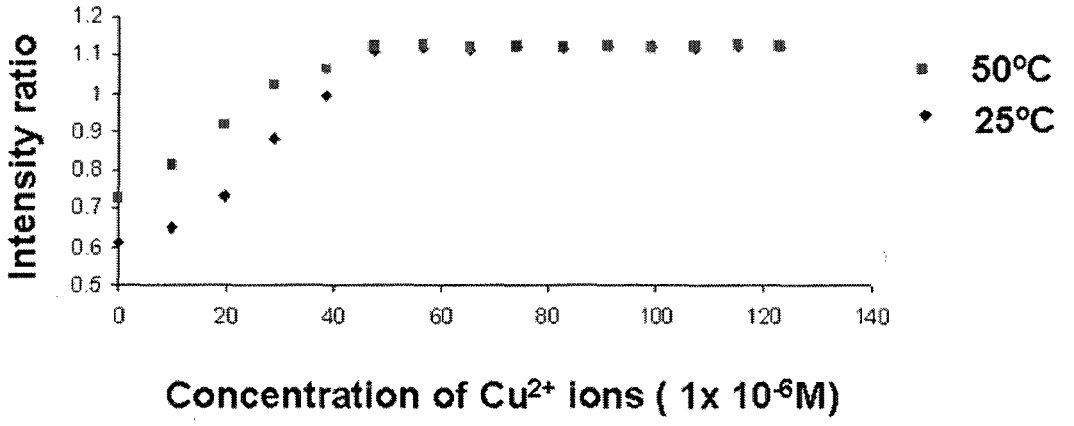

Figure 6.12: 9-VA: 2-NMA fluorescence intensity ratio vs. concentration of Cu^{2+} ions added to poly (NIPAAm-co-DVPAA) suspended in pH 6 MOP buffer.

The equivalence point was 50 x 10^{-6}M Cu^{2+} ions. At pH 6, the 2, 2'-(3-vinylphenylazane diyl) diacetic acid groups within the hydrolyzed polymer network are deprotonated and negatively charged. The resulting 2, 2'-(3-vinylphenylazanediyl) diacetate ions bind to the Cu^{2+} ions forming neutral complex ions which are in the shrunken state and fall out of the solution while the uncomplexed deprotonated 2, 2'-(3-vinylphenylazanediyl) diacetate ions are in the swollen state. It was also observed that polymer microparticles containing hydrolyzed DVPAA bind to Cu^{2+} ions at both 25°C and 50°C, indicating that the presence of the diacetate ions from DVPAA introduces negative charges within the polymer network which repel one another. This makes the polymer to swell at both 25 °C and 50 °C. Also the shrinking of the polymer microparticles at 50° C due to binding of Cu^{2+} ions to the hydrolyzed polymer microparticles containing hydrolyzed DVPAA indicates either an increase in the LCST of the polymer above 50 °C, or a complete loss of the phase transition temperature. The results show that the titration curve has one equivalence point suggesting a 1:1

stoichiometry for the reaction between Cu^{2+} ions and the hydrolyzed DVPAA ligand. The 1:1 stoichiometry was confirmed by calculating the reaction mole ratio for both Cu^{2+} ions and the hydrolyzed DVPAA ligand using the equivalence point for the titration curve.

6.8.6 Fluorometric Titration of the Unhydrolyzed Poly (NIPAAM-co-DVPAA) Polymer Suspension with Standard Solution of Copper (II) Ions

A control experiment was done using unhydrolyzed poly (NIPAAm-co-DVPAA) polymer particles. A suspension of the unhydrolyzed polymer particles was titrated with 10^{-3} M copper (II) ions. There was no observable fluorescence intensity ratio of 9-VA: 2-NMA at both 25 °C and 50 °C indicating that the unhydrolyzed DVPAA ligand does not bind with Cu^{2+} ions. The increase in the ratio of fluorescence intensity at 50 °C was not sufficient to conclude that there is binding between the unhydrolyzed DVPAA ligand and Cu^{2+} ions, but could indicate that there is some hydrolysis of the DVPAA ligand in the presence of Cu^{2+} ions.

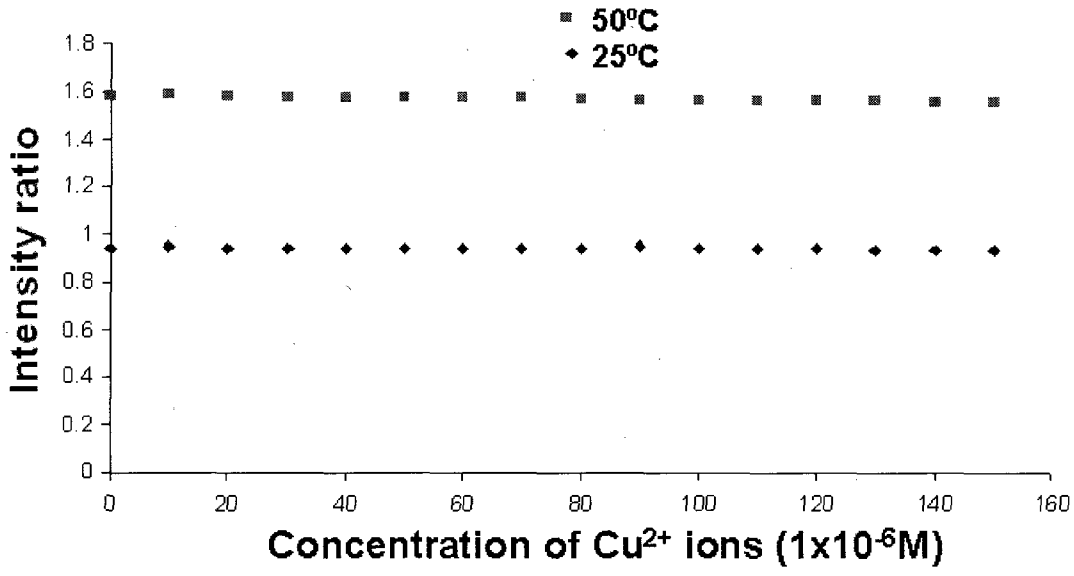

Figure 6.13: 9-VA: 2-NMA fluorescence intensity ratio vs. concentration of Cu^{2+} ions added to unhydrolyzed poly (NIPAAm-co-DVPAA) suspended in pH 6 MOP buffer.

6.8.7 Second Order Light Scattering by Hydrolyzed Poly (NIPAAm-co-DVPAA) Microparticles Suspended in pH 6 MOP Buffer Titrated with 10^{-5}M Cu^{2+} Ions

Second order light scattering of the polymer microparticles were also measured as the polymer microparticles were titrated with 10^{-3}M Cu^{2+} ions at 25 °C and 50 °C. A slight increase followed by a decrease in second order light scattering at the two temperatures was observed as shown in figure 6.14. The slight increase in second order scattering was caused by the formation of a neutral complex still suspended in the buffer solution. The neutral complex contains polymer microparticles in a collapsed form. The decrease in second order scattering was mainly due to the settling of collapsed polymer microparticles down the cuvette. Because the amount of light scattered depends on the number of polymer microparticles within the path of the light,

settling of the microparticles caused a decrease in the second order scattering. The binding of Cu^{2+} ions with the ligand moiety within the polymer microparticles causes the microparticles to coagulate and hence settle to the bottom of the cuvette. This coagulation of the polymer microparticles was observed when Cu^{2+} ions bind to the ligand in the microparticles.

The results can not be used to explain the effect of binding Cu^{2+} ions to the ligand moiety of the polymer micrparticles on the particle size because of its inconsistency with the expected results. The initial slight increase in second order light scattering is attributed to the shrinking of the polymer microparticles due to binding with Cu^{2+} ions and the subsequent decrease is due to polymer microparticles settling at the bottom of the cuvette decreasing the amount of particles within the light path. Because binding Cu^{2+} ions to the hydrolyzed form of the ligand moiety of the polymer microparticles neutralizes the negative charges within the polymer network, the microparticles are expected to collapse with increasing concentration of Cu^{2+} ions. When the particles collapse, their refractive index increases relative to that of the buffer solution and hence scatters more light according to the Fresnel equation [58].

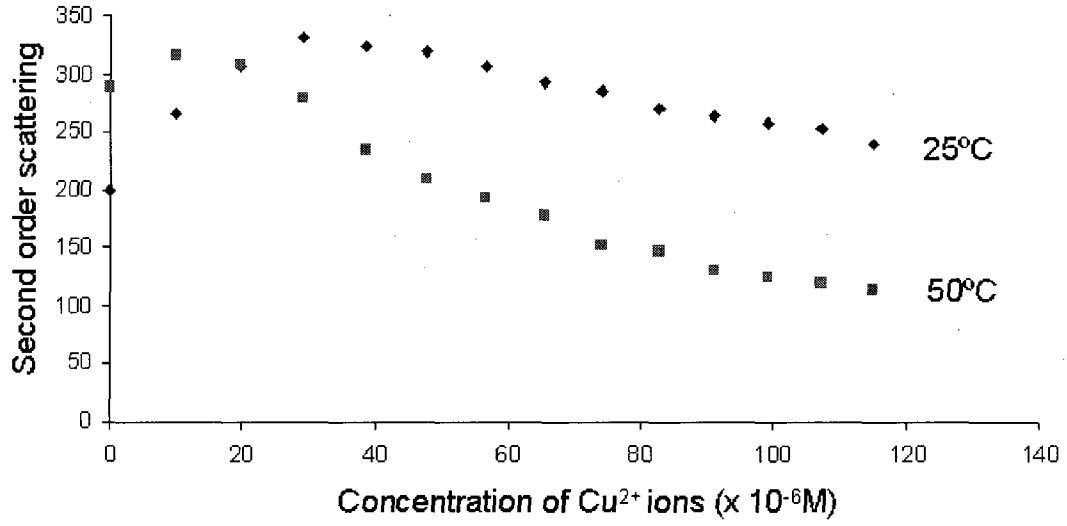

Figure 6.14: Second order scattering of light vs. concentration of Cu^{2+} ions added to poly (NIPAAm-co- DVPAA) suspended in pH 6 MOP buffer.

6.8.8 Fluorometric Titration of Hydrolyzed Poly (NIPAAM-co-DVPAA) Suspension with Standard Solution of Other Ions

A suspension of the hydrolyzed poly(NIPAAM-co-DVPAA) particles in pH 6 MOP buffer were then titrated with 10^{-3} M standard solutions of Pb^{2+} Ni^{2+}, Co^{2+} and Zn^{2+} ions in a cuvette at 25 °C and 50 °C. There was no change in fluorescence intensity ratio of 9-VA: 2-NMA with increases in the concentration of the metal ions either at 25 °C or at 50 °C indicating that the sensor does not respond to these metal ions. Figure 6.15 shows the 9-VA: 2-NMA fluorescence intensity ratio vs. concentration of Pb^{2+} ions at 25 °C and 50 °C

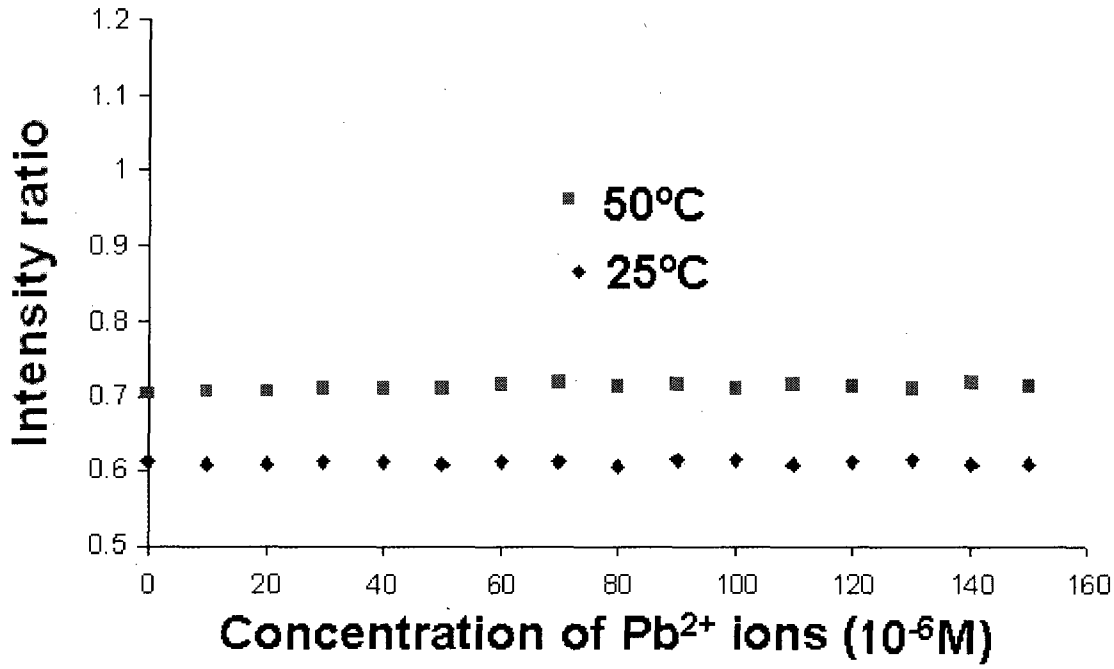

Figure 6.15: 9-VA: 2-NMA *fluorescence intensity ratio vs. concentration of* Pb^{2+} ions added to hydrolyzed poly (NIPAAm-co-DVPAA) suspended in pH 6 MOP buffer.

6.9. Conclusions

Poly (NIPAAm) functionalized with both 2, 2'-acrylamidodiacetic acid (AIDA), and dibutyl (2, 2'-(3-vinylphenylazanediyl) diacetate (DVPAA) were synthesized in acetonitrile. The microparticles had no phase transition temperature and were found to be in the swollen state in pH 6 buffer at both 25 °C and 50 °C because of the negatively charged diacetate ions within the polymer microparticles. Poly (NIPAAm-co-AIDA) polymer microparticles did not bind to Cu^{2+}, Ni^{2+}, Pb^{2+}, and Zn^{2+} ions in pH 6 MOP buffer at either 25 °C or 50 °C. The lack of binding between the metal ions and the AIDA ligand is because the nitrogen in the acrylamidodiacetate ion is an amide group which does not bind with the metal ion rendering the AIDA a weak bidentate ligand.

Polymer microparticles labeled with methacryloxethyl thicarbonyl rhodamine-B and fluorescein o-acrylate were found to be lighter than the pH 6 MOP buffer and migrate to the top of the buffer solution with time while those labeled with 9-VA and 2-NMA are slightly denser than the buffer solution and settle at the bottom of the cuvette. This is expected since the density of pure crystalline poly (NIPAAm) is about 1.118g/mL, which is close to the density of the buffer solution. Copolymerization of poly (NIPAAm) with the two fluorescent monomers and also ligand monomer changes the density of the poly (NIPAAm). The density also increases with the percentage of cross-linking of the polymer microparticles. For the polymer microparticles labeled with methacryloxethyl thicarbonyl rhodamine-B and fluorescein o-acrylate, settling of the microparticles caused no significant effect on the fluorescence intensity ratio although the fluorescence intensities changed significantly. Polymer microparticles labeled with 9-VA and 2-NMA showed no significant change in both the fluorescence intensities and fluorescence intensity ratio with time.

Poly (NIPAAm-co-DVPAA) polymer microparticles were swollen at 25 °C and collapsed at 50 °C with a phase transition temperature of about 29.5 °C. The unhydrolyzed poly (N IPAAm-co-DVPAA) microparticles did not show any binding with Cu^{2+} ions at either 25 °C or 50 °C. The hydrolyzed poly (NIPAAm-co-DVPAA) particles had no phase transition temperature in pH 6 MOP buffer and showed binding with Cu^{2+} ions both at 25 °C and 50 °C. The response of the sensor to the Cu^{2+} ions is supported by the high formation constant (K_f) obtained from the potentiometric titration of the polymer microparticles containing DVPAA ligand moiety. The high formation constant

indicates that the DVPAA ligand from the polymer microparticles strongly binds to the Cu^{2+} ions.

Both hydrolyzed and unhydrolyzed poly (NIPAAm-co-DVPAA) polymer microparticles did not exhibit binding with Zn^{2+}, Ni^{2+}, and Pb^{2+} ions. The lack of binding between the Pb^{2+}, Ni^{2+}, and Zn^{2+} ions with the DVPAA ligand from the polymer microparticles is supported by the fact that N-phenyliminodiacetate ion forms complexes with Zn^{2+}, Ni^{2+}, and Pb^{2+} with formation constants of 2.5×10^3, 4.0×10^3, and 6.3×10^3 respectively. These are relatively low formation constants compared to that of N-phenyliminodiacetate ion-Cu^{2+} indicating weaker binding between the metal ions and the ligand.

CHAPTER 7

PREPARATION OF SWELLABLE FLUORESCENT LABELLED POLY (NIPAAm-co-NMPPAAm) AND POLY (NIPAAm-co-NBPMPA) MICROPARTICLES FOR TRANSITION METAL ION SENSING

7.1 Introduction

Because the response of the sensor depends on the interaction between the ligand and the target analyte, improving the strength of this interaction is of utmost importance in the development of this sensor. This involves the use of ligands with high binding affinities to the target analytes, in this case the transition metal ions. In this chapter, N,N-bis (pyridin-2-ylmethyl)prop-2-en-1-amine (NBPMPA),and N-((4'-methyl-2,2'-bipyridin-4-yl) methyl)-N-propylacrylamide (NMPPAAm) were used as ligands while 9-VA, 2-NMA, fluorescein o-acrylate, and methacryloxethyl thiocarbonyl rhodamine-B were used as fluorescent monomers. Their molecular structures are shown in Figure 5.1 of Chapter 5 of this thesis.

The application of ratiometric fluorescent indicators in biological samples has greatly increased since 2000. A major setback with these types of indicators is the limitation of suitable fluorophores that can be used since the fluorophores should be excited at longer wavelengths. This is because at shorter wavelengths, there is high

fluorescent background and also degradation of most biological samples can easily occur when they are exposed to high-energy radiation. This necessitates the search for fluorophores which can be excited at longer wavelengths. Fluorescein o-acrylate and methacryloxethyl thiocarbonyl rhodamine-B were considered as suitable fluorophore pair due to their longer excitation wavelengths. The emission spectrum of fluorescein overlaps with the excitation spectrum of rhodamine-B, which is a required property for the fluorometric determination method.

Although these fluorophores have longer excitation wavelengths, their use in analysis of transition metal ions may be accompanied by a decrease in sensitivity caused by absorption of the complex formed especially at high concentrations. At low concentrations, the complexes do not absorb significantly due to their low molar absorptivities. Most ligands have low lying π^* molecular orbitals resulting in a transition of electrons between the metal ion orbitals to the π^* molecular orbitals of the ligand. These transitions are weak and occur within the visible region causing a decrease in sensitivity of the sensor because some of the excitation energy is absorbed by the complex and not used to excite the fluorophore.

7.2 Preparation of Poly (NIPAAm-co-NMPPAAm) Labeled with 2-NMA and 9-VA

Poly (NIPAAm-co-NMPPAAm) microparticles labeled with both 2-NMA and 9-VA were synthesized by dispersion polymerization. Binding between the ligand and transition metal ions was investigated. The polymerization and isolation were performed according to the procedure already described in Chapter 3. The polymerization

formulation was 2 mole % NMPPAAm ligand, 0.1 mole % 2-NMA, 0.05 mole % 9-VA, and 5mole % MBA. The total number of moles of monomers used was 10mmoles. 20% w/w of poly (styrene-co-acrylonitrile) was used as a stabilizer. The polymerization was carried out according to the formulation already discussed in chapter 3 of this thesis.

7.3 Analysis of Metal Ions

0.0145g of the resulting polymer microparticles were suspended in 100.00mL MOP buffer at pH 6. The suspension was stirred for 24 hours and 1.00mL was then diluted to 2.5mL. The diluted suspension which had a ligand concentration of 7.8×10^{-6}M was transferred into a quartz cell, inserted into the spectrofuorometer, and titrated with 10^{-5}M metal ion solutions by adding 20µL aliquots. The intensities of the two fluorophores were obtained by exciting the suspended polymer microparticles at 260nm. The emission wavelengths of the two fluorophores were obtained by scanning mode while the absolute intensities were obtained by kinetic mode. The intensity ratios of 9-VA: 2-NMA were determined as the concentrations of the metal ions were increased in the polymer suspension. The fluorescence intensity ratios recorded in this chapter were corrected to account for the effects of both thermal quenching and also settling of the polymer microparticles by subtracting the intensity ratio caused by both settling effect of the polymer microparticles and also fluorescence quenching by copper (II) ions from those caused by changes in copper (II) ion concentration. A graph of the 9-VA: 2-NMA fluorescence intensity ratio vs. the concentrations of the various metal ions was plotted. An experiment was done to investigate how settling of the microparticles affects both the fluorescence intensities of the two fluorophores and the intensity ratio.

7.4 Results and Discussion.

7.4.1 Particle Size and Size Distribution.

Scanning electron micrograph pictures of the polymer particles were taken to determine the particle size and also the size distribution. The particles were found to be dispersed with minimal coagulation as shown in the SEM picture, a property that was supported by the long time taken by the microparticles to settle to the bottom of the cuvette during the settling experiment. The average particle size was 0.32μm and the particle size distribution was in the range of 0.28-0.35μm. in diameter. The scanning electron micrographs of the resulting polymer particles are shown in figure 7.1.

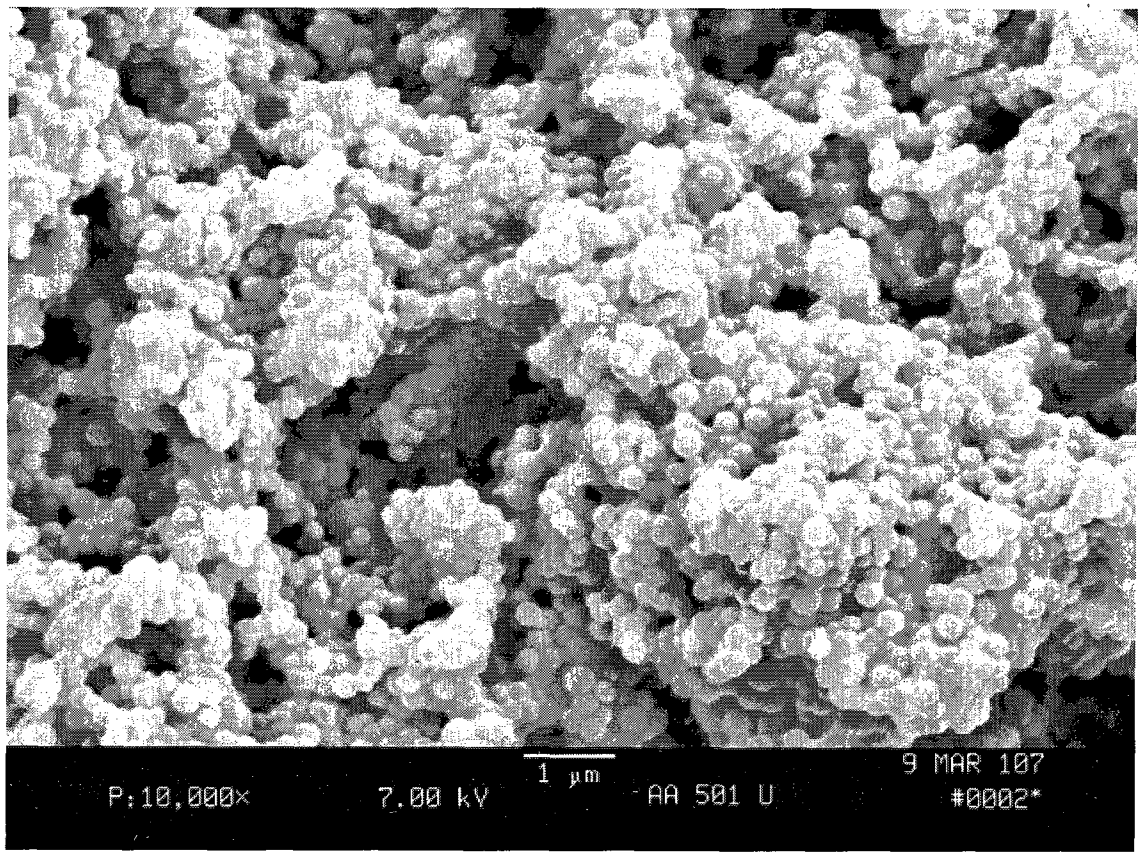

Figure 7.1: Scanning Electron Micrgraphs of Poly (NIPAAm-co NMPPAAm)

7.4.2 Fluorometric Titration of Poly (NIPAAm-co-NMPPAAm) with Copper (II) Ions

A solution containing 10^{-5} M Cu^{2+} ions was prepared from a standard Cu $(NO_3)_2$ solution. The titration was performed according to the procedure in section 7.3. The fluorescence intensity ratio of 9-VA: 2-NMA was calculated at the two temperatures and plotted as shown in figure 7.2. The changes in the fluorescence intensity ratio were found to correlate with the changes in concentration of the Cu^{2+} ions. The fluorescence intensity ratio of 9-VA: 2-NMA decreased with an increase in Cu^{2+} ions in the cuvette both at 25 °C and at 50 °C.

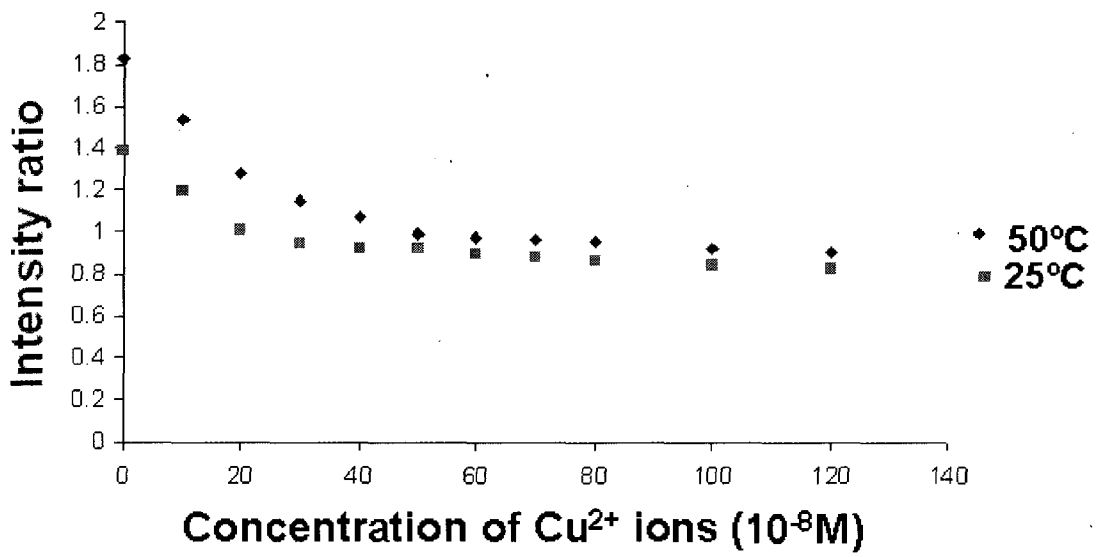

Figure 7.2: 9-VA: 2-NMA fluorescence intensity ratio of Poly (NIPAAm-co-NMPPAAm) vs. concentration of Cu^{2+} ions

The decrease in the intensity ratio is due to the binding of Cu^{2+} ions to the NMPPAAm ligand within the polymer network thereby introducing positive charges which repel each other within the polymer network. The equivalence point was 70 x 10^{-8}M Cu^{2+} ions. The repulsion of the charges caused the polymer particles to swell. The

intensity ratio decreased more at 50 °C than at 25 °C per unit change in Cu^{2+} concentration. This is because at 25 °C, the polymer microparticles are already in a swollen state and binding of the NMPPAAm ligand parts of the polymer microparticles with Cu^{2+} ions does not produce much swelling while at 50 °C, the polymer microparticles are in a collapsed form and binding with Cu^{2+} ions enhances significant swelling. The results show that the titration curve has one equivalence point indicating a 1:1 stoichiometry for the reaction between Cu^{2+} ions and NMPPAAm ligand. The 1:1 stoichiometry was confirmed by calculating the reaction mole ratio for both Cu^{2+} ions and NMPPAAm ligand using the equivalence point for the titration curve.

A comparison of the results with a control experiment prepared from only poly (NIPAAm) alone without the NMPPAAm ligand shows that there is no binding between the unfunctionalized poly (NIPAAm) microparticles and the Cu^{2+} ions. The results of the control experiment were shown in figure 6.6.

Second order light scattering by the polymer microparticles were also measured at 25 °C and 50 °C as 10^{-5}M Cu^{2+} ions were added to the suspension. A decrease in second order light scattering with increasing concentration of Cu^{2+} ions was observed at the two temperatures as shown in figure 7.3. Complexation of Cu^{2+} with the ligand moiety in the polymer microparticles causes the microparticles to swell. This in effect reduces the refractive index of the microparticles and brings it closer to that of the buffer solution. The decrease in refractive index of the microparticles decreases the second order scattering of light by the microparticles. The microparticles remain suspended in the buffer solution without settling to the bottom of the cuvette.

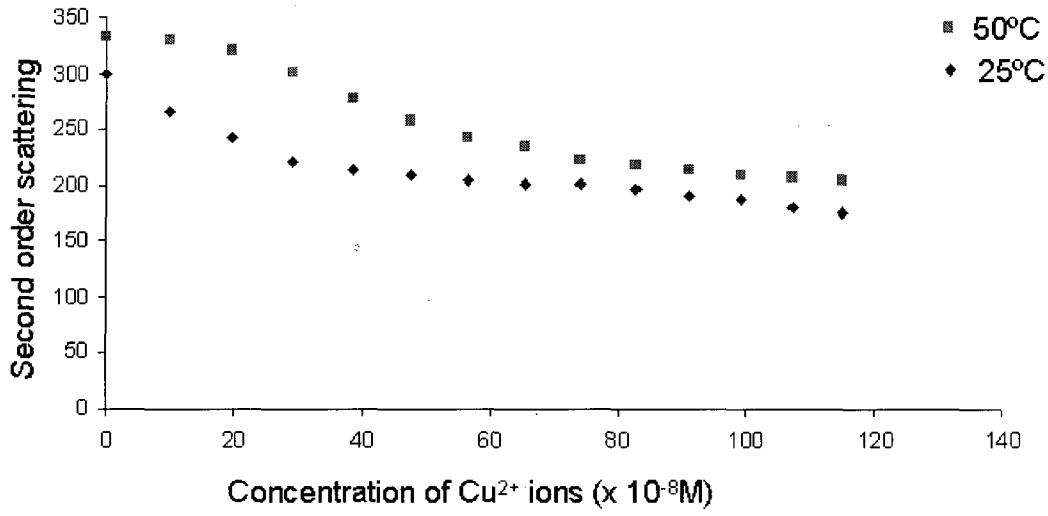

Figure 7.3: Second order light scattering vs. concentration of Cu^{2+} ions added to poly (NIPAAm-co-NMPPAAm) suspended in pH 6 MOP buffer.

7.4.3 Fluorometric Titration of Poly (NIPAAm-co-NMPPAAm) with Nickel (II) Ions

A 10^{-5}M Ni^{2+} ion solution was prepared from standard Ni $(NO_3)_2$ solution. The titration was performed according to the procedure in section 7.3. The polymer suspensions were excited at 260nm and the fluorescence intensity ratio of 9-VA: 2-NMA was calculated as aliquots of 10^{-5} M Ni^{2+} solutions were added to the polymer suspension in a cuvette. A decrease in the 9-VA: 2-NMA fluorescence intensity ratio with increasing concentration of Ni^{2+} ions was observed at 25 °C and 50 °C as shown in figure 7.4. The equivalence point was 70 x 10^{-8}M Ni^{2+} ions. This confirms that there is strong binding between Ni^{2+} and NMPPAAm ligand moiety within the polymer microparticles.

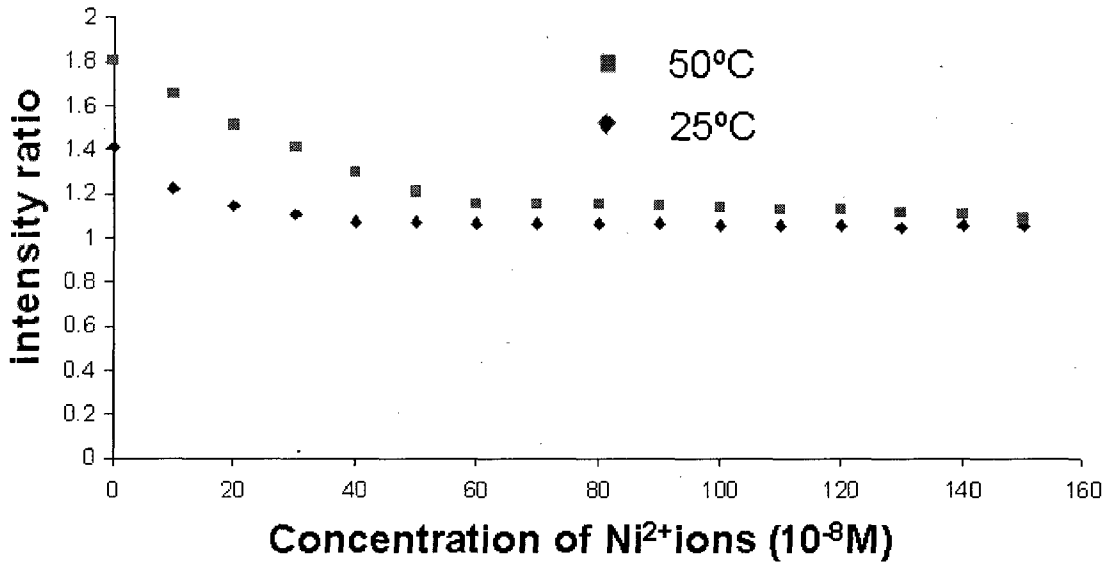

Figure 7.4: 9-VA: 2-NMA fluorescence intensity ratio vs. concentration of Ni^{2+} ions added to poly (NIPAAm-co-NMPPAAm) suspended in pH 6 MOP buffer.

7.4.4 Fluorometric Titration of Poly (NIPAAm-co-NMPPAAm) with Other Metal Ions

10^{-5}M solutions of Zn^{2+}, and Pb^{2+} ions were prepared from standard Zn $(NO_3)_2$, and Pb $(NO_3)_2$ solutions. The titration was performed according to the procedure in section 7.3. The polymer suspension was excited at 260nm and no significant change in the 9-VA: 2-NMA fluorescence intensity ratio was observed. This indicates that the sensor does not respond to Zn^{2+}, and, Pb^{2+} ions. Figure 7.5 shows the 9-VA: 2-NMA fluorescence intensity ratio of poly (NIPAAm-co-NMPPAAm) vs. concentration of Pb^{2+} ions.

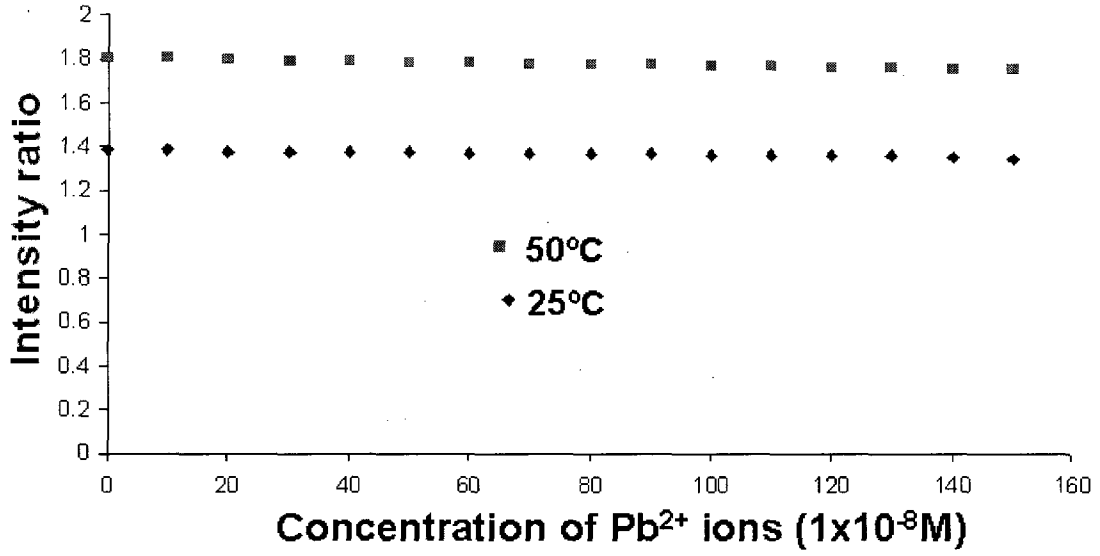

Figure 7.5: 9-VA: 2-NMA fluorescence intensity ratio of poly (NIPAAm-co-NMPPAAm) vs. concentration of Pb^{2+} ions

7.5 Preparation of Poly (NIPAAm-co-NMPPAAm) Labeled with Fluorescein o-acrylate and Methacryloxethyl thiocarbonyl rhodamine-B

Lightly cross-linked copolymers of NIPAAm and NMPPAAm labeled with fluorescein o-acrylate and methacryloxethyl thiocarbonyl rhodamine-B fluorophores were prepared by dispersion polymerization in acetonitrile. The concentration of the crosslinker was optimized for optimum equilibrium swelling and shrinking of the particles without compromising the mechanical strengths of the polymeric material. The concentrations of the two fluorophores were also optimized. The purpose of optimizing the fluorescence intensities was to obtain a reasonable intensity ratio, i.e. fluorescence intensity ratios that are neither too high nor too low. 2 mole % of the NMPPAAm ligand, 0.1 mole % fluorescein o-acrylate, 0.04 mole % methacryloxethyl thiocarbonyl rhodamine-B, and 5 mole % MBA were used in the polymerization formulation. The total number of moles of monomers used was 10mmoles. 20%w/w of poly (styrene-co-

acrylonitrile) was used as the stabilizer. The polymerization was carried out according to the procedure stated in chapter 3 of this thesis.

7.6 Analysis of Metal Ions

0.0145g of the resulting polymer microparticles were suspended in 100.00mL MOP buffer at pH 6. The suspension was stirred for 24 hours and a 1.00mL was then diluted to 2.5mL. The diluted suspension which had a ligand concentration of 7.8×10^{-6}M was transferred into a quartz cell inserted into the spectrofuorometer and titrated with 10^{-5}M solutions of the metal ions by addition of 20µL aliquots. The fluorophores were excited at 480nm and the maximum emission wavelengths of the two fluorophores were obtained using the scanning mode while the maximum fluorescence intensities were obtained by kinetic mode. The fluorometric titrations were done at 25°C and 50°C. The fluorescence intensity ratio of the methacryloxethyl thiocarbonyl rhodamine-B: fluorescein o-acrylate were calculated as the metal ions were added to the polymer suspension at the two temperatures. An experiment was done to investigate how settling of the microparticles affects both the fluorescence intensities of the two fluorophores and the intensity ratio.

7.7 Results and Discussion

7.7.1 Fluorometric titration of Poly (NIPAAm-co-NMPPAAm) Labeled with Fluorescein o-acrylate and Methacryloxethyl thiocarbonyl rhodamine-B with Copper (II) Ions

The results show that the change in fluorescence intensities of the two fluorophores does not correlate to the change in concentration of Cu^{2+} ions in the cuvette. This is because the fluorescence intensities depend on the number of microparticles interacting with the light and therefore depends on the number of particles in the light path of the light source. Because the suspension of the polymer microparticles is non-homogeneous, the number of microparticles within the light path of the light source varies in the suspension, depending on whether the suspension is shaken or not. A more reliable measurement is the fluorescence intensity ratio of the two fluorophores (methacryloxethyl thiocarbonyl rhodamine-B: fluorescein o-acrylate). This ratio was found to decrease with increasing concentration of Cu^{2+} ions both at 25 °C and 50 °C. An equivalence point was observed at 8.5 x 10^{-7}M Cu^{2+} ions. The decrease in fluorescence intensity ratio is due to the high binding affinity between Cu^{2+} ions and the NMPPAAm ligand within the polymer microparticles causing the microparticles to expand. Figure 7.6 shows the fluorescence intensities of methacryloxethyl thiocarbonyl rhodamine-B and fluorescein o-acrylate fluorophores, while figure 7.7 shows the florescence intensity ratio of the two fluorophores.

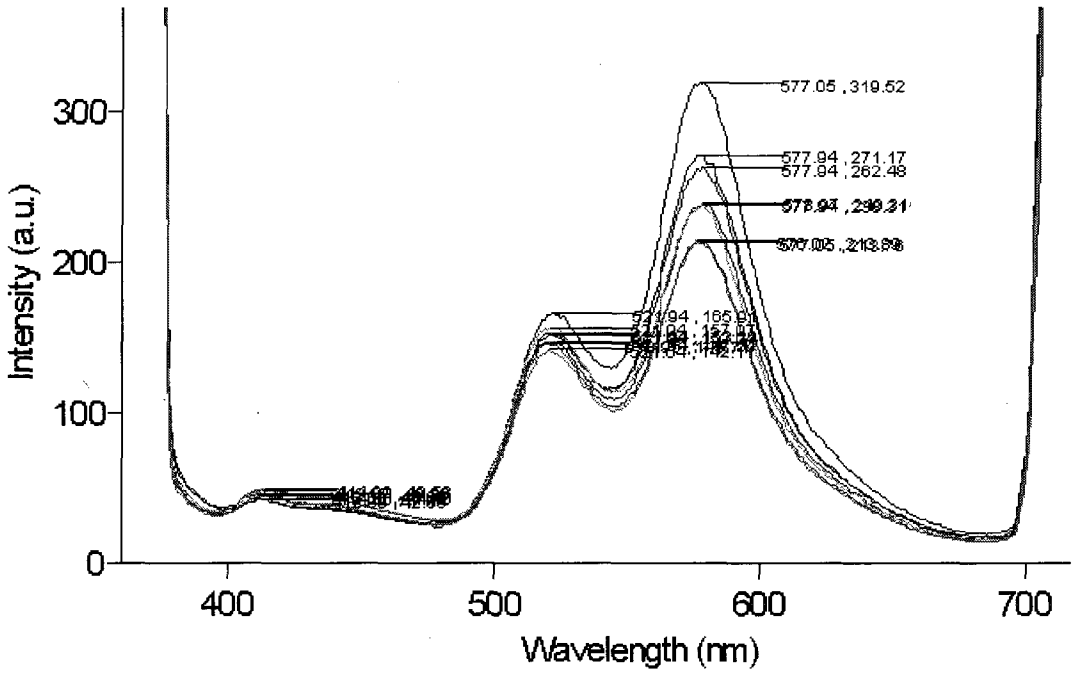

Figure 7.6: Fluorescence spectrum of poly (NIPAAm-co-NMPPAAm) labeled with fluorescein o-acrylate and methacryloxethyl thiocarbonyl rhodamine-B.

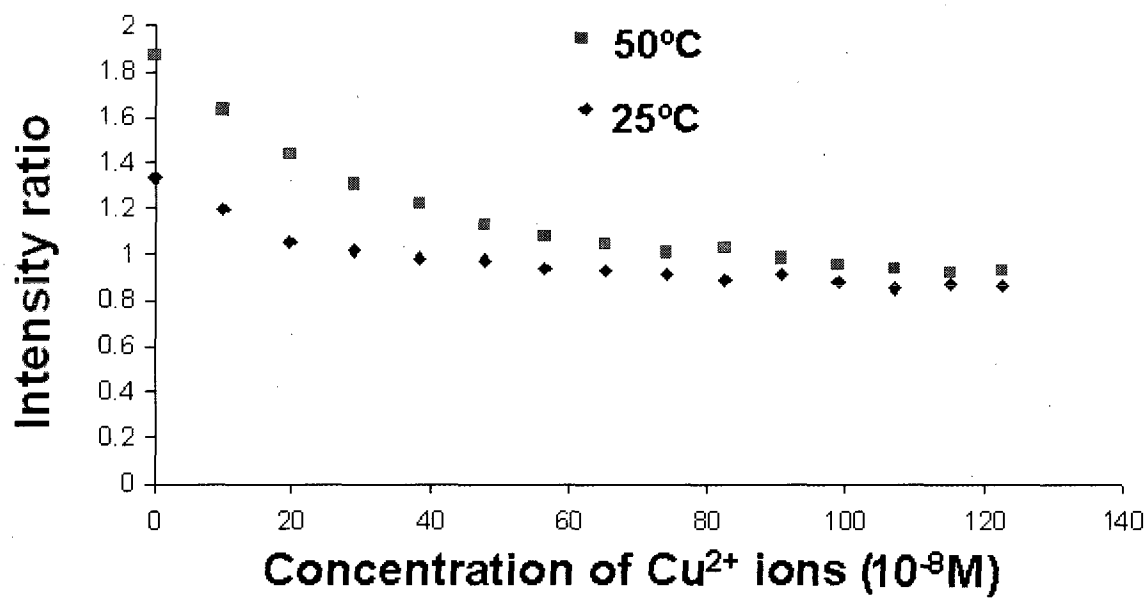

Figure 7.7: Methacryloxethyl thiocarbonyl rhodamine-B: fluorescein o-acrylate intensity ratio vs. concentration of Cu^{2+} ions added to poly (NIPAAm-co-NMPPAAm) suspended in pH 6 MOP buffer.

7.7.2 Fluorometric Titration of Poly (NIPAAm-co-NMPPAAm) Labeled with Fluorescein o-acrylate and Methacryloxethyl thiocarbonyl rhodamine-B with Nickel (II) Ions

There was a decrease in the fluorescence intensities of both methacryloxethyl thiocarbonyl rhodamine-B and fluorescein o-acrylate with an increase in concentration of Ni^{2+} ions up to 70 x 10^{-8} M. The results also show that the methacryloxethyl thiocarbonyl rhodamine-B: fluorescein o-acrylate fluorescence intensity ratio decreased with an increase in Ni^{2+} ion concentration both at 25 °C and 50 °C as shown in figure 7.8. An equivalence point was observed at 70 x 10^{-8}M Ni^{2+} ions. There was no correlation between the fluorescence intensities of the two fluorophores and the Ni^{2+} ion concentration because the polymer suspension was heterogeneous. The decrease in the fluorescence intensity ratio is caused by binding of Ni^{2+}ions to the NMPPAAm ligand moieties in the polymer network making the polymer microparticles expand.

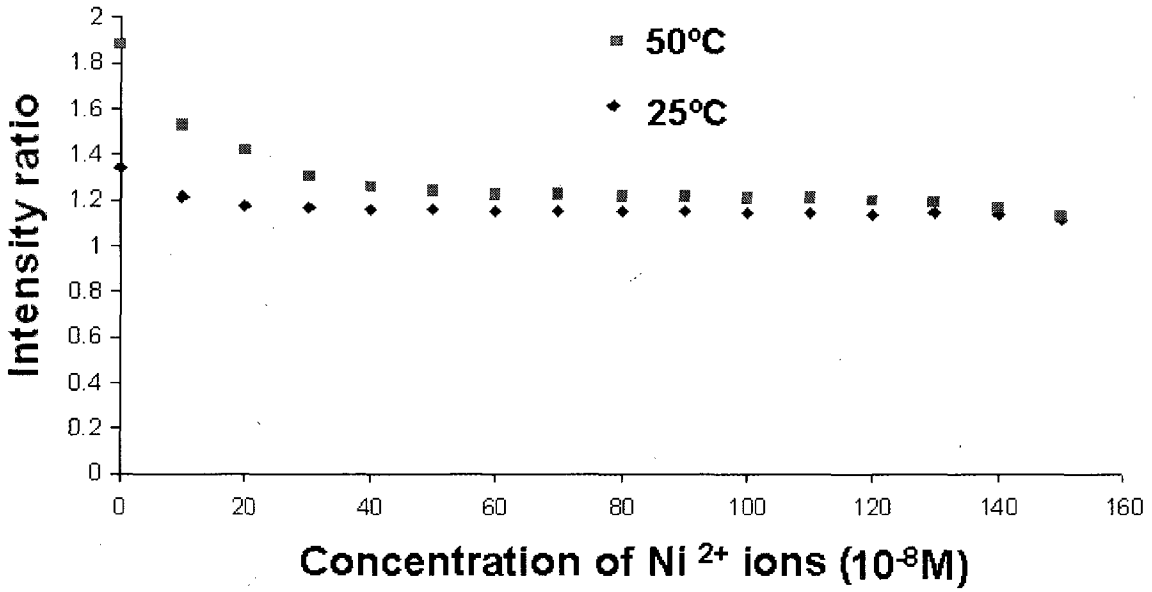

Figure 7.8: Methacryloxethyl thiocarbonyl rhodamine-B: fluorescein o-acrylate intensity ratio vs. concentration of Ni^{2+} ions added to poly (NIPAAm-co-NMPPAAm) suspended in pH 6 MOP buffer.

7.7.3 Fluorometric Titration of Poly (NIPAAm-co-NMPPAAm) Labeled with Fluorescein o-acrylate and Methacryloxethyl thiocarbonyl rhodamine-B with Zn^{2+}, and Pb^{2+} Ions

The results show that the fluorescence intensities of the two fluorophores change inconsistently with increasing concentration of the metal ions because polymer suspensions were non-homogeneous, however, the methacryloxethyl thicarbonyl rhodamine-B: fluorescein o-acrylate fluorescence intensity ratio did not change with increasing concentration of the metal ions either at 25 °C or 50 °C. The results indicate that the sensor does not respond to the metal ions in solutions. Figure 7.9 shows the methacryloxethyl thiocarbonyl rhodamine-B: fluorescein o-acrylate intensity ratio vs. concentration of Zn^{2+} ions.

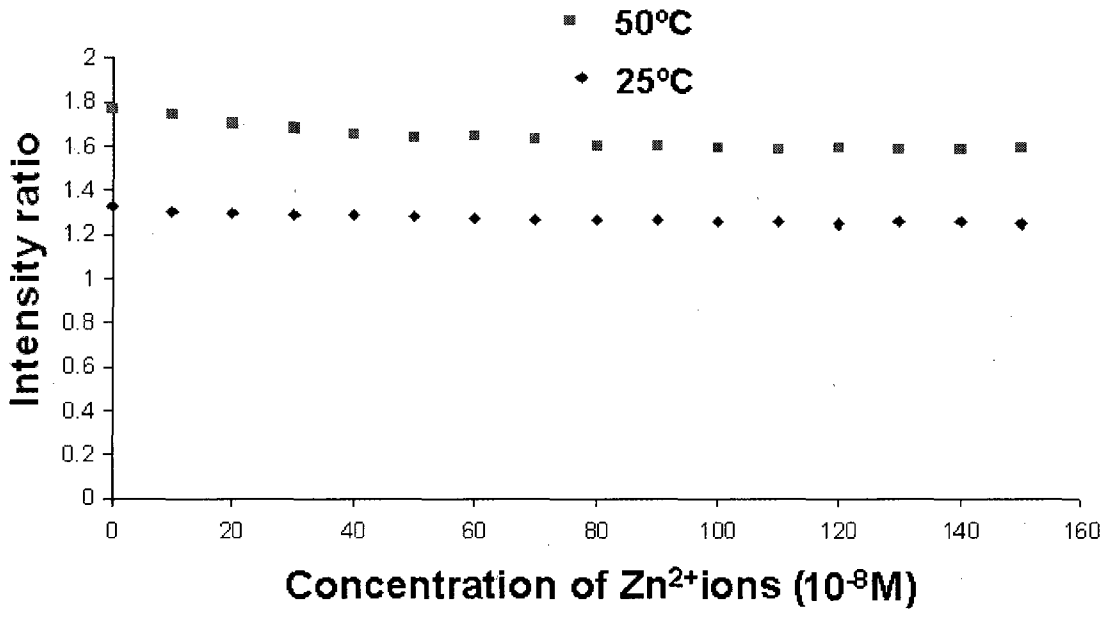

Figure 7.9: Methacryloxethyl thiocarbonyl rhodamine-B: fluorescein o-acrylate intensity ratio vs. concentration of Zn^{2+} ions added to poly (NIPAAm-co-NMPPAAm) suspended in pH 6 MOP buffer.

7.8 Preparation of Poly (NIPAAm-Co-NBPMPA) Labeled with 2-NMA and 9-VA Fluorophores.

Poly (NIPAAm-co-NBPMPA) labeled with 2-NA and 9-VA fluorophores was synthesized according to the polymerization process already discussed in Chapter 3 of this thesis. 2 mole % of the NBPMPA ligand, 0.1mole % 2-NMA, 0.05 mole % 9-VA, and 5 mole % MBA were used in the polymerization formulation. The total moles of monomers used was 10mmoles excluding the 20%w/w of poly (styrene-co-acrylonitrile) stabilizer used. The polymerization was carried out according to the procedure stated in Chapter 3 of this thesis.

7.9 Analysis of Metal Ions

After polymerization, the microparticles were isolated by centrifugation as discussed in chapter 3 of this thesis. 0.013g of Poly (NIPAAm-co-NBPMPA) microparticles were suspended in 100mL pH 6 MOP buffer. 1.00mL of this suspension was transferred into a 2.50mL cuvette and fluorometrically titrated by adding 20µL aliquots of 10^{-5}M metal ions. The titration procedure was done at 25 °C and 50 °C. The emission wavelengths of the two fluorophores were obtained by the scanning mode and the absolute fluorescence intensities were obtained by the kinetic mode. The fluorescence intensity ratios of the two fluorophores were also calculated with each addition of metal ion solution. An experiment was done to investigate how settling of the microparticles affects both the fluorescence intensities of the two fluorophores and the intensity ratio.

7.10 Results and Discussion

7.10.1 Particle Size and Size Distributions

SEM pictures were taken to determine particle size, size distribution, and also to verify if the particles were coagulated. The average particle size was estimated as 0.44µm and the size distribution of the microparticles was found to be between 0.42-0.47µm in diameter. The microparticles were also found to be slightly coagulated as shown in the SEM pictures in figure 7.10 and also the slow settling of the polymer microparticles with time.

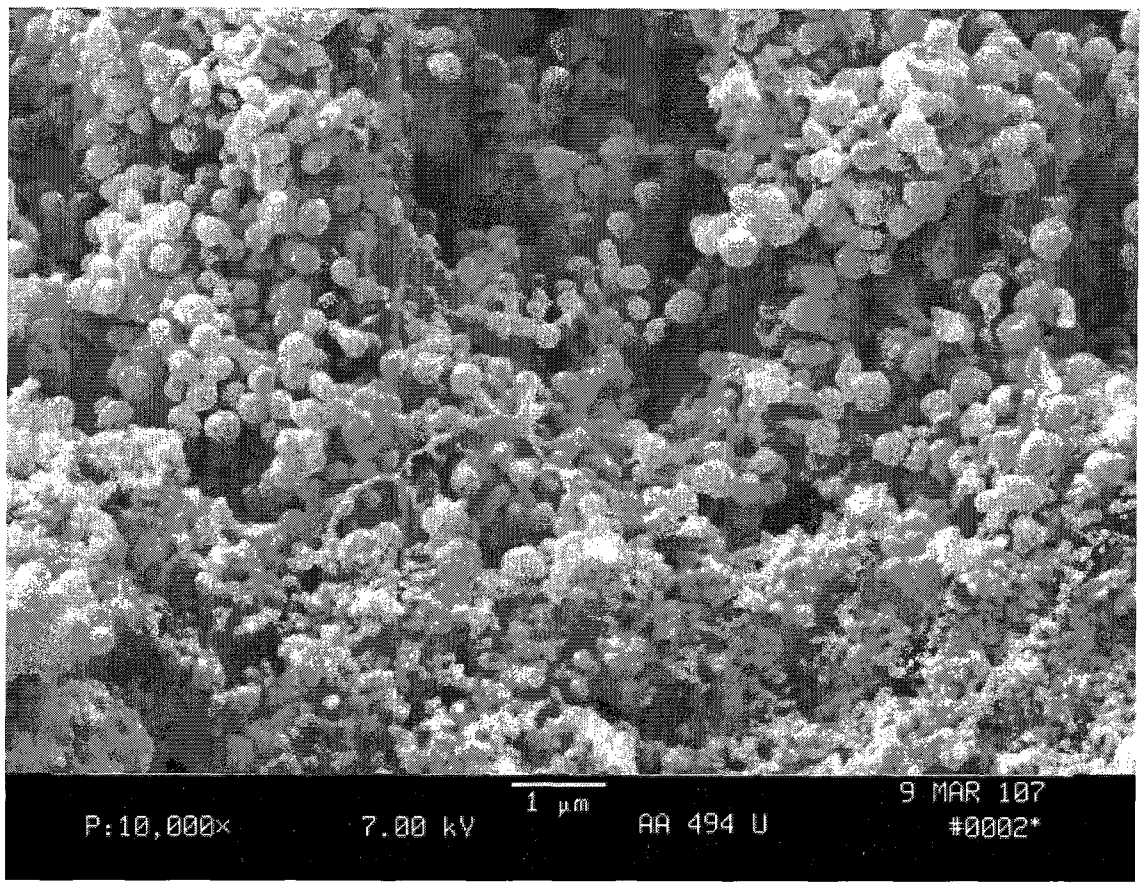

Figure 7.10: Scanning Electron Micrograph of poly (NIPAAm-co- NBPMPA) particle labeled with 2NMA and 9-VA.

7.10.2 Fluorometric Titration of Poly (NIPAAm-co-NBPMPA) Suspension with Standard Solutions of Copper (II) Ions

The polymer suspension was excited at 260nm. The fluorescence intensities of 9-VA and 2-NMA were obtained and the 9-VA: 2-NMA fluorescence intensity ratio was calculated as the concentration of Cu^{2+} ions increased at 25 °C and 50 °C. The fluorescence intensities of the two fluorophores showed a non-correlated relationship with concentration of Cu^{2+} ions due to the non homogeneous nature of the suspension. A decrease in the fluorescence intensity ratio of 9-VA: 2-NMA was observed at 50 °C as the concentration of copper (II) ions increased. The equivalence point was 60 x 10^{-8}M

Cu^{2+} ions. A little decrease in fluorescence intensity ratio was also observed at 25°C. The minimal decrease in the fluorescence intensity ration at 25°C is mainly due to the polymer being in a swollen form and hence less equilibrium swelling ratio with increasing concentration of Cu^{2+} ions. The graph in figure 7.11 illustrates this result both at 25 °C and at 50 °C.

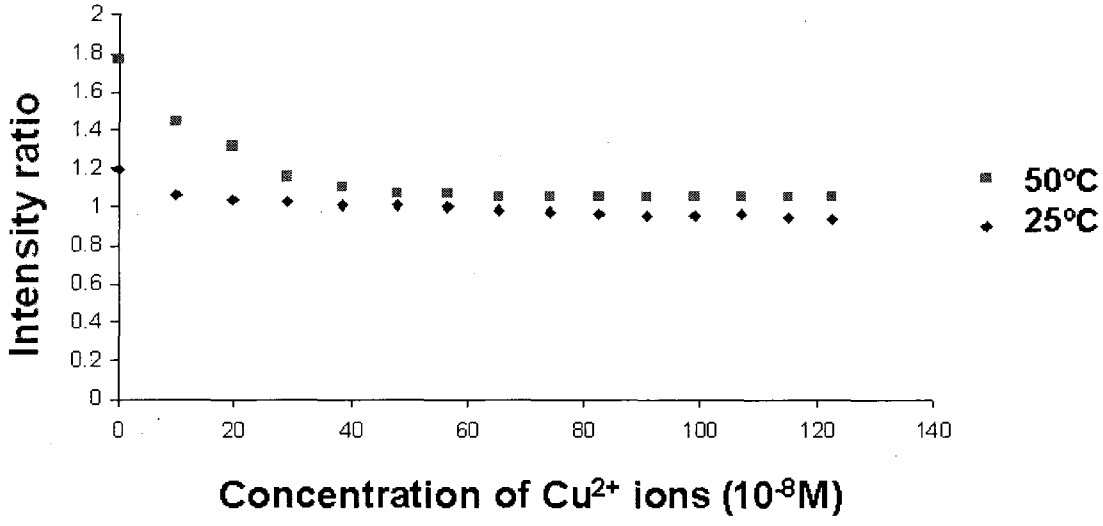

Figure 7.11: 9-VA: 2-NMA fluorescence intensity ratio vs. concentration of Cu^{2+} ions added to poly (NIPAAm-co-NBPMPA) suspended in pH 6 MOP buffer.

7.10.3 Fluorometric Titration of Poly (NIPAAm-co-NBPMPA) Suspension with Standard Solutions of Nickel (II) Ions

The polymer microparticle suspension was titrated with 10^{-5}M Ni^{2+} ions prepared from standard aqueous Ni $(NO_3)_2$ solutions by adding 20µL aliquots while monitoring changes in fluorescence intensities of the two fluorophores. The polymer suspension was excited at 260nm. The fluorescence intensity ratio decreased with increasing Ni^{2+} ion concentration up to 60 x 10^{-8}M as shown in figure.7.12. There was a higher equilibrium swelling ratio at temperatures above the LCST, when the polymer

network is in a collapsed form, than at temperatures below the LCST when the polymer is in a swollen state.

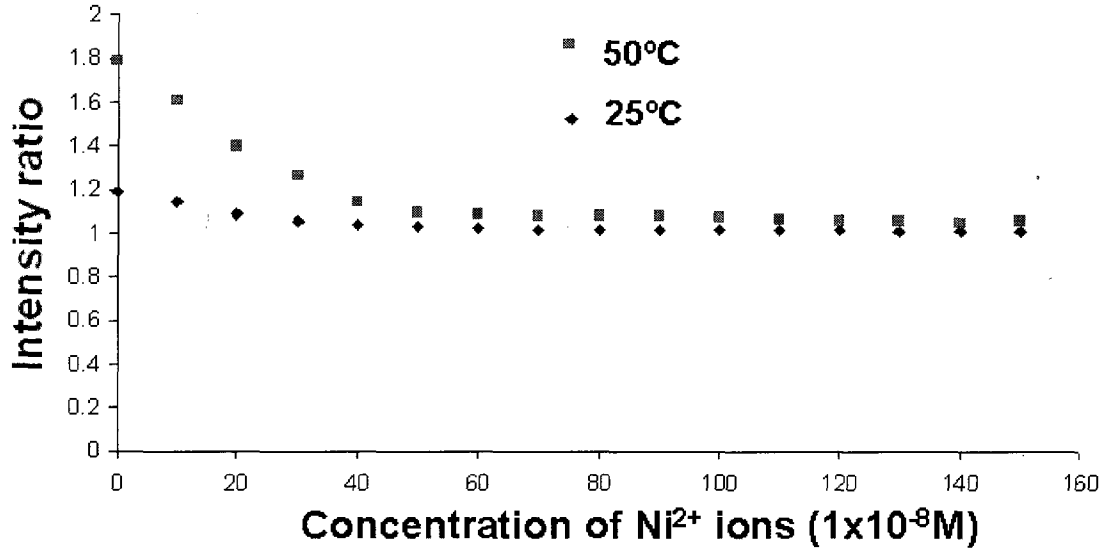

Figure 7.12: 9-VA: 2-NMA fluorescence intensity ratio vs. concentration of Ni^{2+} ions added to poly (NIPAAm-co-NBPMPA) suspended in pH 6 MOP buffer.

7.10.4 Fluorometric Titration of Polymer Suspension with Standard Solutions of Zinc (II) Ions

The polymer microparticle suspension was titrated with 10^{-5}M Zn^{2+} ions prepared from standard aqueous Zn $(NO_3)_2$ solutions by adding 20µL aliquots while monitoring changes in fluorescence intensities of the two fluorophores. The microparticle suspension was excited at 260nm and the fluorescence intensity ratio of 9-VA: 2-NMA was calculated as the concentration of Zn^{2+}ions increased at 25°C and 50°C as shown in figure 7.13. The results show that the fluorescence intensity ratio decreased with increasing concentration of Zn^{2+} ions up to 50 x 10^{-8}M. This result

indicates that there is binding between Zn^{2+} ions and the NBPMPA ligand of the polymer network.

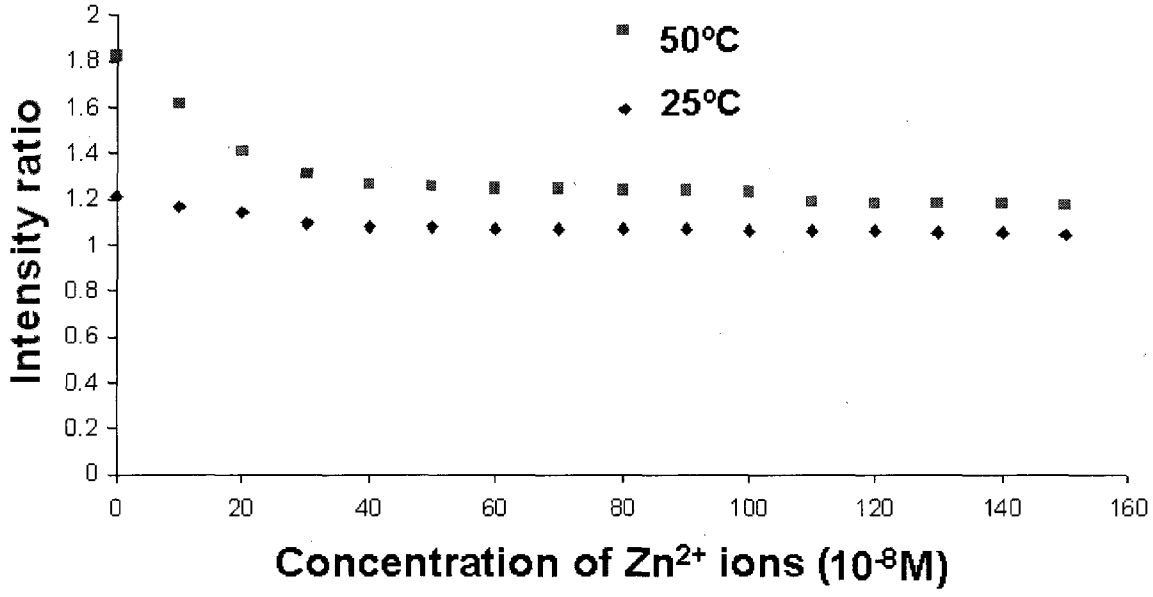

Figure 7.13: 9-VA: 2-NMA fluorescence intensity ratio vs. concentration of Zn^{2+} ions added to poly (NIPAAm-co-NBPMPA) suspended in pH 6 MOP buffer.

7.11 Conclusions

Fluorescent labeled swllable Poly (NIPAAm) functionalized with N, N-bis (pyridin-2-ylmethyl) prop-2-en-1-amine (NBPMPA), and N-((4'-methyl-2, 2'-bipyridin-4-yl) methyl)-N-propylacrylamide (NMPPAAm) ligands were synthesized. The florescent-labeled poly (NIPAAm-co-NMPPAAm) microparticles show strong binding affinity with both Cu^{2+}, and Ni^{2+}, and no binding with Zn^{2+} at pH 6. The sensor response to Cu^{2+} ions is further supported by the high value of the formation constant obtained earlier by potentiometric titration for the complex formed between the Cu^{2+} and polymer microparticles containing the NMPPAAm ligand moiety. This formation constant was

slightly less than the literature K_{f1} value for the bipyridine-Cu^{2+} complex (1.0×10^8). The sensor showed lack of response for both Pb^{2+} and Zn^{2+} ions because of low binding affinity of the NMPPAAm ligand for the two ions as evidenced by the K_{f1} values of the bipyridine-metal ion complex for these metal ions obtained from literature. The literature K_{f1} values for the bipyridine ligand complexes with Pb^{2+}, and Zn^{2+} ions were 7.9×10^2 and 1.35×10^5 respectively [118].

Poly (NIPAAm-co-NBPMPA) exhibited strong binding towards Cu^{2+}, Ni^{2+}, and, Zn^{2+} at pH 6. The response of the sensor to Cu^{2+} ions indicated that the NBPMPA ligand from the polymer microparticles strongly binds to Cu^{2+}-ions. This binding between the NBPMPA ligand and the Cu^{2+}-ions is supported by the conditional formation constant (3.1×10^8) obtained by the potentiometric titration between the poly (NIPAAm-co-NMPMPA) polymer microparticles and the Cu^{2+} ions in Chapter 5. This formation constant, even though it is far less than the formation constant obtained from the literature for the di-2-picolylamine-Cu^{2+} complex (2.5×10^{14}), is a clear indication that the NMPMPA ligand moiety strongly binds with the Cu^{2+} ions. In acidic medium, the formation constant decreases with decreasing pH. The sensor also showed response for both Ni^{2+} and Zn^{2+} ions indicating that the NBPMPA ligand moiety in the polymer microparticles strongly binds to these ions. Literature K_{f1} values for the complex formed between the di-2-picolylamine and Ni^{2+} and Zn^{2+} ions are 5×10^8 and 3.7×10^7 respectively which suggest strong binding between the ligand and the metal ions. Unfunctionalized poly (NIPAAm) was found to have no binding with the metal ions.

CHAPTER 8

MOLECULARLY IMPRINTED POLYMER MICROPARTICLES FOR THEOPHYLLINE AND GLUCOSE SENSING

8.1 Introduction

Molecular imprinting is an emerging technology which allows the synthesis of materials containing highly specific receptor sites with an affinity for target compounds. Molecularly imprinted polymers (MIPs) can mimic some of the functions of enzymes through the creation of three-dimensional cavities of specific size and shape for the recognition of the biomolecules. MIPs have been applied in the development of sensors, assays, polymers with special functions such as drug release matrices and separation materials.

The molecular recognition between molecular receptors (hosts) and substrate (guests) in a matrix containing structurally related molecules involves both binding and discrimination. Molecularly imprinted gels have cavities with affinity for the imprint molecule or its analog through which either the imprint molecule or its analog can pass. The cavities are correctly shaped, sized, and appropriately functionalized to bind the imprint molecule or its analog. Interactions between receptors and substrates occur only if the binding sites of the receptor and substrate molecules complement each other in chemical functionality, shape, and size. Depending on the binding sites of both the receptor and the substrate, the interactions between them can either be hydrophobic, hydrogen bonding, or ionic, or it can involve more that one type of interaction.

Wenzhe Fan showed that theophylline (THO) molecularly imprinted polymer responds selectively to theophylline concentrations as low as 10^{-7} M [85]. He prepared lightly crosslinked theophylline imprinted poly (NIPAAm-co-MAA) in acetonitrile and extracted the theophylline template. In his work, he used turbidity of the polymer particles immobilized in PVA membranes to monitor the interaction between the THO and MAA moiety of the polymer particles. He observed that as the concentration of THO increases, turbidity of the particles in the membrane increases indicating that the polymer particles were collapsing with introduction of low concentrations of THO at pH 7.

In this chapter, two sensors were developed; a ratiometric fluorescent sensor for theophylline analysis, and a glucose sensor, using the change in turbidity of the polymer microparticles with changing analyte concentration. The ratiometric fluorescent sensor was prepared using fluorescent-labeled theophylline imprinted polymer microparticles. The microparticles were prepared by dispersion polymerization using fluorescein o-acrylate, and methacryloxethyl thiocarbonyl rhodamine-B as donor and acceptor fluorophores respectively and MAA as the functional monomer. The selectivity of the sensor was tested using caffeine, a molecule with similar molecular structure as theophylline with an additional methyl group. The glucose sensor was prepared using β-D-glucopyranose imprinted polymer microparticles with acrylamide as the functional monomer. The polymer microparticles were immobilized in PVA membranes and the turbidity of the immobilized polymer microparticles was measured at 500nm. The selectivity of the sensor was tested using β-D-galactopyranose.

8.2 Preparation of Theophylline (THO) Imprinted Poly (NIPAAm-co-MAA) Microparticles Labeled with Fluorescein and Methacryloxethyl thiocarbonyl rhodamine-B

THO imprinted poly (NIPAAm-co-MAA) polymer particles labeled with fluorescein o-acrylate and methacryloxethyl thiocarbonyl rhodamine-B were prepared by dispersion polymerization in acetonitrile. The monomers were dissolved in acetonitrile and sonicated for 30 minutes to ensure uniform dispersion of the monomers in the solvent. Both dissolved and undissolved oxygen in the flask were removed from the flask by purging nitrogen into the reaction flask for 20 minutes. The flask was sealed and immersed in a water bath which was maintained at 60°C. Polymerization was carried out for 16 hours with continuous stirring. Table 8.1 shows the formulation for the polymer preparation.

Reagent	Quantity
NIPAAm	1.0180g (9.000mmol)
AIBN	0.0320g (0.200mmol)
MBA	0.0771g (0.500mmol)
Poly(styrene-co-acrylonitrile)	0.2240g
Fluorescein-o-acrylate	0.0193g (0.048mmol)
Methacryloxethyl rhodamine-B	0.0137g (0.020mmol)
THO	0.0180g (0.200mmol)
MAA	0.0173g (0.200mmol)
Acetonitrile	50mL

Table 8.1: Typical formulation for the polymerization of THO imprinted poly (NIPAAm-co-MAA) particles.

The MIP microparticles were isolated by centrifugation according to the procedure described in Chapter 3. After isolation of the microparticles, extraction of the theophylline was achieved by suspending the microparticles in a mixture of methanol-acetic acid (9:1) by volume. The extraction process was repeated five times. The polymer microparticles were then washed three times with water and then dried.

8.3 Preparation of Non-imprinted Poly (NIPAAm-co-MAA) Particles Labeled with Fluorescein o-acrylate and Methacryloxethyl thiocarbonyl rhodamine-B

Non-imprinted poly (NIPAAm-co-MAA) polymer particles labeled with fluorescein o-acrylate and methacryloxethyl thiocarbonyl rhodamine-B were prepared using the procedure similar to that of the THO imprinted polymers. The resulting non-imprinted polymer microparticles were isolated by centrifugation and washed about four times with de-ionized water.

8.4. Results and Discussion

8.4.1 Particle Size and Size Distribution

SEM pictures were taken to determine particle size, size distribution and also to determine whether the microparticles were coagulated or not. The diameter of the microparticles was difficult to determine due to coagulation of the microparticles as can be seen in figure 8.1.

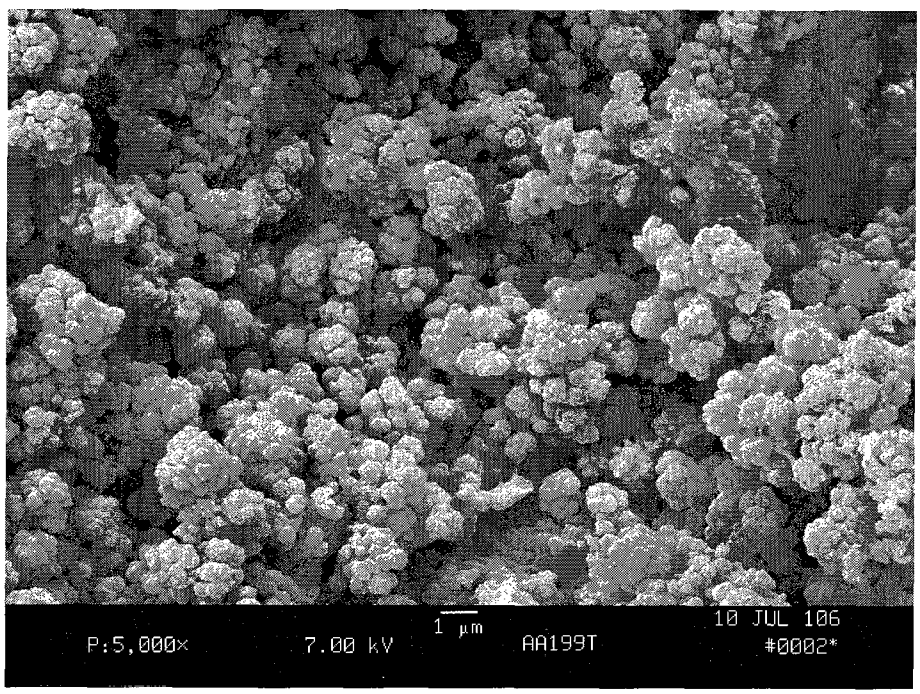

Figure 8.1: Scanning Electron Micrograph of poly (NIPAAm-co- MAA) Microparticles.

8.4.2 Effect of Temperature on THO Imprinted Polymer Microparticles

0.05g of the microparticles were suspended in pH 7 phosphate buffer with the ionic strength adjusted to 0.1M using potassium chloride. A 2.5mL aliquot of the polymer suspension was transferred into a cuvette and inserted in to a spectrofluorometer. The microparticles were excited at 450nm and fluorescence intensities of fluorescein o-acrylate and methacryloxethyl thiocarbonyl rhodamine-B was observed at 517nm and 585nm respectively as the temperature was increased from 25°C to 45°C. The emission intensity of the fluorescein o-acrylate peak decreased

whereas that of methacryloxethyl thiocarbonyl rhodamine-B increased significantly as the temperature of the polymer suspension increased. The results show that as the temperature of the suspended microparticles increases, the poly (NIPAAm-co-MAA) microparticles shrink and phase separate from the solution. An increase in the methacryloxethyl thiocarbonyl rhodamine-B: fluorescein o-acrylate fluorescence intensity ratio was observed. Figure 8.2 shows the variation of methacryloxethyl thiocarbonyl rhodamine-B: fluorescein o-acrylate fluorescence intensity ratio with temperature of the suspended polymer particles. The phase transition temperature of the poly (NIPAAm-co-MAA) microparticles also increased to about 35°C.

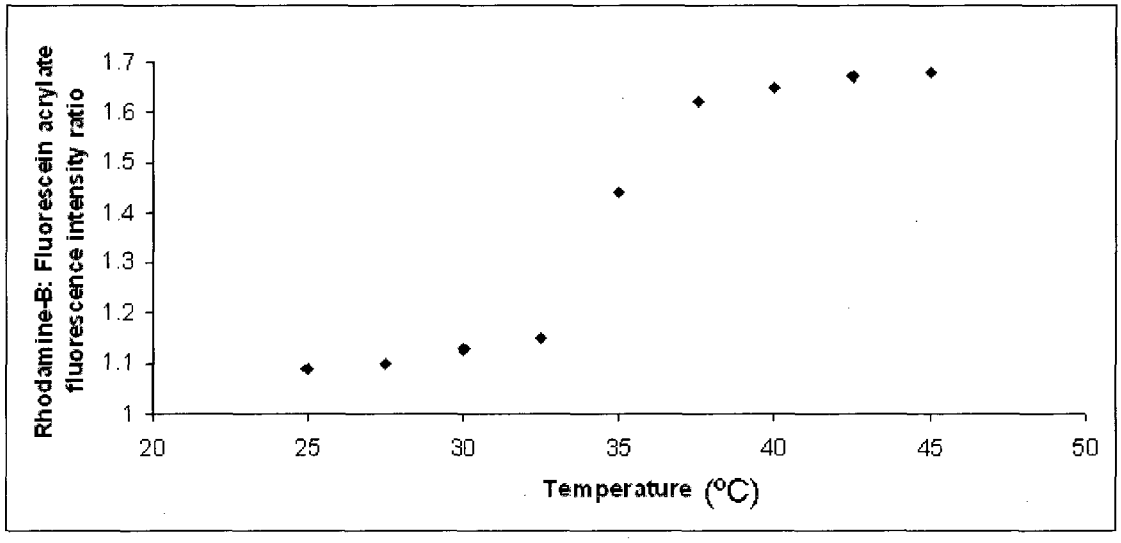

Figure 8.2: Thermal response of poly (NIPAAm-co-MAA) microparticles labeled with fluorescein o-acrylate and methacryloxethyl thiocarbonyl rhodamine-B

8.4.3 Application of THO Imprinted Polymer Microparticles in Analysis of THO

THO imprinted polymer microparticles suspended in phosphate buffer at pH 7 were investigated for their response to THO concentrations. 0.05g of the polymer microparticles were suspended in 2.5mL of pH 7 phosphate buffer with the ionic strength adjusted to 0.1M using potassium chloride and titrated with various standard solutions of THO. The microparticles were excited at 450nm and the fluorescence emissions of fluorescein o-acrylate and methacryloxethyl thiocarbonyl rhodamine-B were obtained at 517nm and 585nm respectively at various concentrations of THO. A decrease in fluorescence intensity of fluorescein o-acrylate and an increase in fluorescence intensity of methacryloxethyl thiocarbonyl rhodamine-B were observed as the concentration of THO was increased. This resulted in an increase in the methacryloxethyl thiocarbonyl rhodamine-B: fluorescein o-acrylate fluorescence intensity ratio with increasing THO concentration. A graph of the fluorescence intensity ratio of methacryloxethyl thiocarbonyl rhodamine-B: fluorescein o-acrylate vs. -log [THO] was plotted and shown in figure 8.4.

A possible explanation for the profile observed is that at pH 7, methacrylic acid is deprotonated while THO is protonated. There is electrostatic attraction between the positively charged protonated THO and the negatively charged deprotonated methacrylate ions within the polymer network causing the polymer microparticles to collapse or shrink. As the polymer microparticles collapse, the two fluorophores come closer together and energy is transferred from the fluorescein o-acrylate groups to the methacryloxethyl thiocarbonyl rhodamine-B groups. This transfer of energy between the

two fluorophores causes the intensity of fluorescein o-acrylate to decrease while that of methacryloxethyl thicarbonyl rhodamine-B increases.

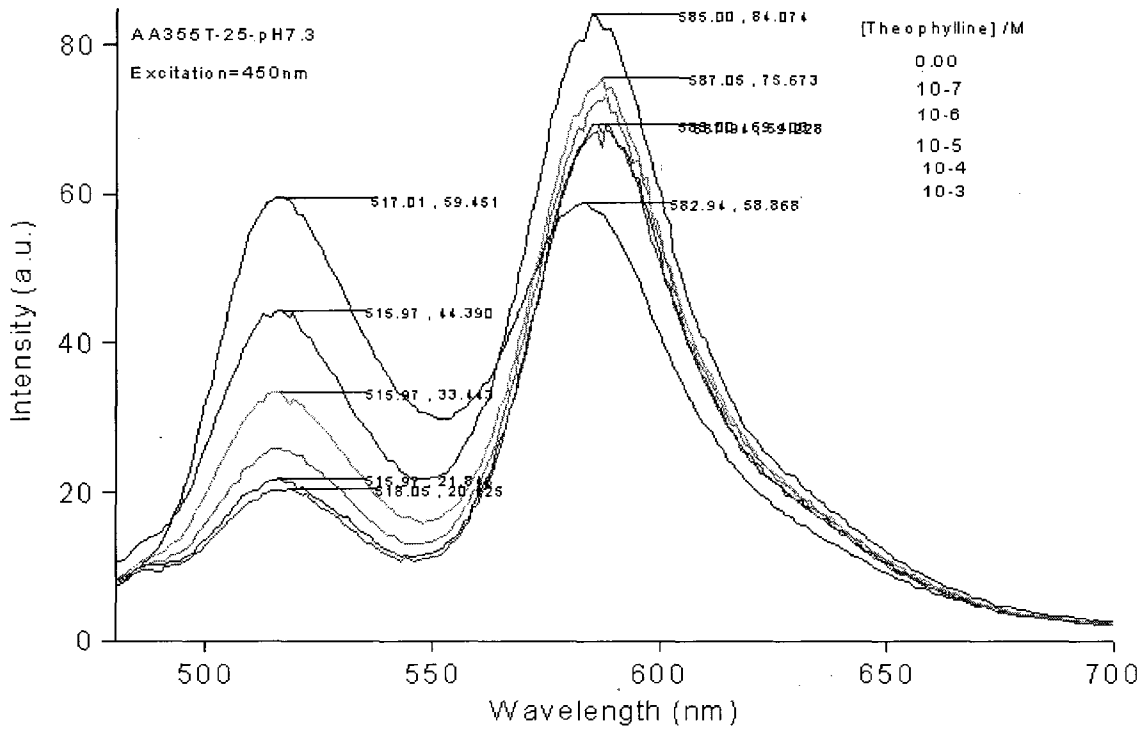

Figure 8.3: Spectrum of methacryloxethyl thiocarbonyl rhodamine-B and fluorescein o-acrylate within poly (NIPAAm-co- MAA) microparticles suspended in pH 7 phosphate buffer titrated with THO.

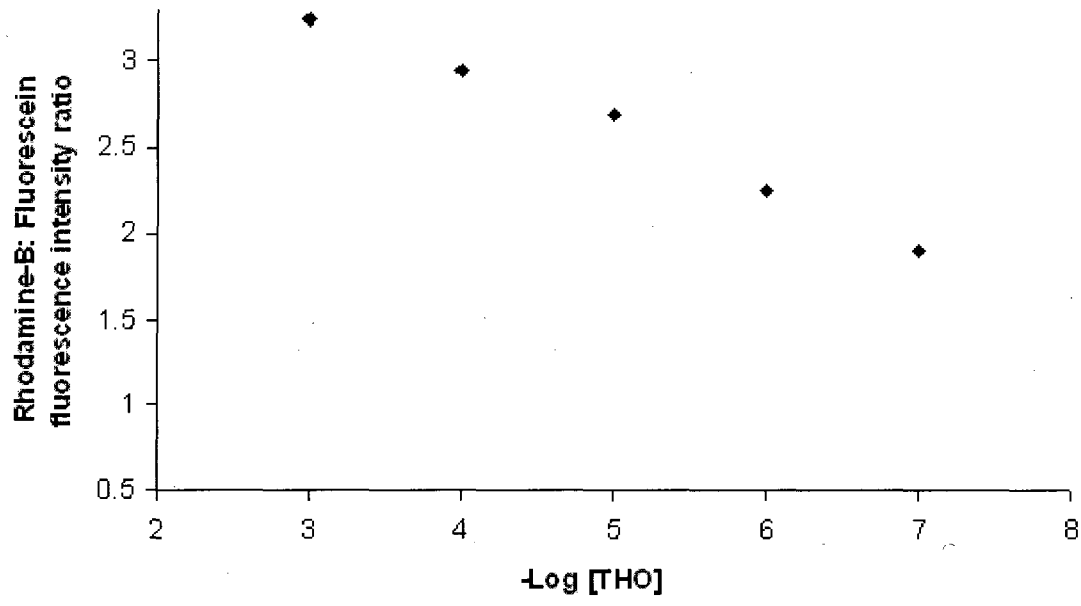

Figure 8.4: Theophylline response for THO imprinted poly (NIPAAm-co-MAA) microparticles.

8.4.4 Analysis of Caffeine by THO Imprinted Polymer Microparticles

Caffeine was used to test the selectivity of the THO imprinted polymer microparticles. A series of standard solutions of caffeine were prepared and analyzed using the THO imprinted polymer microparticles suspended in a pH 7 phosphate buffer with ionic strength adjusted to 0.1M using KCL. A 2.5mL aliquot of the polymer suspension was transferred into a 3mL cuvette and fitted in to the spectrofluorometer. The microparticles were excited at 450nm and fluorescence intensities of methacryloxethyl thicarbonyl rhodamine-B and fluorescein o-acrylate were obtained at 517nm and 585nm respectively as the concentration of caffeine increased in the cuvette. Figure 8.5 shows the results of analysis of caffeine by THO imprinted polymer microparticles suspended in pH 7 phosphate buffer.

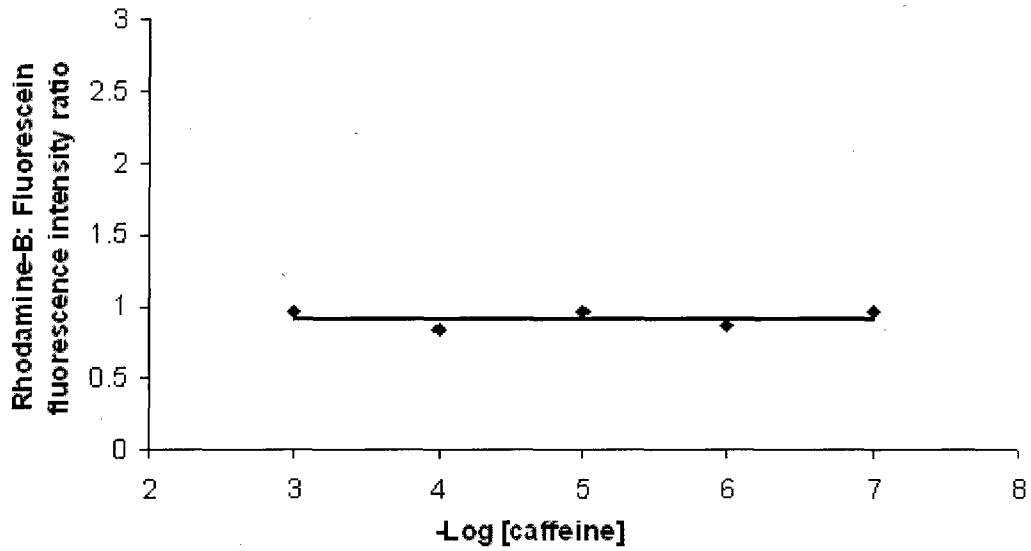

Figure 8.5: Caffeine response for THO imprinted poly (NIPAAm-co-MAA) Microparticles.

8.4.5 Analysis of THO by Non-imprinted Polymer Microparticles

The thermal responses for non-imprinted polymer microparticles were found to be similar to the THO-imprinted polymer microparticles. However, the microparticles were non-responsive to THO solutions introduced into the polymer suspension. There were no changes in the fluorescein o-acrylate: methacryloxethyl thiocarbonyl rhodamine-B fluorescence intensity ratio with increase in THO concentrations. This shows that there was no binding between the polymer microparticles and the THO molecules.

8.5 Molecular Imprinting of β-D-glucopyranose

8.5.1 Preparation of β-D-glucopyranose Imprinted Poly (NIPAAm-co-acrylamide) Particles

In this project, lightly cross-linked glucose imprinted polymer particles were prepared by dispersion polymerization according to the formulation shown in table 8.2 using NIPAAm, acrylamide, and ß-D-glucopyranose as the principal monomer, recognition monomer, and imprint molecule respectively. MBA and PVP were used as the cross-linker and stabilizer respectively while KPS was used as the initiator. All the monomers, cross-linker, stabilizer and initiator were first dissolved in water in a 100mL flask then sonicated for 20 minutes for complete dispersion of the solutes into the solvent. Oxygen was removed from the reaction mixture by purging oxygen in to the flask for 20 minutes. The flask and its content were then heated in a water bath held at 60°C and left for 16 hours for the polymerization process to be completed.

Reagent	Quantity
NIPAAm	1.018g (9mmol)
Acrylamide	0.035g (0.5mmol)
β-D-glucopyranose	0.036g (0.2mmol)
MBA	0.077g (0.5mmol)
PVP	0.224g
KPS	0.050g (0.18mmol)
Water (solvent)	40.00mL

Table8.2: Typical formulation for the synthesis of β-D glucopyranose imprinted poly (NIPAAM-co-acrylamide) particles.

8.5.2 Extraction of the β-D-glucopyranose from Polymer Network

The polymer microparticles were isolated by centrifugation. After the microparticles were isolated and cleaned, β-D-glucopyranose was extracted by suspending the particles in 0.1M nitric acid solution in a 100mL flask immersed in a temperature controlled water bath maintained at 30°C and stirred for 6 hrs. At this temperature, the polymer particles are swollen and the bound β-D-glucopyranose molecules can be extracted from the particles. The dilute nitric acid solution oxidizes the straight chain form of the β-D-glucose converting it to glucaric acid as shown in the following equation.

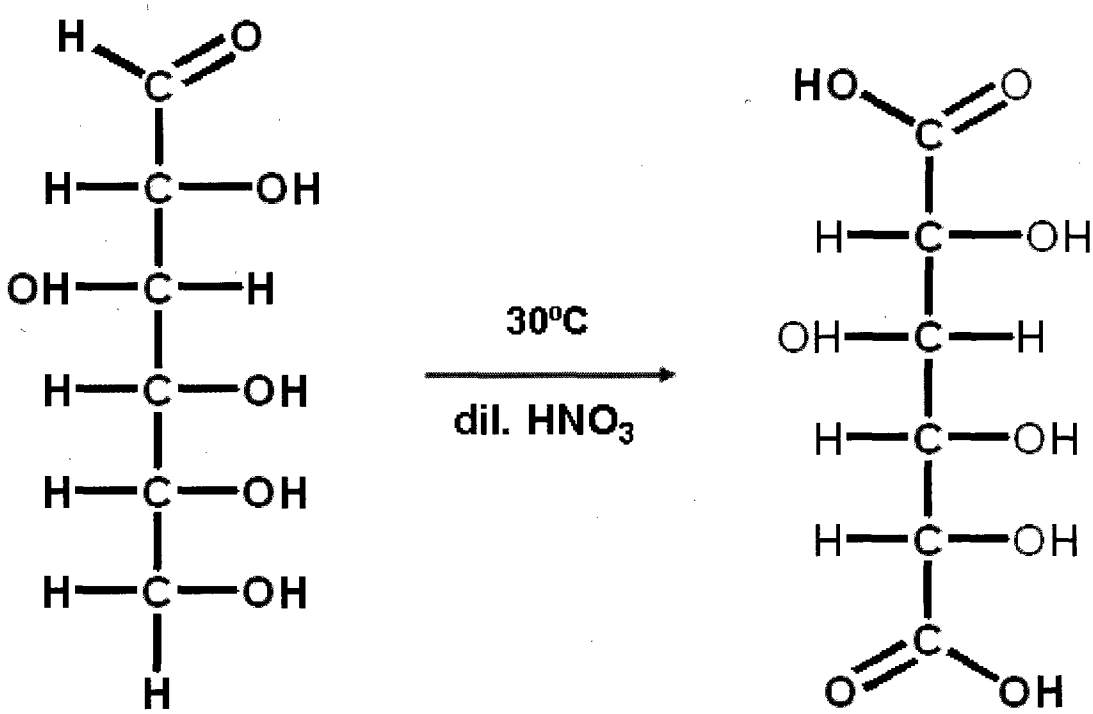

Figure8.6: Oxidation of straight chain form of β -D-glucose by dilute nitric acid.

The polymer microparticles were then washed several times by resuspending them in de-ionized water and centrifuging until the final supernatant was neutral. The pH of the supernatant was tested using a pH meter. This was to ensure that both the acidic glucaric and nitric acids were removed from the particles. The polymer particles were then embedded in PVA membranes prepared according to the formulation described in chapter 3 of this thesis. The membranes were stored in de-ionized water to prevent them from ripping.

8.6 Preparation of Non-Imprinted Poly (NIPAAm-co-acrylamide) Particles

Non-imprinted polymer (NIP) particles were prepared using the same polymerization procedure as the β-D-glucopyranose imprinted polymer but without β-D-glucopyranose. The particles were then isolated by centrifugation, resuspended in de-ionized water, and centrifuged again. The process was repeated three times to ensure that all the unreacted monomers were removed. They were then embedded in PVA membrane and stored in de-ionized water for glucose analysis.

8.7 Analysis of β-D-glucopyranose and β-D-galactopyranose by Turbidity Measurements

The membranes containing β-D-glucopyranose extracted-MIP microparticles were then secured in a membrane holder and fitted in a cuvette. 2.5mL of pH 7 MOP buffer with ionic strength adjusted to 0.1M with KCl was immediately added to the cuvette and left for about 1hr. Standard solutions of β-D-glucopyranose were also prepared in pH 7 MOP buffer with ionic strength adjusted with 0.1M KCl. Binding of β-D-glucose to the polymer microparticles in the membranes was investigated by adding aliquots of 100μL of the standard β -D-glucopyranose solutions to the PVA membrane in pH 7 MOP buffer fitted in the cuvette. To investigate the selectivity of the sensor, standard solutions of β-D-galactopyranose were prepared in pH 7 MOP buffer with ionic strength adjusted with 0.1M KCl. Aliquots of 100μL of the β-D-galactopyranose standard solutions were added to the PVA membrane containing the glucose MIP microparticles.

Turbidity measurements of the membrane containing polymer microparticles were taken as the various aliquots of the standard solutions of either β-D-glucopyranose or β-D-galactopyranose were added to the cuvette maintained at constant temperatures of 25°C and 40°C. The procedure was repeated using NIP microparticles to investigate their interactions with β-D-glucopyranose. The two temperatures were chosen for analysis because the polymer particles are temperature sensitive due to thermal properties of poly (NIPAAm). At 25°C, the polymer microparticles are in the swollen state, while at 40°C, they are in the collapsed state as shown by the temperature response of the microparticles. Absorbance measurements were taken at 500nm.

8.8 Results and Discussions

8.8.1 Effect of Temperature on Glucose Imprinted Polymer Particles

The effect of temperature on the β-D-Glucopyranose imprinted poly (NIPAAm-co-acrylamide) microparticles was studied by measuring turbidity of the particles embedded in PVA membranes at various temperatures. Increase in turbidity with increasing temperature was observed. The phase transition temperature of the polymer also increased slightly to about 35.8°C. The increase in phase transition temperature depended on the percentage of acrylamide monomer used in the copolymerization. Polymer microparticles prepared with higher percentage of acrylamide were found to have a higher phase transition. Introduction of acrylamide in the polymer network increases the hydrophilic nature of the polymer making the polymer swell. Figure 8.7 below shows the temperature response of poly (NIPAAm-co-

acrylamide) microparticles embedded in PVA membrane. The microparticles were prepared according to the formulation given on table 8.1.

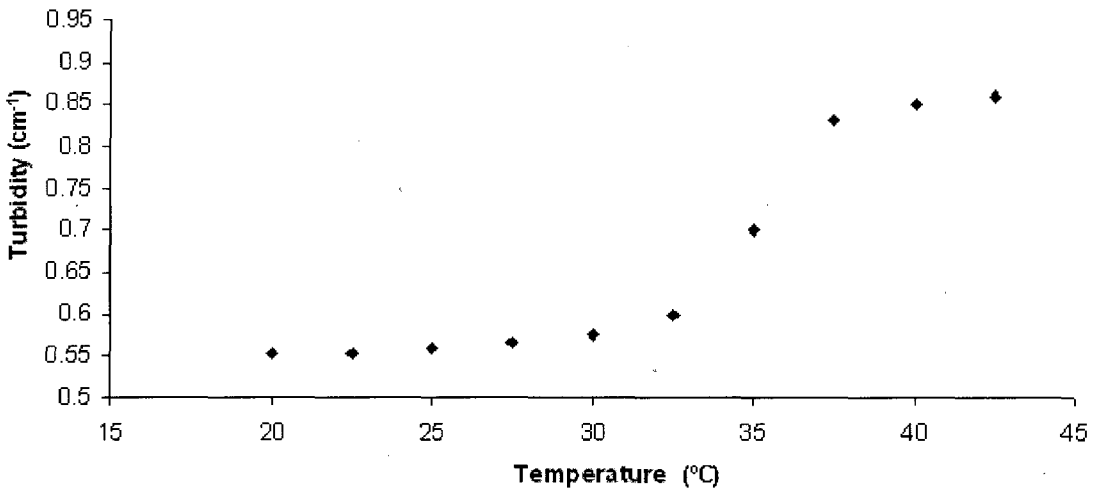

Figure 8.7: Temperature response of Poly (NIPPAAm-co-acrylamide) Microparticles.

8.8.2 β-D-Glucopyranose Response of Non-imprinted Poly (NIPAAm-co-acrylamide) Particles

The binding of β-D-glucopyranose to the non-imprinted polymer microparticles was investigated using turbidity measurements. A graph of turbidity vs. –log [β-D-glucopyranose] was plotted. The results show that there was no change in absorbance with increase in concentration of β-D-glucopyranose at both 25°C and 40°C indicating that non-imprinted polymer microparticles do not bind with β-D-glucopyranose molecules. Figure 8.8 shows the spectrum and of absorbance of non-imprinted polymer microparticles in a PVA membrane in pH 7 MOP buffer as the concentration of β-D-glucopyranose increases at 25°C. Figure 8.9 shows a graph of turbidity vs. –log [β-D-glupyranocose] at 25°C and 40°C.

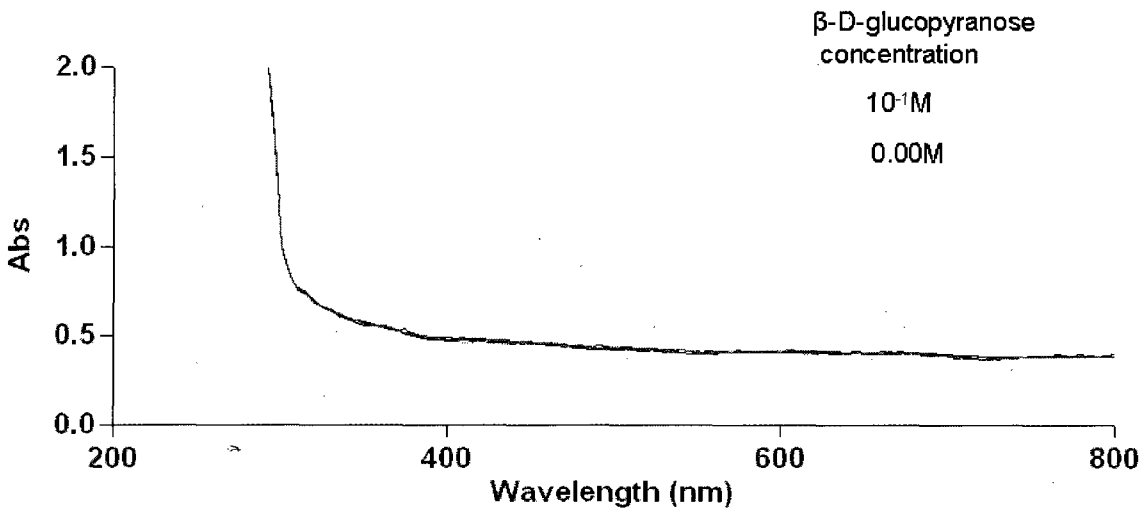

Figure 8.8: Absorbance vs. wavelength spectrum of Non β-D-glupyranocose imprinted poly (NIPAAm-co-Acrylamide) microparticles suspended in PVA membrane at 25°C titrated with various concentrations of β-D-glucopyranose.

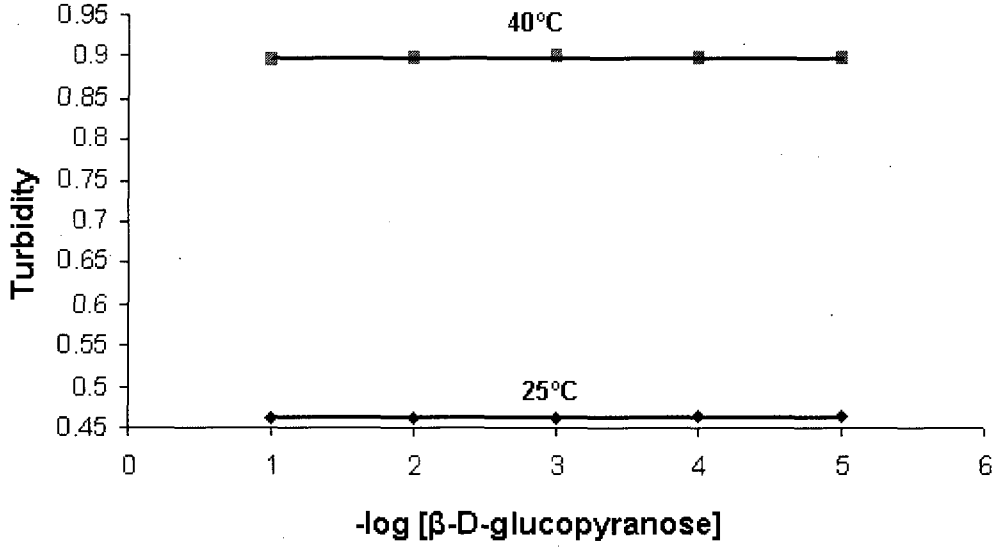

Figure 8.9: Graph of turbidity of non-imprinted poly (NIPAAm-co-acrylamide) microparticles vs. concentration of β-D-glucopyranose at 40°C.

8.8.3 Analysis of β-D-Glucose by Glucose Imprinted Poly (NIPAAm-co-acrylamide) Particles.

Figure 8.10 shows the absorbance spectrum of β-D-glucopyranose imprinted poly (NIPAAm-co-acrylamide) microparticles in a PVA membrane at 25°C as concentration of β-D-glucopyranose increases. There was insignificant change in turbidity with increase in concentration of β-D-glucopyranose indicating that there is no binding or interaction between the glucose molecules and the polymer particles at 25°C. This little increase in turbidity with increase in β-D-glucopyranose concentration is attributed to the fact that at temperatures lower than the LCST of poly (NIPAAm), the imprinted cavities are distorted due to the swollen state of the hydrogel in water. There is also competition in the interaction between the β-D-glucopyranose molecules and the water molecules especially at temperatures when the polymer particles are in swollen state.

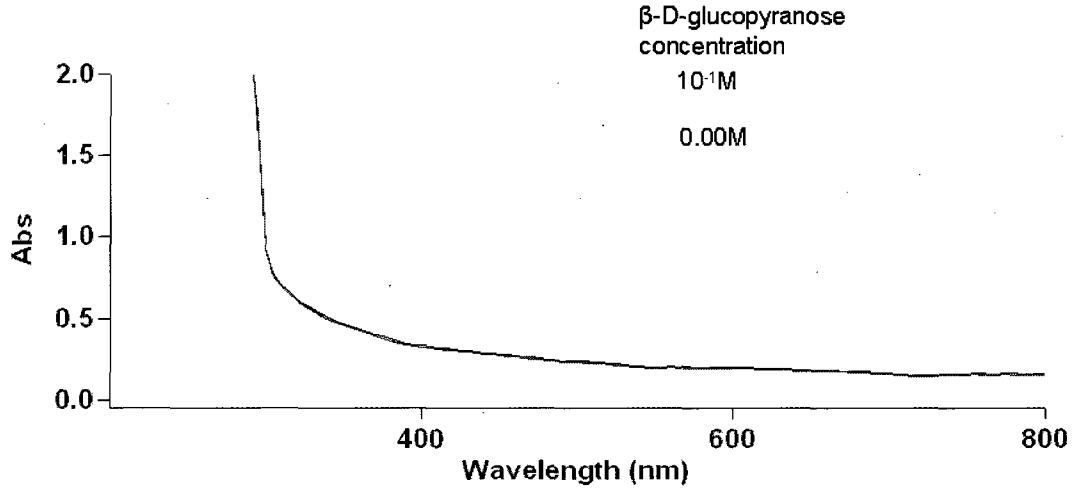

Figure 8.10: Absorbance vs. wavelength spectra of poly (NIPAAm-co-acrylamide) microparticles suspended in PVA membrane at 25°C titrated with various concentrations of β-D-glucopyranose.

Figure 8.11 shows the absorbance spectrum of β-D-glucopyranose imprinted poly (NIPAAm-co-acrylamide) microparticles in PVA membranes at 40°C as the concentration of β-D-glucopyranose is increased. The results show that as the concentration of β-D-glucopyranose increases, the absorbance also increases. This indicates that there is interaction between the β-D-glucopyranose molecules and the polymer particles. The –OH groups of the β-D-glucopyranose molecules hydrogen bond with the amide groups of the acrylamide molecules within the polymer particles causing the polymer to collapse. The collapsing of the polymer microparticles are indicated as increase in turbidity. A graph of turbidity vs. –log [β-D-glucopyranose] was plotted and the results are represented by figure 8.12.

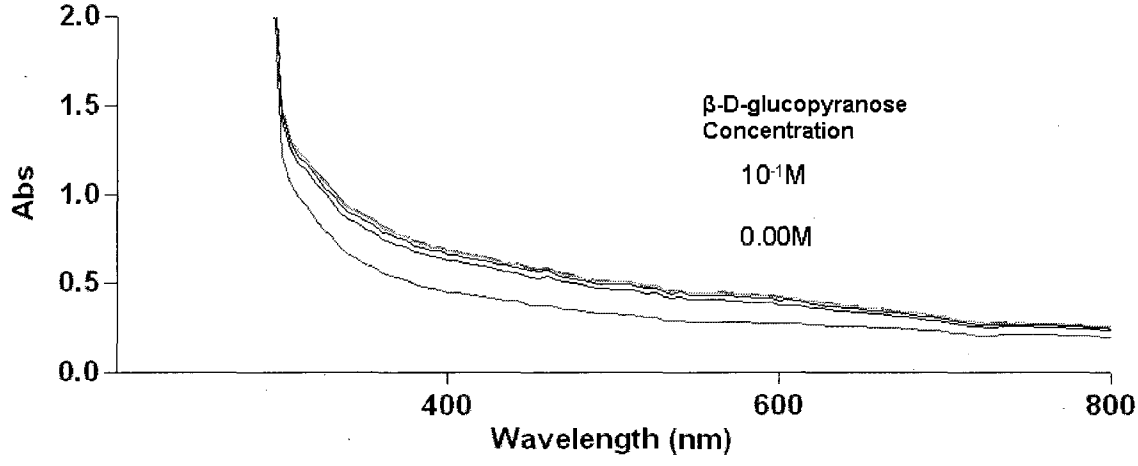

Figure 8.11: Absorbance vs. wavelength spectra of poly (NIPAAm-co-acrylylamide) particles suspended in PVA membrane at 40°C titrated with various concentrations of β-D-glucopyranose.

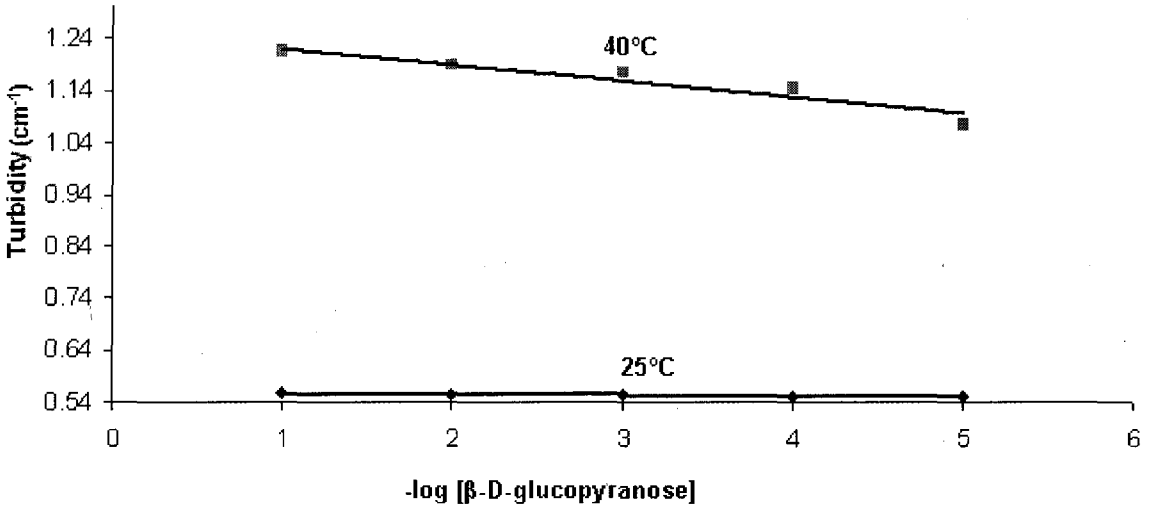

Figure 8.12: Graph of turbidity of poly (NIPAAm-co-acrylamide) particles in PVA membrane vs. log concentration of β-D-glucopyranose at 25°C and 40°C.

The lightly cross-linked polymer network holds the functional groups in fixed positions enabling the groups to form suitable binding sites for interaction with β-D-glucopyranose. They also enable the polymer to both retain its swelling-shrinking property without losing its mechanical strength and also allows for easy diffusion of the β-D-glucopyranose molecules into the polymer network during analysis. During the preorganization stage of the imprinting process, the amide group of the acrylamide monomer forms hydrogen bonds with the hydroxyl groups of the glucopyranose molecule.

8.8.4 β-D-Galactopyranose Response of poly (NIPAAm-co-acrylamide Microparticles

Figure 8.13 below shows the absorbance spectrum of β-D-glucopyranose imprinted poly (NIPAAm-co-acrylamide) microparticles in a PVA membrane at 25°C with increasing concentration of β-D-galactopyranose. The absorbance was obtained at

25°C and also at 40°C. The results show that β-D-glucopyranose imprinted polymer particles have lower binding affinity towards β-D-galactopyranose at 40°C compared to β-D-glucopyranose. There was no binding between β-D-galactopyranose and the polymer particles at 25°C. Turbidity of the membranes containing polymer microparticles were calculated for the various concentrations of β-D-galactopyranose added according to equation 9. A graph of turbidity vs. –log [β-D-galactopyranose] was plotted and the results are shown in figure 8.14.

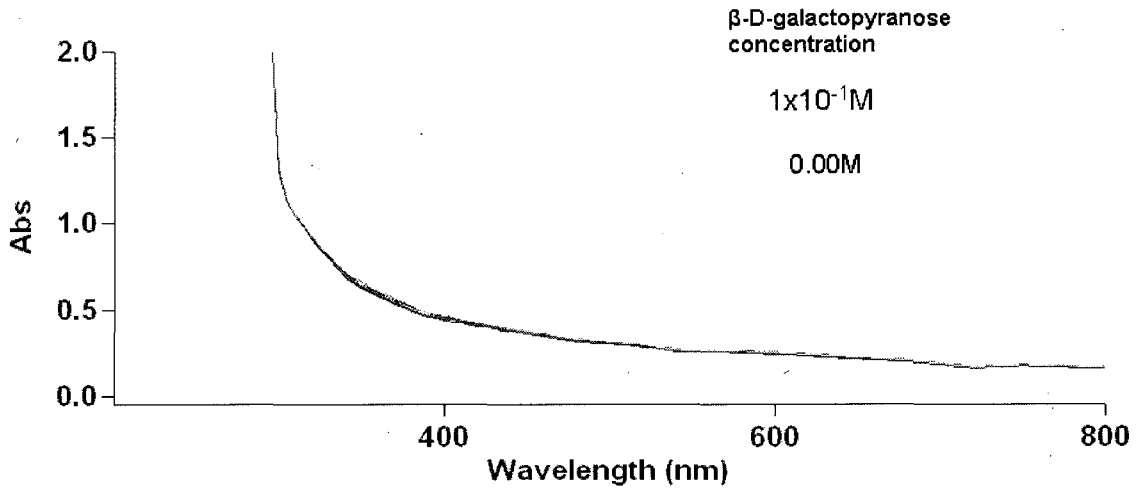

Figure 8.13: Absorbance vs. wavelength spectrum of poly (NIPAAm-co-acrylamide) microparticles suspended in PVA membrane at 25°C titrated with various concentrations of β-D-galactopyranose.

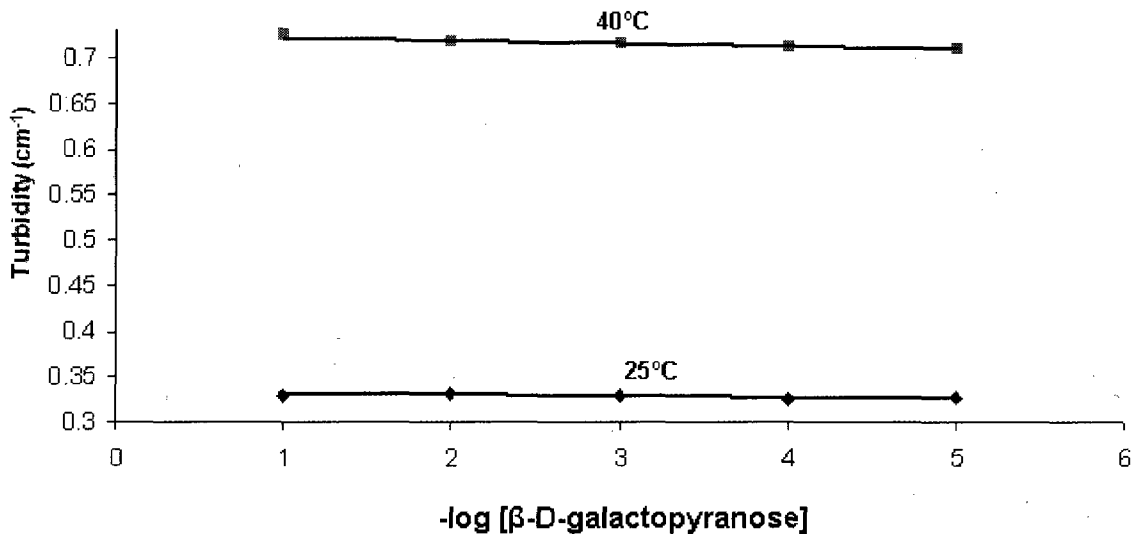

Figure 8.14: Graph of turbidity of poly (NIPAAm-co-acrylamide) vs. concentration of β-D-galactopyranose at 25°C and 40°C.

8.9 Conclusions

Lightly cross-linked molecularly imprinted polymer particles were prepared in acetonitrile and water for recognition of theophylline and β-D-glucopyranose respectively. The polymer microparticles exhibited swelling and shrinking properties that varied with the concentration of theophylline. The recognition of both theophylline and β-D-glucopyranose was enhanced at temperatures above the phase transition temperature of the polymer particles when the polymer microparticles were collapsed and the presence of the imprint molecules caused the polymer microparticles to collapse further. Theophylline imprinted polymer did not bind to caffeine. The experimental results show that β-D-glucopyranose imprinted polymer showed strong binding to the template but weak binding to β-D-galactopyranose. It was also observed that there was no significant binding between the non-imprinted polymers (NIPs) and either theophylline or β-D-glucopyranose.

CHAPTER 9

CONCLUSIONS AND FUTURE WORK

9.1 Conclusions

A chemical sensor based on polymer swelling and shrinking was developed using dispersion polymerization in both water and acetonitrile. Fluorescent labeled poly (NIPAAm) microparticles functionalized with acrylamide, MAA, IDA, DVPAA, NMPPAAm, and NBPMPA were also prepared successfully by dispersion polymerization. The microparticles were prepared using PVP and poly (styrene-co-acrylonitrile) as steric stabilizers and cross-linked using MBA. Poly (NIPAAm) microparticles showed thermal responsive properties with a lower critical solution temperature (LCST) of about 33°C and the LCST depended on amount, hydrophilic, or hydrophobic nature of comonomers used in copolymerizing NIPAAm. Poly (NIPAAm) microparticles labeled with 9-VA, 2-NMA, fluorescein o-acrylate, and methacryloxethyl thiocarbonyl rhodamine B fluorophores also showed thermal responsive properties. In the polymerization process, the amount of cross-linker was optimized for swelling ability of the polymer microparticles. Low cross-linking levels results in gel like microparticles with non-uniform swelling and shrinking. High cross-linking produces rigid polymer microparticles with little swelling and shrinking ability.

Poly (NIPAAm-co-AIDA) microparticles labeled with 9-VA and 2-NMA were prepared and evaluated for response with Cu^{2+} ions. Only the polymer microparticles prepared by copolymerizing NIPAAm with very low percentage of AIDA (less than 2

mole %) showed a thermal phase transition while those prepared with more than 2mole % lost the thermal phase transition at pH 6.

Swllable poly (NIPAAm-co-DVPAA) microparticles labeled with 9-VA and 2-NMA were prepared and hydrolyzed. The hydrolyzed polymer microparticles were sensitive to as low as 10^{-5}M Cu^{2+}. The hydrolyzed microparticles were also found to be sensitive 10^{-5}M Ni^{2+} ions, but showed insignificant sensitivity to the same concentration level of both Zn^{2+} and Pb^{2+} ions at either 25°C and 40°C. The unhydrolyzed polymer microparticles were not sensitive to any of the metal ions. The unhydrolyzed polymer microparticles also had LCST below 32°C while the hydrolyzed form prepared by copolymerizing NIPAAm with less than 2mole% of DVPAA had the LCST increased to above 34°C. The unhydrolyzed polymer microparticles prepared by copolymerizing NIPAAm with about 5mole% of DVPAA showed no phase transition temperature up to about 45°C. The microparticles aggregated with increasing Cu^{2+} ion concentrations. Potentiometric titrations of the hydrolyzed poly (NIPAAM-co-DVPAA) microparticles suspended in MOP buffer, pH 6 with a standard solution of Cu^{2+} ions showed a binding constant of 8.4×10^5.

Fluorescent labeled lightly cross-linked poly (NIPAAm-co-NMPPAAm) and poly (NIPAAm-co-NBPMPA) microparticles were also prepared and their response to transition metal ions such as Cu^{2+}, Pb^{2+}, Ni^{2+}, Zn^{2+} were evaluated. Both the polymer microparticles showed swelling and shrinking properties that depended on the percentage of cross-linking. The polymer microparticles had phase transition temperatures below 32 °C and were sensitive to the metal ions at concentrations as low as 10^{-8}M at both 25 °C and 50 °C. The sensitivity of the polymer microparticles was

higher at 50 °C that at 25 °C. The polymer microparticles had higher sensitivity for Cu^{2+} and Ni^{2+} ions compared to the other metal ions. When the polymer microparticles were potentiometrically titrated with standard solutions of Cu^{2+}, the binding constants for poly (NIPAAm-co-NMPPAAm) and poly (NIPAAm-co-NBPMPA) were 2.6×10^7 and 3.1×10^8 respectively.

Poly (NIPAAm-co-acrylamide) microparticles imprinted with β-D-glucopyranose were prepared and studied for both β-D-glucopyranose and β-D-galactopyranose response. The microparticles were embedded in PVA membranes and the optical properties of the membranes containing the imprinted polymer microparticles were evaluated. The glucose imprinted polymer microparticles had a higher sensitivity for β-D-glucopyranose when the polymer microparticles were in the collapsed form than when the particles were in the swollen form. The response time of the collapsed polymer microparticles to β-D-glucopyranose was long due to decreased rate of diffusion of the glucose molecules into the collapsed polymer network. The microparticles also responded to β-D-galactopyranose but with a lower sensitivity compared to that of β-D-glucopyranose. Also molecularly imprinted poly (NIPAAm-co-MAA) microparticles labeled with fluorescein o-acrylate and methacryloxethyl thiocarbonyl rhodamine B fluorophores were prepared for theophylline sensing. The polymer microparticles were found to be sensitive to as low as 10^{-7}M theophylline and not sensitive to caffeine.

9.2 Future Work

The future work will be based mostly on the results obtained from this research project. The work will focus on improving some of the features of the sensor such as increasing the sensitivity, selectivity, and also exploring the use of other fluorophore pairs that are readily available and can be excited at longer wavelengths. 9-VA and 2-NMA fluorophores have short excitation wavelengths which render them unsuitable to be applied in sensors for biological samples. Also preparation of monodisperse polymer microparticles free from coagulation is a challenging task and needs to be explored further. Because the response of the sensor also depends on the extent to which the microparticles are dispersed, it is vital to develop ways to prepare monodisperse polymer microparticles. The sensor response also depend on the swelling and shrinking ability of the polymer particles to a great extent and it is therefore important to prepare uniform sized microparticles which swell or shrink uniformly with changes in either environmental conditions (temperature, pH or ionic strength) or analyte concentrations.

In the case of poly (NIPAAm-co-DVPAA) particles, the particles can only bind with metal ions in hydrolyzed form but the hydrolyzed form has deprotonated carboxylic acid groups which increases polymer solubility in aqueous medium or increases the phase transition temperature of the polymer. The solubility of the polymer particles interferes with their mechanical strengths. It is therefore necessary to reduce the phase transition temperature of the polymer particles by copolymerizing NIPAAm with monomers such as tertiary butyl acrylamide (NTBA). A sensor operating at lower temperatures is suitable for applications under physiological conditions.

LIST OF REFERENCES

1. Francioso, L.; Prato, M.; Siciliano, P.; *Sensors and Actuators*, **2008**, 130, 359-365.

2. Hsu, C. T.; Lyuu, H. J.; Young, T. H.; Conte, E. D.; Zen, J. M.;

   Sensors and Actuators, **2006**, 113, 22-28.

3. Janata, J., *Anal. Chem.*, **2001**, 73, 150a.

4. Arnold, M.A.; *Anal. Chem.* **1992**, 64, A1015.

5. Murray, R. W.; Dessy, R. E.; Heineman, W. R.; Janata, J., Seitz, W. R.; Chemical Sensors and Microinstrumentation, *American Chemical Society*, Washington D.C. **1989**.

6. Spichiger-Keller, U. E.; *Chemical Sensors and Biosensors for Medical Applications*, Weiheim, Wiley-VCH, **1998**.

7. St. John, P.; Davis, R.; Cady, N.; Czajka, J.; Batt, C.; Craighead, H.; *Anal. Chem.* **1998**, 70, 1108.

8. Nagata, R.; Yokuyama, K.; Clarke, S. A.;Karube, I.; *Biosens. Bioelectrons.* **1995**,10, 377.

9. Hart, A. L.; Turner, A.; Hopcroft, D. *Biosens. Bioelectrons.* **1996**, 11, 263.

10. Janata, J.; *Principles of Chemical Sensors*; Plenum Press: New York, **1989**.

11. Lau, K. S.; Wong, K. H.; Yeung, S. K.; *J. Chem. Educ.* **1993**, 70 (4), 336.

12. Seitz, W. R.; CRC Crit. Rev. *Anal. Chem.* **1988**, 19, 135.

13.Bergman, I.; *Nature* **1968**, 218, 396.

14. Freeman, T. M.; Seitz, W. R.; *Anal. Chem.* **1978**, 50, 1242.

15. Peterson, J. T.; Goldstein, S. R.; Fitzgerald, R. V.; Buckhold, D. K.; *Anal. Chem.* **1980**, 52, 864.

16. Saari, L.A.; Seitz, W., R.; *Anal. Chem.* **1983**, 55, 667

17. Taitt, C. R.; Shubin, S.; Angel, R.; Ligler, F. S.; *Appl. Environ. Micro.* **2004**, 70, 152-158

18. Leiner, M. J. P.; *Sensors and Actuators: B*, **1995**, 29, 169.

19. Grate, J. W.; Martin, S.; White, R.; *Anal. Chem.* **1993**, 65, 940A.

20. Dorety, S. A.; PhD. Dissertation, University of New Hampshire, **2000**.

21. Tanaka, T.; *Phys. Rev. Lett.* **1978**, 40, 820.

22. Shakhsher, Z., Seitz, W. R.; Legg, K. D.; *Anal. Chem.* **1994**, 66, 1731.

23. Rooney, M. T.; PhD. Dissertation, University of New Hampshire, **1996**.

24. Pan, S.; Conway, V.; Shakhsher, Z.; Emerson, S.; Bai, M.; Seitz, W. R.; Legg, K. D.; *Anal. Chim. Acta.* **1993**, 279, 195.

25. Civielo, M.C.; MS. Thesis, University of New Hampshire, **1997**.

26. Milde, S. P.; PhD. Dissertation, University of New Hampshire, Durham, NH **2001**.

27. Fan, W.; PhD. Dissertation, University of New Hampshire, Durham, NH, **2003**.

28. Peppas, N. A.; Bergmann, N. M.; *Prog. Plym. Sci.* **2008**, 33, 271-288.

29. Oral, E.; Peppas, N. A.; *J. Biomed. Mater. Res. A.* **2004**, 68A, 439-47.

30. Williams, S. R.; The biological chemistry of the elements, in: The Inorganic Chemistry of Life Claredon Press, Oxford, **1991**.

31. Sigel, H.;in: Sigel, H. (Ed.), *Metal ions in Biological Systems*: *Properties of Copper*, **1981**, 12.

32. Wagoner, D. J.; Bartnikas, T. B., Gitlin, J. D.; The Role of Copper in Neurodegenerative Disease, *Neourobiol, Dis.* **1999**, 6, 221-230.

33. Changela, A.; Chen, K.; Xue, Y.; Holschen, J.; Outten, C.E.; O'Halloran, T. V.; Mondragon, A.; *Molecular Basis of Metal-ion Selectivity and Zeptomolar Sensitivity*; **2003**, 301, 1383-1387.

34. Rae, T. D. Schmidt, P. J.; Pufahl, R. A.; Cullotta, V. C.; O'Halloran, T. V.; Undetectable Intracellular Free Copper: The Requirement of a Copper Chaperone for Superoxide Dismutase, *Science*, **1999**, 284, 805-808.

35. Finney, L. A.; O'Halloran, T. V.; Transition Metal Speciation in the Cell: Insights from the Chemistry of Metal Ion Receptors, *Science,* **2003**, 300, 931-936.

36. High, B.; Bruce, D.; Richter, M. M.; Determining Cpper Ions in Water Using Electrochemiluminescence, *Anal. Chim. Acta.* **2001**, 449, 17-22,

37. Tapia, L.; Suazo, M.; Hodar, C.; cambiazo, V.; Gonzalez, M.; *Copper Exposure Modifies the Content and Distribution of Trace Metals in Mammalian Cultured Cells, Biometals*, **2003**, 16, 169-174.

38. Mayr, T.; Wemer, T.; Highly Selective Optical Sensing of Copper (II) Ions Based on Fluorescence Quenching of Immobilized Lucifer Yellow, *Analyst,* **2002**, 127, 248-252.

39. Chen, Y. F.; Rosenzweig, Z.; Luminescent CdS Quantum Dots as Selective Ion Probes, *Anal. Chem.* **2002**, 74, 5132-5138.

40. Zheng, Y. J; Orbulescu, J.; Ji, X.; Andreopoulos, F. M.; Pham, S. M.; Leblanc, R. M.; Development of Fluorescent Film Sensors for the Detection of Divalent Copper, *J. Am. Chem. Soc.* **2003**, 125, 2680-2686.

41. Zheng, Y. J.; Gattas Asfura, K. M.; Konka, V.; Leblanc, R. M.; A *Dansylated Peptide for the Detection of Copper ions, Chem. Commun.* **2002**, 2350-2351.

42. Zheng, Y. J.; Cao, X. H.; Orbulescu, J.; Konka, V.; Andreopoulos, F. M.; Pham, S.M.; Leblanc, R. M.; *Anal. Chem.* **2003**, 75, 1706-1712.

43. Colson, B. J.; Robinson, V. J.; *Analyst,* **1997**, 122, 1451-1455.

44. Sadhu, K. K.; Bag, B.; Bharadwaj, K. P.; *Inorg. Chem.* **2007**, 46, 8051-8058

45. Hopt, A.; Korte, S.; Fink, H.; Panne, U.; Niessner, R.; Jahn, R.; Kretzschmar, H.; Herms, J.; *Journal of Neuroscience Methods*, **2003**, 128, 159-172.

46. Rahimi, Y.; Goulding, A.; Shrestha, S.; Mirpuri, S.; Deo, S. K.; *Biochemical and Biophysical Research Communications*, **2008**, 370, 57-61.

47. Broder, J.; Majunder, A.; Srinivasamoorthy, G.; Keith, C.; Lauderdale, J.; Sornborger, A.; *J. Opt. Soc. Am.* **2007**, vol. 24, 9, 2921.

48. Du, Y.; Yan, J.; Zhou, W.; Yang, X.; Wang, E.; *Electrophoresis,* **2004**, 25, 3853-3859.

49. Kaval, N.; PhD. Dissertation, University of New Hampshire, Durham, NH, **2002**.

50. Seymour, R. B.; Carraher, C. E.; *Polymer Chemistry, 2nd Ed.*; Marcel Deker, New York, **1988**.

51. Steven, M. P.; *Polymer Chemistry: An Introduction*: Oxford University Press: New York. **1999**.

52. Miele, E.; PhD. Dissertation, university of New Hampshire, **1999**.

53. Crowie, J. M. G.; Polymers: Chemistry and Physics of Modern *Materials*, Intext Educational Publishers, New York, **1973**.

54. Billmeyer, F. W.; *Textbook of Polymer Science, 3rd Ed.*; John Wiley & Sons, New York: **1984**.

55. Young, R. J.; *Introduction to Polymers*, Hepman and Hall, **1986**.

56. Lovell, P. A.; *Emulsion Polymerization and Emulsion Polymers*, John Wiley and Sons, New York, **1997**.

57. *Dispersion Polymerization in Organic Media*, John Wiley and Sons Ltd. London, **1975**.

58. Nakashima, T.; Shimizu, M.; Kukizaki, M.; *Membrane Emulsion Operation Manual, 1st Ed.*, 1-4 -14, Tsuneshisa, Miyazaki City 880, Japan, **1971**.

59. Domszy, R. C.; Alama, R.; Edwards, C. O.; Mandelkern, L.; *Macromolecules*, **1986**, 19, 310.

60. Candau, F.; Ottewill, R. H.; *Scientific Methods for the Study of Polymer Colloids and their Applications,* Kluwer Academic Publishers, Boston, **1988**.

61. Wang, H. PhD. Dissertation, University of New Hampshire Durham, NH. **2002**.

62.Gibanel, S.; Heroguez, V.; Forcada, J.; *J. Polym. Sci. Part A: Polym. Chem. **2002**, 40, 2819.*

63. Flory, P.J.; *Principles of Polymer Science*, Cornell University Press, Ithaca, New York, **1953**.

64. Stobel, H. A.; Heineman, W. R., *Chemical Instrumentation: A Systematic Approach*, John Willey and Sons, NY: **1989**.

65. Zhang, Z.; Shakhsher, Z.; Seitz, W. R.; *Mikrochimica Acta.* **1995**, 121, 41.

66. Homola, J.; Yee, S.; Gauglitz, G.; *Sensors and Actuators B*, **1999**, 54, 3.

67. Hatefi, A.; Amsden, B. J.; J. *Control. Release*, **2002**, 80, 9-28.

68. Yao, K. D.; Peng, T.; Goosen, F. A.; Min, J. M.; He, Y. Y.; *J. Appl. Polym. Sci.* **1993**, 48, 343.

69. Tanaka, Y.; Kagami, Y.; matsuda, A.; Osada, Y.; *Macromolecules* **1995**, 28, 2574.

70. Heskins, M.;Guillet, E. J.; *J Macromol. Sci. Chem.* **1968**, 2, 1441-1445.

71. Shibayama, M.; Isono, K.; Okabe, S.; Karino. T.; Nagao, M.; *Macromolecules*, **2004**, 37, 2909-2918.

72. Liu, V.; Jastromb, W. E.; Bhatia, S. N.; J. *Biomed. Mater. Res.* **2002**, 60, 126-134.

73. Meunier, F.; Elaissari, A.; *In: Colloidal Polymers: Synthesis and Characterization*; Elaissari, A.; Ed.; Mercel Dekker: New york, **2003**; 117-143.

74. Chen, H.; Hsieh, Y. L.; *J. Polym. Sci. part A: Polym Chem.* **2004**, 42, 3293-3301.

75. Akiyma, Y.; Kikuchi, A.; Yamato, M.; Okano, T.; *Langmuir*, **2004**,

20, 5506-5511.

76. Cunliffe, D.; *Biotechnol. Lett.* **2000**, 22, 141-145.

77. Kempe, M.; *Anal. Chem.* ; **1996**, 68, 1948.

78. Ramstrom, O.; Ye, L.; Krook, M.; Mosbach, L.; *Anal Commun.*; **1998**, 35, 9.

79. Al-Kindy, S.; Badia, R.; Suarez-Rodriguez, J. L.; Diaz-Garcia, M, E.; *Critical Reviews in Anal. Chem*, **2000**, 30, 291.

80. Pauling, L. J.; *J. Am. Chem. Soc.* **1940**, 62, 2643.

81. Oral, E.; Peppas, N. A.; *polymers*, **2004**, 45, 6163-6173.

82. Hart, B. R.; Shea, K. J.; *J. Am. Chem. Soc.*, **2001**, 123, 2072.

83. Hart, B. R.; Shea, K. J.; Rush, D. J.; *J. Am. Chem. Soc.*, **2000**, 122, 460.

84. Spivak, D.; Shea, K. J.; *J. Org. Chem.*; **1999**, 64, 4627.

85. Spivak, D.; Gilmore, M. A.; Shea, K. J.; *J. Am. Chem. Soc.*, **1997**, 119, 4388.

86. Remcho, V. T.; Tan, Z. J.; *Anal. Chem.* **1999**, 248A.

87. Kriz, D.; ramstron, O.; Mosbach. K.; *Anal. Chem.* **1997**, 69, 345A.

88. Takashi, I.; Woo-sang, L.; Hiroyuki, N.; Toshifuni, T.; *J. of Chromatogr.* B, **2004**, 804, 197-201.

89. Wulf, G.; *Chem. Int. Ed. Engl.*, 34, **1995**, 1812.

90. Takeuchi, T.; Haginaka, J.; *J. of Chromatogr.* B, 728, **1999**, 1.

91. Harris, D.; Bertolucci, M.; *Symmetry and Spectroscopy*, **1989**, Dover Publications, New York.

92. Zumdahl, S. S.; *Chemical Principles, 5th Edition*, **2005**, Houghton New york.

93. Anderson, W. P.; Edwards, W. D.; Zerner, M. C.; *Inorg. Chem.* **1986**, 25, 2728-2732.

94. Wulfsberg, G.; *Inorganic Chemistry, University Science Books*, **2000**, 191-206, 357-362.

95. Harris, D. C.; *Quantitative Chemical Analysis, 7th Edition*, W. H. Freeman and Company, **2007**, New York, page 229.

96. Shriver, D.; Arkins, P.; *Inorganic Chemistry, 3rd Edition*, W. H. Freeman and Company, New York, **1999**.

97. Miessler, G. L.; Tarr, D. A.; *Inorganic Chemistry, 2nd Edition*, Prentice Hall: New Jersey, **1999**.

98. Kalyanasundaram, K.; *Photochemistry of Polypyridine and Porphyrin Complexes*, Academic, New York, **1992**.

99. Volger, A.; Kunkey, H.; Coord. *Chem. Rev.* **2000**, 208, 321.

100. Lancashire, R. J.; *Selection Rules for Electronic Spectroscopy*, **2006**.

101. Chen, R. F.; *Biochemical Fluorescence*: *Concepts*. **1965**, 408.

102. Roth, M.; *Fluorometric Assays of Enzymes: Methods of Biochemical Analysis*, Vol. 17, Wiley Interscience, New York, **1969**.

103. Gilbault, G. G.(Editor); *Fluorescence Theory, Instrumentation, and Practice*, Mercel Dekker Inc. Publishers, New York, **1967**.

104. Berlman, L. R.; *Handbook of Fluorescence Spectra in Aromatic Molecules*, Academic Press; New York, Vol. I, **1965**, Vol. I, 1971.

105. Hercules, D. M.(Editor); *Fluorescence and Phosphorescence Analysis*, Wiley Interscience Publishers, New York, London, Sydney, **1965**.

106. RÜdiger, R.; Marco, M.; Rosario, R.; Tullio, P.; *Nature Reviews Molecular Cell Biology*, **2003**, 4, 579-586.

107. Elangovan, M., Day, R. N.; Periasamy, A.; *J. Microsc.* **2002**, 205, 3-14.

108. Elangovan, M., Wallrabe, H.; Chen, Y.; Day, R. N.; Barroso, M.; Periasamy, A.; *Methods*, **2003**, 29, 58-73.

109. Giordano, L.; Jovin, T. M.; Irie, M.; Jares-Erijman, E. A.; *J. Am. Chem. Soc.* **2002**, 124, 7481-7489.

110. Wang, X.; Chang, S.; Yang, J.; Zhou, M.; Cao, D.; Tan, *J.; Applied Optics*, **2007**, 46, 35, 8446-8452.

111. Heeg, B.; Rumbles, G.; *Appl. Opt.,* **1981**, 20, 2934-2940.

112. Heeg, B.; DeBarber, P. A.; Rumbles, G.; *Appl. Opt.* **2005**, 44, 3117-3124.

113. Gilbault, G. G.(Editor).; *Practical Fluorescence*, Mercel Dekker Inc. Publishers, New York, **1973**.

114. Inger (Jr), J. D.; Crouch, S. R.; *Spectrochemical Analysis, Prentice* Hall Publishers, New Jersey, **1988**.

115. Liao, Q, G.; li, Y. F.; Huang, C. Z.; *Talanta*, **2007**, 71, 567-572.

116. Wilson, J. D.; Foster, T. H.; *Optics Letters*, **2005**, 18 vol. 30, 2442-2444

117. Yu, L. R.; Li, Y. Q.; Sui, W.; *Spectrosc. Spect. Anal.* **2002**, 22, 819.

118. Fu, Q.; Sun, W.; *Applied Optics*, **2001**, vol. 40, No. 9, 1354-1361.

119. Sayan, C.; *American Journal of Physics*, **2007**, 75, 9, 824-826.

120. Alberty, R. A.; Silbey, R. J.; *Physical Chemistry, 2nd Edition*, John Wiley, New York, **1997**.

121. Haralabakopoulos, A. A.; Tsiourvas, D.; Paleos, C. M.; *Journal of Applied Polymer Science*, **1998**, 69, 1885-1890.

122. Martell, A. E., Smith, R. M, Critical Stability Constants, vol. 1, 351 **1982.**

123. Martell, A. E., Smith, R. M, Critical Stability Constants, vol.5, 248, **1982.**

124. Martell, A. E., Smith, R. M, Critical Stability Constants, vol.2, 246, **1982.**